Equipment Manual

Boss Manipulator™ & 5390 Controller

For GTEM!™ Models 5311 and 5317

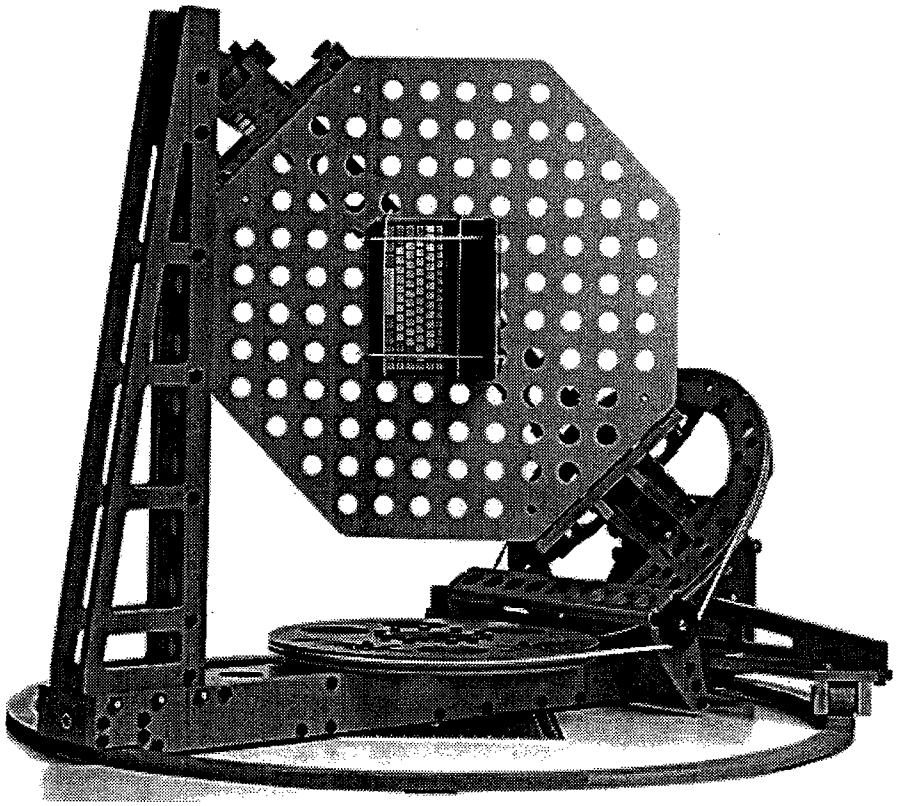

ETS™

EMC TEST SYSTEMS, L.P. – An ESCO Company

E M C O

USA
2205 Kramer Lane, Austin, Texas 78758-4047
P.O. Box 80589 Austin, Texas 78708-0589
Tel 512.835.4684 Fax 512.835.4729

FINLAND
Euroshield OY
Fankkeen Teollisuusalue
27510, Eura, Finland
Tel 358.2.838.3300 Fax 358.2.865.1233

E-MAIL & INTERNET
support@emctest.com
http://www.emctest.com

REV B - PN 399205

TABLE OF CONTENTS

LIST OF ILLUSTRATIONS

LIST OF TABLES

WARRANTY

The Electro-Mechanics Company (EMCO) warrants that our products are free from defects in materials and workmanship for a period of two years from the date of shipment. If you notify us of a defect within the warranty period, we will at our option, either repair or replace those products which prove to be defective. If applicable, we will also recalibrate the product.

There will be no charge for warranty services performed at the location we designate. You must, however, prepay inbound shipping costs and any duties or taxes. We will pay outbound shipping costs for a carrier of our choice, exclusive of any duties or taxes. You may request warranty services to be performed at your location, but it is our option to do so. If we determine that warranty services can only be performed at your location, you will not be charged for our travel related costs.

This warranty does not apply to:

1. Normal wear and tear of materials;
2. Consumable items such as fuses, batteries, etc.;
3. Products which have been improperly installed, maintained, or used;
4. Products which have been operated outside of specifications;
5. Products which have been modified without authorization; and,
6. Calibration of products, unless necessitated by defects.

THIS WARRANTY IS EXCLUSIVE. NO OTHER WARRANTY, WRITTEN OR ORAL, IS EXPRESSED OR IMPLIED, INCLUDING BUT NOT LIMITED TO, THE IMPLIED WARRANTIES OF MERCHANTABILITY AND FITNESS FOR PARTICULAR PURPOSE.

THE REMEDIES PROVIDED BY THIS WARRANTY ARE YOUR SOLE AND EXCLUSIVE REMEDIES. IN NO EVENT ARE WE LIABLE FOR ANY DAMAGES WHATSOEVER, INCLUDING BUT NOT LIMITED TO, DIRECT, INDIRECT, SPECIAL, INCIDENTAL, OR CONSEQUENTIAL DAMAGES, WHETHER BASED ON CONTRACT, TORT, OR ANY OTHER LEGAL THEORY.

Please contact our sales department for a Return Material Authorization (RMA) Number before shipping equipment to us. Telephone USA +1-512-835-4684 or facsimile USA +1-512-835-4729.

NOTICE: This product and related documentation must be reviewed for familiarization with safety markings and instructions before operation.

SAFETY SYMBOL DEFINITIONS

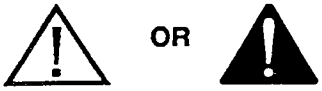

REFER TO MANUAL
When product is marked with this symbol refer to instruction manual for additional information.

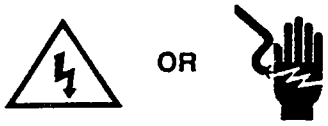

HIGH VOLTAGE
Indicates presence of hazardous voltage. Unsafe practice could result in severe personal injury or death.

PROTECTIVE EARTH GROUND (SAFETY GROUND)
Indicates protective earth terminal. You should provide an uninterruptible safety earth ground from the main power source to the product input wiring terminals, power cord, or supplied power cord set.

CAUTION

CAUTION
Denotes a hazard. Failure to follow instructions could result in minor personal injury and/or property damage. Included text gives proper procedures.

GENERAL SAFETY CONSIDERATIONS

BEFORE POWER IS APPLIED TO THIS INSTRUMENT, GROUND IT PROPERLY through the protective conductor of the AC power cable to a power source provided with protective earth contact. Any interruption of the protective (grounding) conductor, inside or outside the instrument, or disconnection of the protective earth terminal could result in personal injury.

BEFORE POWER IS APPLIED TO THIS INSTRUMENT, SET ITS PRIMARY POWER INPUT to the voltage of the AC power source. Failure to set the AC power input to the correct voltage could cause damage to the instrument when power is applied.

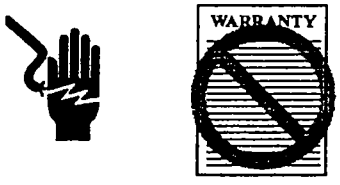

BEFORE SERVICING: CONTACT EMCO - servicing (or modifying) the unit by yourself may void your warranty. If you attempt to service the unit by yourself, disconnect all electrical power before starting.There are voltages at many points in the instrument which could, if contacted, cause personal injury. Only trained service personnel should perform adjustments and/or service procedures upon this instrument. ***Capacitors inside this instrument may still be CHARGED even when instrument is disconnected from its power source.***

TO AVOID A SAFETY HAZARD, replace fuses with the same current rating and type (normal blow, time delay, etc.). Order any replacement parts direct from EMCO.

TO AVOID UNDUE MECHANICAL STRESS on the GPIB I/O CONNECTOR, limit connector stacking to no more than three cables on one connector.

ONLY QUALIFIED PERSONNEL should operate (or service) this equipment.

BOSS MANIPULATOR™ AND MODEL 5390 CONTROLLER
For GTEM!™ Models 5311 and 5317

INTRODUCTION

The Electro-Mechanics Company (EMCO) Boss Manipulator and its Model 5390 Controller are designed for use with EMCO Gigahertz Transverse Electromagnetic cells (GTEM!) to accomplish a variety of EMC tests including those for compliance with the rules and regulations of the Federal Communications Commission (FCC) and the European Union (EU). The use of the GTEM! for such testing complies with the intent of §5.4.2 Alternate Test Sites, in ANSI C63.4-1992 [1][1].

The Boss Manipulator used in the GTEM! facilitates rapid testing of an equipment under test (EUT) using not only the standard three-position test procedure, but nine, twelve, twelve-plus-four, and other test procedures that are needed to provide near-field measurements and to characterize special EUTs as well. The Model 5390 Controller permits both manual and computer control of the Boss Manipulator; thus providing both automated and manual EMI emissions and immunity testing to meet all commercial and military requirements for an EUT.

The objective of this equipment manual is to let the operator use the fullest capabilities of the manipulator to enhance EMC tests in GTEM!s. This manual explains the need for the manipulator, describes both it and its controller and tells how to use them.

EMC measurements in the GTEM! require that the EUT be measured in at least three orthogonal positions so that enough data are collected to predict or "correlate" the performance of the EUT to measurements on an open-area test site (OATS) or in a semi-anechoic chamber. Whether measuring the EMI emissions or immunity of an EUT, tests must be made with it in several positions. Positioning the EUT for each measurement can be done manually, but this is quite time consuming and can require two or three people to reposition the EUT inside the GTEM!. Not only does changing the EUT position take time, but supplies of dielectric materials of low permittivity are needed to support it in each measurement position. With the aid of computer-controlled instruments, the GTEM! is capable of very rapid collection of measured data; thus it can easily take longer to manually change the EUT positions than it does to collect the data.

The time to manually position the EUT can be the major part of the total test time when nine or more positions are needed. It is easy to see that if the data are taken by computer-controlled instruments, then a device is needed which will let the computer reposition the EUT under program control. The Boss Manipulator with its controller fills that need.

[1]Numbers in square brackets denote documents listed in the References section of this manual.

GENERAL DESCRIPTION

The EMCO Boss Manipulator system consists of a platform apparatus, a motor base, the Model 5390 Controller, and a Hand-Held Control Unit. The platform apparatus mounts inside the GTEM! on the floor, and the motor base mounts outside the GTEM! underneath the floor. These are shown in Figures 1 and 3. The Model 5390 Controller may be used on a desk or mounted in a rack. The controller and the hand-held unit give the operator complete manual control of the manipulator, and controller gives the operator automatic remote control through a GPIB connection to an external computer.

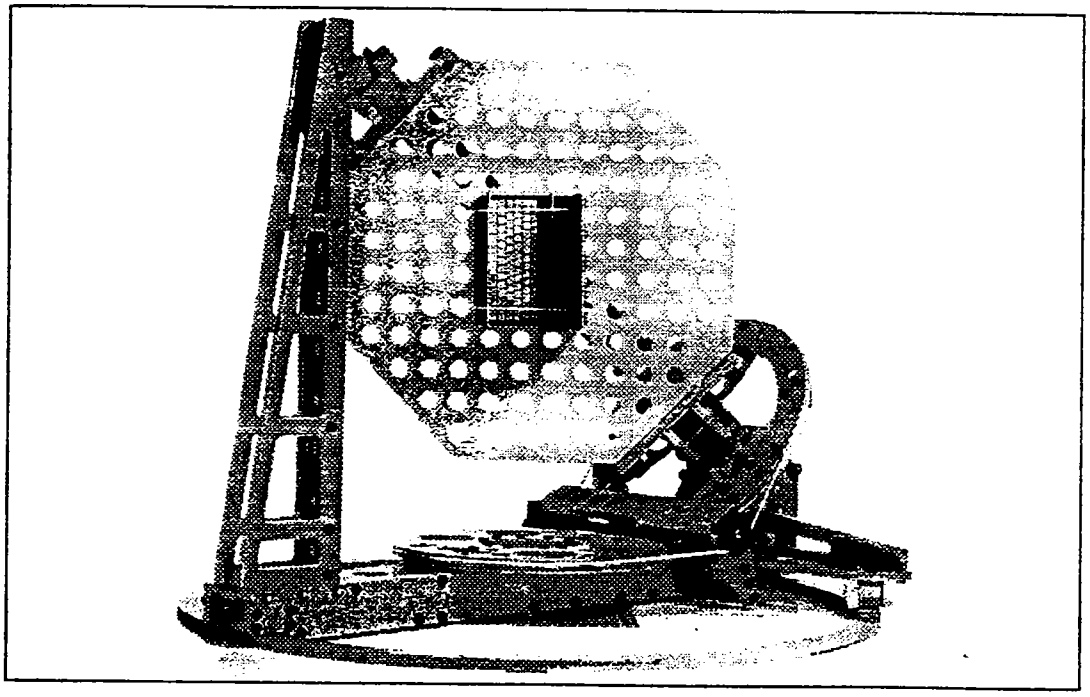

Figure 1. Picture of Boss Manipulator

Boss Manipulator

Platform Apparatus. The platform apparatus has two axes, an azimuth axis perpendicular to the floor of the GTEM! and an orthogonal (ortho-) axis set at an angle of 35.3° to the Floor. The frame of the platform apparatus rests on a circular phenolic bearing or guide-ring on the floor of the GTEM! and rotates 370° around the azimuth axis. The EUT platform rotates ±125° around the ortho-axis. This is shown in Figure 3. The EUT platform, or simply, the platform, is perforated to reduce its weight, to reduce its effects on the electromagnetic fields around the EUT, and to provide anchoring points for securing the EUT during testing. It is removable so that multiple platforms can be used to stage and queue several EUTs for testing. All of the platform apparatus is constructed of dielectric materials which have low permittivity. To reduce perturbation of the electromagnetic fields by the platform apparatus, all of the parts are cut away or perforated, e.g., the platform, so that only the minimum amount of material, needed for strength, is inside the GTEM! near the EUT. The effect of the manipulator on test results is discussed in "Impact of Manipulator on Measurements," on page 15, and in a report by Osburn,

et. al. [2], (see Appendix B). The part of the metal drive shaft from the motor base which penetrates the floor of the GTEM! is kept short to prevent or minimize any field perturbations.

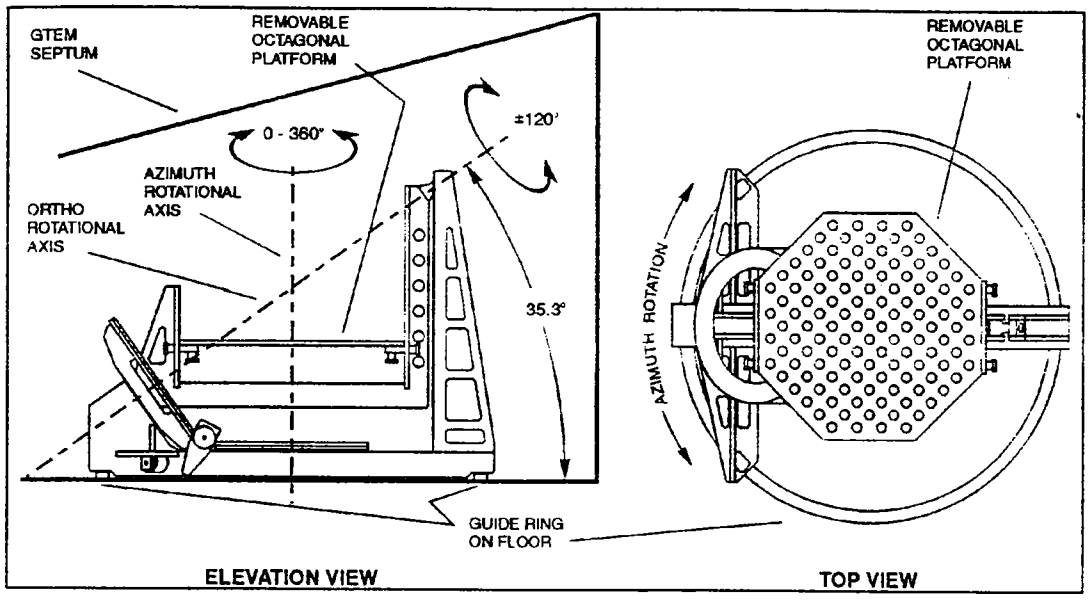

Figure 2. Simplified CAD Drawing of Platform Apparatus.

Motor Base. The motor base mounts under the floor of the GTEM! so that it is outside of the cell. It has a reversible motor with a gear box which drives two concentric shafts that drive the platform apparatus inside the cell. The inner shaft is driven directly by the motor and gear box, and the outer shaft is driven through a solenoid-operated electric clutch. The outer shaft drives the frame of the platform apparatus in azimuth and the inner shaft drives the ortho-axis assembly. To change the azimuth, the clutch is engaged and the motor turns both shafts so that there is no relative motion between the ortho-axis assembly and the frame. The motor rotates clockwise (CW) to increase the azimuth. To rotate the platform around the ortho-axis, the clutch is disengaged and the motor turns only the inner shaft. The motor rotates counter-clockwise (CCW) to produce clockwise platform rotation around the ortho-axis. The motor base also contains control circuits and relays which control the motor and the clutch solenoid, position encoders which sense and indicate the positions of the two axes of the manipulator, and power supplies to run the control circuits and encoders.

Model 5390 Controller

The EMCO Model 5390 Controller is designed specifically to control the Boss Manipulator. It permits both manual and computer control of the manipulator, providing both automated and manual EMI emissions and immunity testing of EUTs. The front panel of the Model 5390, shown

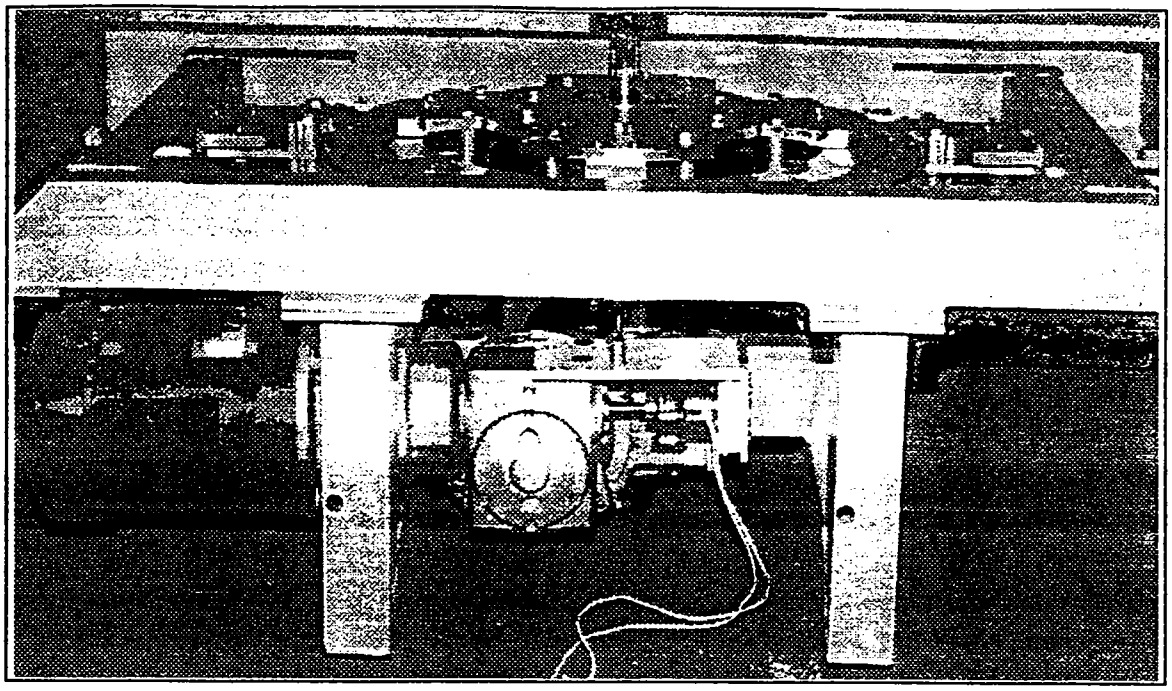

Figure 3. Picture of Manipulator Motor Base.

in Figure 4, contains a 240 x 64-dot, back-lighted, graphic liquid crystal display (LCD), a numeric keypad, and a multi-purpose positioner knob or cursor device. The LCD displays device parameters and operational information, the numeric keypad is used for entering or altering device parameters and invoking functions, and the positioner knob/cursor device is used for stepping through menu items and manually positioning the axes of the manipulator.

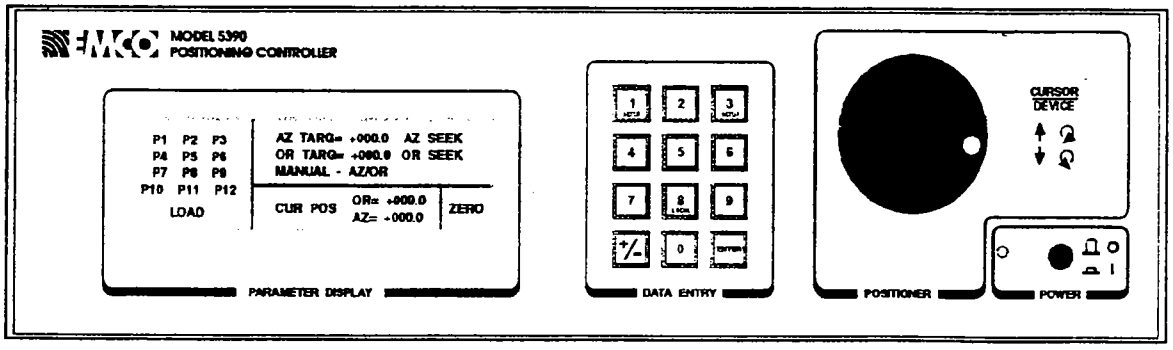

Figure 4. Front Panel of the Model 5390 Boss Manipulator Controller

The Device Interface Port connector located on the rear panel of the Model 5390 provides the connection to the manipulator. The control cable connects to the Device Interface Port of the controller at one end and the motor base at the other end.

Control of the manipulator may be accomplished either in the local mode through direct interaction with the front panel controls, or in the remote mode via the IEEE Std 488.1-1987 general purpose interface bus (GPIB) [4]. The Model 5390 is connected to the GPIB through the 24-pin "D" connector located on the rear panel. In the remote mode of operation, the required

GPIB instruction set from IEEE Std 488.2-1992 [4] and a full Boss Manipulator (device-unique) instruction set are available in the firmware. These are described in other sections of this manual.

Hand-Held Control Unit

The Hand-Held Control Unit gives the operator local control of the manipulator at the GTEM! during test setup. With it, the operator can move either or both axes of the manipulator to see that the EUT is securely mounted in the manipulator and that it has adequate clearances from the other parts of the GTEM!, particularly the septum and the absorbers. The Hand-Held Control Unit is mounted on a comfortable handle with a small panel containing four control switches. The switches are "rocker" type switches which can be operated by the operator's thumb. It is shown in Figure 5. Using the switches the operator can select the hand-held unit or the main controller, the axis to rotate and the direction to rotate it. The Control switch must be in the "MAIN" position when the hand-held unit is not being used. The Hand-Held Control Unit has an integral cable which connects to the motor base of the manipulator so that it is easy to use near the GTEM!.

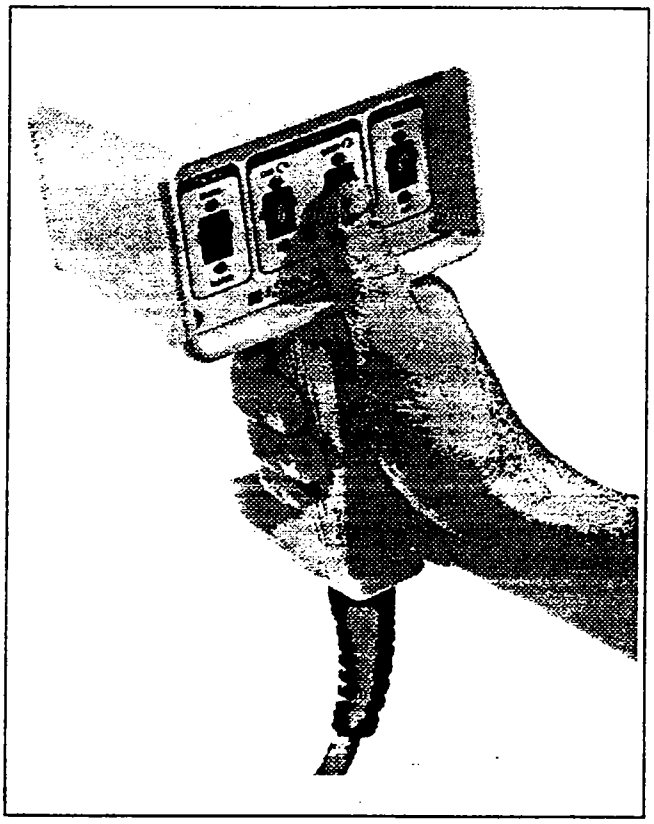

Figure 5. Picture of Hand-Held Control Unit.

SPECIFICATIONS

The specifications of the Boss Manipulator and its components are shown in the following tables.

Table I

Boss Manipulator Specifications

Electrical			
Voltage	230 V_{rms} AC (Set at Factory)	Frequency	50 - 60 Hz, 1-phase
		Current	10 A @ 115 V or 5 A @ 230 V
Cir Bkr	20 A, 2-pole	Ctrl Cir Fuse	2 A Fast
Electr's Fuse	0.4 A Fast	Azmth Brake	2 A Slow, 2 ea
Environmental			
Operating Temp.	0° C - 40° C	Rel. Humidity	≤90% non-condensing
Shock & Vib.[1]	EIA RS-414-A [5]		
Note	[1]Limit shock and vibration to values less than those found in RS-414-A.		
Mechanical			
Motor Speed	1 RPM		
Air Pressure Setting	100 PSI (To Manipulator Brakes)		
Platform Apparatus:		Model 5317 Boss	Model 5311 Boss
Length		1.7 m	1.05 m
Width		1.7 m	1.05 m
Height		1.3 m	0.8 m
Weight (Including platform)		100 kg	64 kg
Octagonal Platform:			
Width (across flats)		0.9 m	0.55 m
Thickness		20 mm	20 mm
Weight (Included above)		8 kg	5 kg
Maximum Payload:			
Diameter		0.9 m	0.55 m
Height		0.7 m	0.42 m
Weight		50 kg	50 kg

Table II

Model 5390 Controller Specifications

Electrical		**Mechanical**	
Voltage	90 - 250 V_{rms} AC	Height	133 mm (EIA 5.25-in.)
Frequency	50 - 400 Hz, 1-phase		
Max Power Req.	<90 VA	Width x Depth	438 mm x 381 mm
Fuse	2 A, 250 V, Time Delay	Weight	4.5 kg
Max Leakage (Ea Line to Gnd):		**Environmental**	
	250 V, 50 Hz: 1.25 mA;	Operating Temp.	0° C - 40° C
	120 V, 60 Hz: 1.00 mA	Humidity, Rel.	≤90%, non-condens'g.
EMI Filter	Corcom 3EQ8 or equal	Shock & Vib.[2]	EIA RS-414-A [5]
Control Cables	18 Pr Shielded, 10 m Lg Belden 8118 or equal[1]	**Notes:**	
		1. Max control cable length, 50 m.	
Device Connectors	32-pin MS-38999	2. Limit shock and vibration to values less than those found in RS-414-A.	
GPIB Connector	24-pin "D"-Type		

Table III
Hand-Held Control Unit Specifications

Electrical		**Mechanical**	
Voltage	5 V	Height (Incl. handle)	203 mm
Frequency	DC	Width	114 mm
Control Cable	6 m	Depth	89 mm
Device Connector	6-pin MIL-C-5015	Weight (Incl. case)	6.6 kg
Environmental		**Note**	
Operating Temp.	0° C - 40° C	[1]Limit shock & vibration to values less than those found in EIA RS-414-A.	
Rel. Humidity	≤90% non-condensing		
Shock & Vibration[1]	EIA RS-414-A [5]		

UNPACKING AND ASSEMBLY INSTRUCTIONS

Installation of the Boss Manipulator requires some disassembly and modification of the GTEM!. Please leave all unpacking and assembly to the EMCO installer. Upon receiving the equipment, inspect the crates and packages containing the components of the Boss Manipulator for damage and report any damage found to the delivering shipper. Please place the crates and packages in the same room with the GTEM!, or in a room as near to it as possible, to await the arrival of the EMCO installer.

PREPARATION FOR USE

Power and Grounding Requirements

The Boss Manipulator motor base will accept AC power which is nominally 115 V or 230 V, 50-60 Hz, single phase. The voltage for the motor base must be set to the correct value at the factory before shipment. The brake solenoids appropriate for the voltage that will be used must be installed in the motor base prior to shipment and different interconnecting plugs for the other components in the motor base must be used for different voltages. Factory settings of operating voltage are shown on the label on the motor base.

CAUTION

Operation of a manipulator motor base set up for 115 V on 230 V may cause extensive damage to the components of the motor base. Operation of a manipulator motor base set up for 230 V on 115 V may damage the motor. If in doubt, call the factory at +1-512-835-4684 to verify which operating voltage is correct.

The Model 5390 Controller accepts any AC power source input within the range of 90 to 250 V, 50 to 400 Hz. No voltage selection is required.

WARNING

Before switching on this equipment, the protective earth terminals of this equipment must be connected to the protective conductor of the power system. The power cords shall only be connected to socket outlets provided with a protective earth contact. This protective action must not be defeated through the use of an extension cord without a protective earth conductor.

For the application of AC power, two three-conductor power cables are shipped with the manipulator. Connecting these cables to an appropriate AC power source causes both the motor base and the controller chassis to be connected to earth ground. There are also ground conductors in the control cable which connect the motor base and controller grounds together.

CAUTION

The protective earth terminal of both power cables must be connected to the *same* protective ground (earth) conductor in the AC power source and it must be the *same* one that is connected to the chassis of the GTEM!.

Motor Base, Model 5390 Controller and Hand-Held Control Unit Connections

Connection between the Model 5390 Controller and the Boss Manipulator motor base is accomplished by means of one multi-conductor cable. The standard length of this cable is 10 m, but lengths up to 50 m may be used. The cable terminates in circular bayonet-style connectors which are identical at both ends. The cable is symmetrical so that either end may be connected to the Model 5390. When connecting the control cable to either the motor base or the Model 5390 Device Interface Port connector, observe the keying of both the cable and panel connectors and align them properly during insertion to prevent possible damage to the connector shell. Also, excessive lengths of cabling (more than 1.8 metres) should not be allowed to hang freely from the rear panel of the Model 5390, as this will place excessive mechanical stress on the connector and the panel.

If either end of the control cable is not connected or if the required AC power is not present at the motor base when the Model 5390 power is turned on, the Parameter Display screen will show a two-line error message instead of the Main Menu. See Appendix A at the back of this manual for an explanation of these error messages. To eliminate the error message and get the Main Menu, place the power switch OFF, make sure both ends of the control cable are connected to the equipment and that there is AC power connected to the motor base, and then place the power switch ON.

CAUTION

Always turn off the AC power to the Model 5390 when connecting or disconnecting the control or GPIB cables.

GPIB Interconnections

The Model 5390 is compatible with the General Purpose Interface Bus (GPIB) and its command sets as described in IEEE Std 488.1 [3] and IEEE Std 488.2 [4]. A 24-pin "D"-Type connector located on the rear panel of the instrument provides for connection to the GPIB. When making this connection, avoid stacking more than three cables on the connector as this may cause excessive stress on the connector and the rear panel of the instrument. Be sure to tighten the two connector lock screws finger tight to avoid intermittent connection during operation.

The talker/listener bus address of the Model 5390 may be set through the front panel controls. Instructions on how to perform this operation may be found in the section of this manual entitled "Setup Menu." Instructions for programming of the GPIB interface of the instrument may be found in the section of this manual entitled "Programming Model 5390 for Remote Operation."

The Hand-Held Control Unit control cable connector plugs into a mating connector on the panel of the motor base near the device interface port (main control cable) connector. Be sure the control switch on the hand-held unit is set to "Main" before connecting its cable to the motor base.

Model 5390 Controller Rack Mounting

The Model 5390 may be ordered with a Rack-Mount Option. This option may be either factory or field installed. This option provides capability for installing the instrument in a universal EIA 19-inch rack or cabinet. The instrument requires 5.25 inches, approximately 133 mm, of rack height (three standard rack height units). When installing the Rack-Mount Option, the feet must be removed from the Model 5390 cabinet and the rack-mounting ears must be installed on the sides of the cabinet at the front. The following steps describe this installation:

1. Remove and save the four screws nearest the front panel on each side of the Model 5390 cabinet;
2. Place the rack-mounting brackets included in the rack mount option at each side of the cabinet with the rack ears at the front and pointing outward, and align the four holes in the brackets with those in the side of the cabinet;
3. Use the four screws from Step 1 to fasten the rack-mounting brackets to the sides of the cabinet;
4. Turn the cabinet upside down and remove the four feet, one screw holds each foot (save these for possible reuse later).

OPERATION

The Boss Manipulator is easy to operate under control of the Model 5390 controller. It will place the EUT in all of the positions which are required for GTEM! measurements. GTEM! measurements are based on theory developed over the past several years. Measurement theory is given in The GTEM! manual [6], pages 22 - 37 and Appendix A, and reports which have been

made by EMCO and others [7, 8, 9, 10, 11]. The essence of GTEM! theory is distilled in the following sections of this manual to help the operator use the manipulator.

Theory of Operation

Measurements in a GTEM!. A GTEM! may either receive or transmit; thus electromagnetic interference (EMI) measurements in a GTEM! may be of either emissions or immunity. Among emissions measurements are far-field, near-field, and some special measurements. To predict the performance of the EUT during measurements of its emissions on an open-area test site (OATS), its emissions must be measured in a specific set of positions in the GTEM!. Predicting EUT performance on an OATS by making measurements in a GTEM! is also called "correlation," and the mathematical process is often called the "correlation algorithm."

Simplified Far-Field Measurements may be made of an EUT in a GTEM! to predict or correlate its OATS-measured emissions [6, 7, 8]. These measurements are usually made to show compliance to standards, e.g., CISPR 22 or FCC Part 15, in which it is only necessary to know the maximum E-Field versus frequency within a specified range of heights at a certain distance. For example, FCC tests for home computers search heights from one to four metres above the ground at a distance of three metres over the frequency range of 30 MHz to 5 GHz. These simplified measurements require emissions to be measured with the EUT in only three orthogonal positions. This is called the 3-measurement, 3-input correlation algorithm. The main simplifying assumption in this algorithm is that the EUT has gain no greater than a dipole, i.e., a dipole radiation pattern.

Near-Field Measurements may be made of an EUT in a GTEM! to correlate its emissions over the frequency range of 9 kHz to 30 MHz [9]. This is called the 9-measurement, 9-input correlation algorithm, and requires measurement of emissions with the EUT in nine positions. The EUT is assumed to be much smaller than a wavelength in its largest dimension; a reasonable assumption below 30 MHz for EUTs that will fit into a GTEM!. While this algorithm was originally intended for near-field measurements below 30 MHz, it also works well for far-field measurements above 30 MHz. It is valid from 9 kHz to 5 GHz.

Special Measurements are sometimes required because the EUT may have gain greater than a dipole [10], and thus may have a cardioid or other unidirectional pattern. Above about 500 MHz, some EUTs may have an incidental unidirectional pattern because of the way they are constructed, but others have a unidirectional pattern because they are intentional transmitters with an antenna built in. There are two algorithms which may be used, depending on what one wants to know about the EUT. The simplest one is the 12-measurement, sorted 3-input correlation algorithm, and the other one is the 12+4-position correlation algorithm. In both of these algorithms, the EUT is viewed as a cube and measurements are taken of the emission from each of its faces in both polarizations.

The 12-measurement, sorted 3-input correlation is used when it is not necessary to know anything about the shape of the radiation pattern of the EUT. It is often used to test small Telecom Terminal Equipment, such as cellular telephones, up to 10 GHz. It is valid from 30 MHz to at least 10 GHz.

The 12+4-position correlation algorithm is used when one needs to estimate the shape of the radiation pattern of the EUT. It is valid from 30 MHz to 5 GHz.

Immunity Measurements may be made in the GTEM! [7, 11] to satisfy standards such as MIL-STD-462 or IEC 1000-4-3. If the operator does not know the shape of the radiation (sensitivity) pattern of the EUT, then its front, back, and both sides must all be exposed to the test signal in both horizontal and vertical polarizations. To do this, eight positions must be tested so that the four usually vertical sides of the EUT are tested in both polarizations facing the apex of the GTEM!. If the operator already knows that only one side, e.g., the back, of the EUT is sensitive to external electromagnetic fields, then the testing can be reduced to exposing only its one sensitive side to the apex of the GTEM! in both polarizations.

Installing the EUT. For the purposes of this discussion, consider the EUT as a cube. We will identify the sides of the EUT as faces of the cube and establish a set of Cartesian axes for it. Then we can show how to set it on the manipulator platform.

Naming the EUT Faces. Figure 6 shows a three-dimensional Cartesian axis system with a cube centered on it. The face from which a positive axis emerges is named for that axis, i.e., "+X" is the face of the cube from which the positive X-axis emerges. Name the front of the EUT "–Z" and the back "+Z". Looking at the "+Z" face (the back), name the right-hand side "+X" and the left-hand side "–X". Name the top "+Y" and the bottom "–Y".

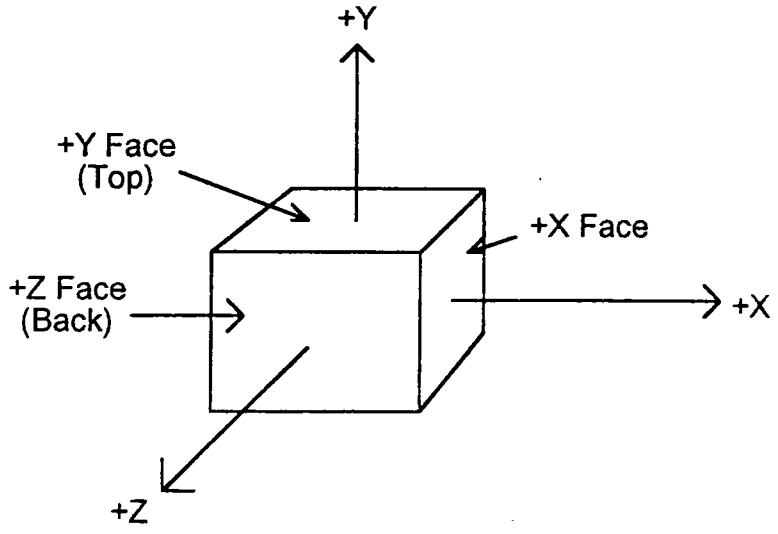

Figure 6. EUT as a Cube on Cartesian Axes Showing Names of Faces.

This is the coordinate system for the EUT. Note that the three orthogonal positions of the EUT exchange the EUT coordinates relative to the GTEM! coordinates. The first position is identified as XYZ, the second as YZX, and the third as ZXY; and the voltages measured at the apex of the GTEM! in the three positions are called V_{XYZ}, V_{YZX}, and V_{ZXY}.

EUT Face Directions on Platform. Figure 7 shows how the EUT is set on the manipulator platform so that the positions of the EUT coincide properly with the axis positions tabulated in Tables IV, V, and VI.

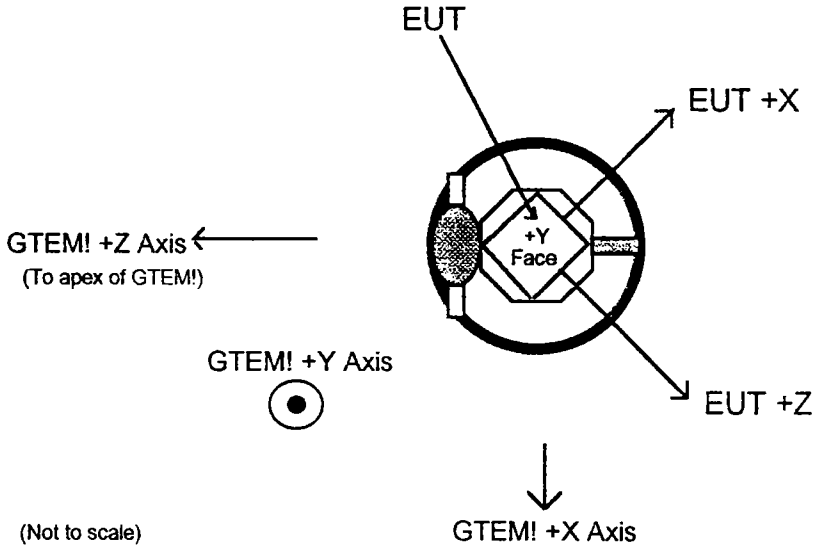

Figure 7. Position of EUT on Manipulator During Loading Showing Directions of EUT Faces and Axes.

EUT Positions. To make control of the manipulator easier during all the different kinds of tests, the Model 5390 controller provides 12 preset positions and other positions which the operator can control. The emissions tests all require sets of positions which are built on the basic three orthogonal positions needed by the 3-measurement, 3-input correlation. The immunity tests require positions based on the test standard; these are not necessarily extensions of the basic set of three orthogonal positions.

The Twelve Preset Positions are listed in Table IV below. The positions are in degrees from the zero position of each axis; "+" is clockwise and "–" is counter-clockwise. "Az." stands for azimuth and "Or." for orthogonal. These 12 preset positions are pictured in Figures C-1 through C-12 in Appendix C.

Table IV
Preset Positions for the Boss Manipulator

Pos.	Az.	Or.	Pos.	Az.	Or.	Pos.	Az.	Or.
P1	45	–120	P2	45	0	P3	45	+120
P4	135	+120	P5	135	0	P6	135	–120
P7	225	–120	P8	225	0	P9	225	+120
P10	315	+120	P11	315	0	P12	315	–120

These 12 preset positions are arranged so that there is a position in which each of the six sides of the EUT faces the apex of the GTEM! in each polarization, vertical and horizontal. They are also

arranged in four sets of three orthogonal positions; each row in Table IV is a set of three orthogonal positions.

Sets of Positions Needed. For the 3-measurement, 3-input correlation, use any set of three orthogonal positions. But the best positions to use are P4, P5 and P6, or P7, P8 and P9, because there is less manipulator mass between the EUT and the apex of the cell.

For the 9-measurement, 9-input correlation, use any set of three orthogonal positions and make six more by rotating the azimuth ±45° for each ortho-axis setting. For example, select P10, P11 and P12 as the basic set, then after measuring the EUT in position P10, rotate the azimuth first to 270° (315–45) and make a measurement, then rotate the azimuth to 360° (315+45) and make a measurement. The nine positions which are developed around the basic P10, P11 and P12 set are shown in Table V. Similar sets of nine positions can be constructed from other basic three-position sets.

Table V
Example Positions for 9-Measurement, 9-Input Correlation

Pos.	Az.	Or.	Pos.	Az.	Or.	Pos.	Az.	Or.
P10–45	270	+120	P11-45	270	0	P12-45	270	-120
P10	315	+120	P11	315	0	P12	315	-120
P10+45	360	+120	P11+45	360	0	P12+45	360	-120

For the 12-measurement, sorted 3-input correlation, and for the 12+4 position correlation, use all 12 of the preset positions. The results of using all 12 positions are measurements of all six faces in two polarizations. Select the face with the highest measured emissions level. This may be a different face at different frequencies. Define this face as +X in orientation XYZ and select two more faces such that three orthogonal positions YZX and ZXY are satisfied. For example, if the strongest emissions were measured in position P5, then from Table IV the other two positions would be P4 and P6.

1. For the 12-measurement, sorted 3-input correlation, the data already measured in the three positions described above, e.g., P5, P4 and P6, are then input to the 3-measurement, 3-input correlation. This correlation, which eliminates the assumption of gain no greater than a dipole, can be used to do tests in which the EUT is replaced by a dipole on the OATS and the limit levels are in terms of the power at the dipole terminals needed to produce the same emission level measured from the EUT. This correlation is discussed in more detail in [10] and [13] (see Appendix B).

2. For the 12+4 position correlation, select four additional measurement positions that are ±45° to the position of highest emissions, and measure the EUT emissions in these positions. For example, if the strongest emissions in the first 12 measurements were measured in position P5, then the other four positions would be (Az., Or., respectively) 90°, 0°; 180°, 0°; 180°, -120°; and, 270°, -120°. These could also be stated as P5 ±45° azimuth and P7 ±45° azimuth. Use these data to estimate the directivity, and thus the gain, of the EUT. Then use the previously measured data at P5, P4 and P6, and the

estimated gain as inputs to the 3-measurement, 3-input correlation. See [10] and [13] (Appendix B) for a more detailed discussion of this correlation.

For EMI immunity measurement, eight of the preset positions will provide tests of all four sides in both polarizations. These positions are shown in Table VI. In the table, the test face is the side of the EUT facing the apex of the GTEM!; identifying test faces of the EUT and installing it on the manipulator are described below. If it is necessary to test the top and bottom too, use all 12 preset positions.

Table VI
Preset Positions Used in Immunity Tests

Test Face	Pol.	Preset Pos.	Az.	Or.	Test Face	Pol.	Preset Pos.	Az.	Or.
+Z	V	P5	135	0	+X	V	P8	225	0
+Z	H	P7	225	−120	+X	H	P4	135	+120
−Z	V	P11	315	0	−X	V	P2	45	0
−Z	H	P1	45	−120	−X	H	P10	315	+120

The operator should study the immunity test standard that applies to the EUT, e.g., IEC 1000-4-3, before attempting to make immunity measurements.

Zero Position. This position may be set by the operator using the Setup Menu of the Model 5390 controller. The recommended settings for the Zero position are 0° for both axes. It is important that the proper zero positions be established before trying to make measurements using the manipulator. The EMCO installer will have set the zero positions of both axes during installation, but check them before making measurements. If the Zero position is not as depicted in Figure 8, use the Hand-Held Control Unit (discussed below) to move the axes to these positions and then Set Zero using the Setup Menu of the Model 5390 controller.

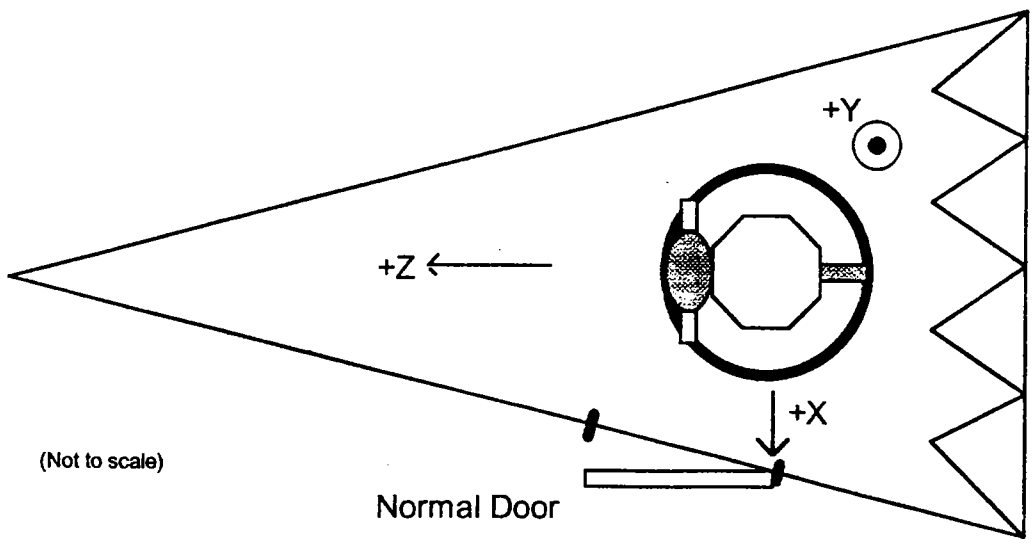

Figure 8. Plan View of GTEM! With Manipulator Showing GTEM! Axes and Manipulator in Zero Position

When Zero is properly set, the azimuth axis should rotate CCW to the mechanical stop at −5° and CW to the mechanical stop at +365°; and starting with the platform level, the ortho-axis should rotate CCW to the mechanical stop at −125° and CW to the mechanical stop at +125°.

Load Position. This position may also be set by the operator using the Model 5390 controller. The recommended settings for the Load position are 0° for both axes. These are the Factory default settings. Alternate settings which may be used for the Load position are 315° for the azimuth axis and 0° for the ortho-axis. This position will allow loading the EUT with its front facing the apex of the cell.

Factory Default Limits. The factory default limits are based on the Zero position being as described above. Both the azimuth and orthogonal axes must be at 0° when the platform is level, the frame of the platform apparatus is aligned with the longitudinal axis (Z-axis) of the GTEM!, and the tall frame post is next to the RF absorbers at the back of the cell. This is depicted in Figure 8. The default limits and the mechanical limits of rotation are −5° (CCW) and +365° (CW) on the azimuth axis and −125° (CCW) and +125° (CW) on the ortho-axis.

Impact of Manipulator on Measurements

Whenever materials which have permittivity (ε) or permeability (μ) greater than air (or vacuum) are placed in an electromagnetic field, the field will be perturbed. The amount the field is perturbed depends on the amount of material, the magnitude of its ε or μ relative to air, and where the material is located in the field. For example, a small amount of high-ε material located in a region of high E-Field will perturb the field much more than if it were located in a region of low E-Field, and a small amount of high-μ material located in a region of high H-Field will perturb the field much more than if it were located in a region of low H-Field. Except for the drive shaft which penetrates the GTEM floor, the manipulator is made of dielectric material. It would be desirable if the permittivity of the material were nearly unity, e.g., $\varepsilon \approx 1.06$ for Styrofoam™. Foamed plastics have low values of ε because there is much more air than plastic in them. This condition can be approached with other dielectric materials by cutting material away and boring holes in it as much as its needed strength can tolerate. This has been done with the manipulator. The small amount of steel in the manipulator drive shafts which penetrate the GTEM floor is located in a region of low H-Field, thus its contribution to perturbing the field is small.

Osburn, et. al. [2], (see Appendix B) performed a series of experiments to determine how much the manipulator affected the measurements of emissions made in the GTEM. The results of these experiments showed that the average difference between measurements of an EUT with and without the manipulator was 0.18 dB with a standard deviation of 0.58 dB. The average measured E-Field data are shown in Figure 9 and the differences in Figure 10. These were emissions measurements, but by reciprocity, EMI immunity measurements should be affected the same amount.

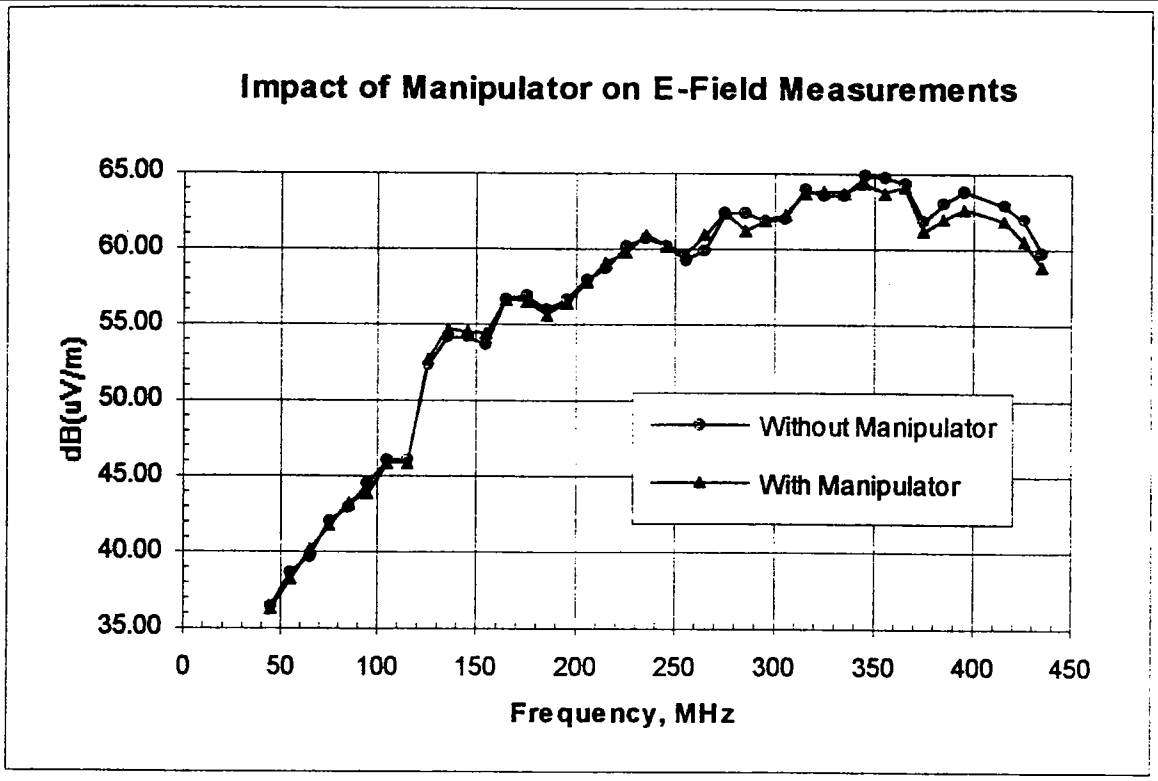

Figure 9. Average Measured E-Field Data.

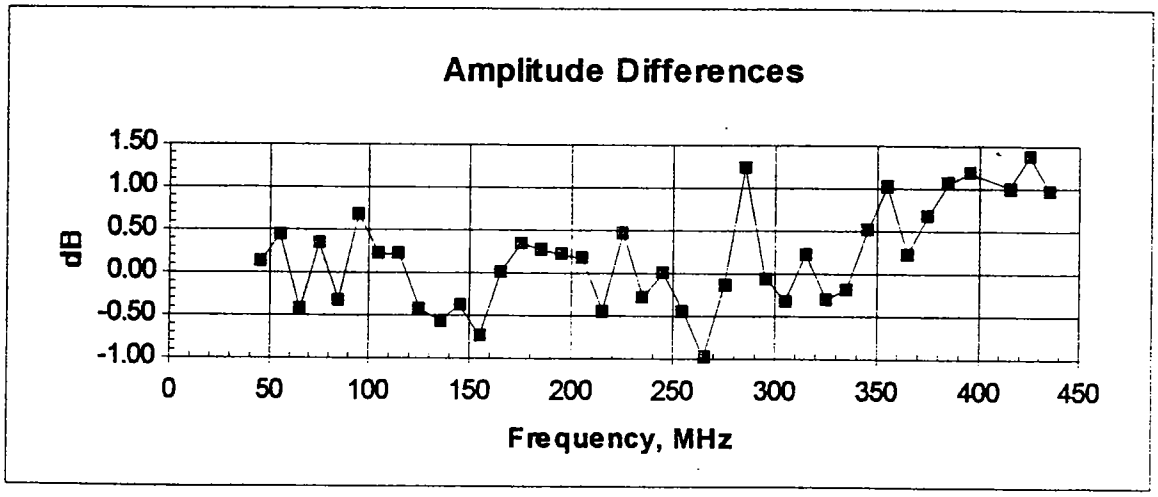

Figure 10. E-Field Differences With and Without Manipulator

Accommodating Large EUTs

An EUT which is too large or too heavy for the manipulator may be tested in the GTEM! if the platform apparatus is first removed. Removal of the platform apparatus will leave the phenolic guide-ring or bearing and a short length of the concentric shaft (including the azimuth drive yoke) from the motor base protruding above the floor of the GTEM!. Do not remove these parts or the

motor base, instead protect the guide-ring, shaft, and yoke by filling in the spaces around and between them and covering them with soft or frangible dielectric materials of low permittivity.

WARNING

Get help! The platform apparatus is heavy! The Model 5317 Boss weighs 100 kg (>220 lb.) and the Model 5311 Boss weighs 64 kg (>140 lb.).

To avoid directional calibration problems, the platform apparatus must be reinstalled so that the axes have the same positions relative to the motor base shafts as when it was removed.

1. Set both axes of the manipulator to their zero positions. Information on how to do this is contained in the section entitled, "Model 5390 Local Mode," below.

Note

From this point on, be sure that neither axis is rotated. Both the platform apparatus and the motor base must remain at zero until after the platform apparatus is reinstalled.

2. Disconnect power from the motor base and turn off the Model 5390.

3. Remove the EUT platform and its height adjustment brackets. (This removes seven to ten kilograms from the total weight.)

4. Carefully lift the platform apparatus up until it clears the shaft and move it towards the door of the GTEM!. It will have to be lifted approximately 10 cm to clear the shaft.

5. After the platform apparatus is clear of the shaft, move the apex end of it towards the GTEM! door, being careful not to rotate the orthogonal axis.

6. Move the platform apparatus to the door, lift it carefully over the threshold of the door jam, and move it out of the GTEM!

7. Store it in an area where it will be protected from damage and rotation of the orthogonal axis.

8. To reinstall the platform apparatus, reverse the above steps. The end of the frame with the tall post must go into the GTEM! first and be placed next to the Absorbers. When setting the platform apparatus in place, be sure that the azimuth yoke lugs fit correctly into the frame slots.

Controllers

Model 5390. The Model 5390 is a menu-driven instrument which has two modes of operation, local and remote, that are described below. There are three menus, two in the local mode and one

in the remote mode. The Setup Menu and the Main Menu are available in the local mode, and the Remote Menu is displayed in the remote mode. The Main Menu is displayed at power on.

Using the Model 5390, the operator has complete control over both axes of the manipulator and thus the orientation or positioning of the EUT. The EUT Platform moves or rotates around the ortho-axis and the frame of the platform apparatus moves or rotates around the azimuth axis. Each one is controlled independently by the Model 5390. The operator may position the manipulator manually using the local mode, or under program control using the remote mode.

In the local mode, the operator may manually bring the two axes of the manipulator to their zero positions, their load positions, twelve preset positions, or any other desired positions within their travel ranges by using the parameters and commands available in the Main Menu. For example, to test a device for compliance with Part 15 of the FCC Rules and Regulations, the operator can set the manipulator axes (the frame and platform) in their load positions to make it easy to install the EUT. Once the EUT is installed and operating properly, the operator may choose to perform the testing either automatically under remote program control or under local, manual control. Usually it is faster and more efficient to do the tests under computer control using test controlling software, but there may be circumstances in which the operator wants to have manual control over the tests. In this event, the operator can position the manipulator to each of three orthogonal positions to take the three sets of orthogonal data, or to some other position for a unique or special test. All of the parameters and functions needed to position the manipulator, and thus the EUT, are discussed in the paragraphs under Local Mode below.

In the remote mode, the controlling computer can position the manipulator frame and EUT platform as necessary to do any of the tests. The EMCO GTEM! Evaluation and Test Software (GETS!™)[2] is designed to provide all of the manipulator positioning needed by the test algorithm being used. Here, the operator's entire interaction is with the controlling computer, its display, and the Remote Screen displayed by the Model 5390. While GETS! will do everything, there may be times when the operator wants to write a special controlling program. In this event, he or she should refer to the commands and examples in Tables VII through XIII and other information in Remote Mode below.

Hand-Held Control Unit. The Hand-Held Control Unit is a convenient controller for the operator to use during test setup. It plugs into the motor base so that it is easy to use at the GTEM!, and it gives the operator the ability to move both axes of the manipulator. It is a simple control unit with only four switches as shown in Figure 5. The left-most switch transfers control from the Model 5390 (MAIN) to the Hand-Held unit (HAND). This switch must be in the MAIN position to enable the Model 5390 to control the manipulator. It should also be in that position while the operator connects it to the motor base. The right-most switch selects the axis to control, the choices being orthogonal (OR) and azimuth (AZ). The two switches in the middle cause the selected axis to be moved or rotated clockwise (CW) or counter-clockwise (CCW).

[2]GETS! is a registered trade mark of the Electro-Mechanics Company.

Model 5390 Local Mode

In the local mode of operation, either the Main Menu or the Setup Menu is presented on the Parameter Display, shown in Figure 3, which displays the operational parameters that may be altered and functions that may be invoked. The Main Menu is always displayed first after the power is turned on. The displayed menu, the operational parameters, and the functions may be selected and changed or invoked using the Cursor Device, also called the Cursor Knob, and the Data Entry (numeric) Keypad, also called the Keypad.

A parameter must be selected before it may be altered, and similarly a function must be selected before it may be invoked. The currently selected parameter or function is high-lighted, that is, displayed in reverse video (light characters on a dark background). The selection is changed by rotating the Cursor Device (Knob). Rotating the Cursor Knob clockwise will sequentially select menu items in a forward (left to right and top to bottom) direction, while rotating the Cursor Knob counter-clockwise reverses the order of selection of menu items. The cursor wraps around the menu so that it will repeatedly go through the menu in either direction if the Cursor Knob is continuously rotated in either direction. It is usually quicker to rotate the Cursor Knob towards the menu item in the shortest direction, e.g., if the desired item is ZERO and the currently selected item is P2, rotate the Cursor Knob counter-clockwise. Changing menus, entering new parameter values, or invoking functions is accomplished by using the (Data Entry) Keypad.

To change parameter values, rotate the Cursor Knob either direction until the desired parameter is selected (high-lighted). If the selected menu item is an operational parameter, the Keypad will be open for numeric entry. As each key is pressed, the corresponding digit will be pushed from right to left into the selected parameter value on the display.

To invoke functions, rotate the Cursor Knob to select (high-light) the desired function. The key on the Keypad which will invoke the function, usually the ENTER key, will then be illuminated. Press this key and the selected function will be performed until the key is again pressed.

Main Menu. The main menu layout is shown in Figure 11. It shows all of the Functions which may be invoked and Parameters whose values may be altered during manual operation of the manipulator. The parameters which may be altered are Azimuth Target (AZ TARG) and Orthogonal Target (OR TARG). The values in them are stored in non-volatile memory so that they are remembered until altered, even during loss of AC power to the instrument. The arguments for these two positional parameters must be within the range of ±999; they must also be within the limiting values of these parameters that were programmed in the Setup Menu.

The Main Menu is displayed first when the power is turned on unless the manipulator motor base is not connected to the controller or does not have power. If there is a connection problem or a motor base power problem, a two-line error message will be displayed instead of the Main Menu. See Appendix A for an explanation of these error messages, and "Motor Base, Controller and Hand-Held Control Unit Connections" on page 8 for the action to take in this event.

There are 12 preset positions which are stored in read-only memory (ROM) that the operator cannot alter but may select from this menu. They are numbered P1 - P12. The LOAD and ZERO

functions may be invoked in this menu but may be altered only in the Setup Menu. AZ SEEK and OR SEEK are the azimuth and orthogonal seek functions which may be invoked in this menu. AZ TARG and OR TARG, the target parameters for AZ SEEK and OR SEEK, may be set in this menu. The MANUAL AZ/OR function may be invoked in this menu, placing control of the azimuth or orthogonal axes (the frame and platform, respectively) of the manipulator under control of the Positioner Knob (also known as the Cursor Knob). Finally, the Current Position (CUR POS) area of this menu shows the positions of the two manipulator axes while they are moving and after they cease to move.

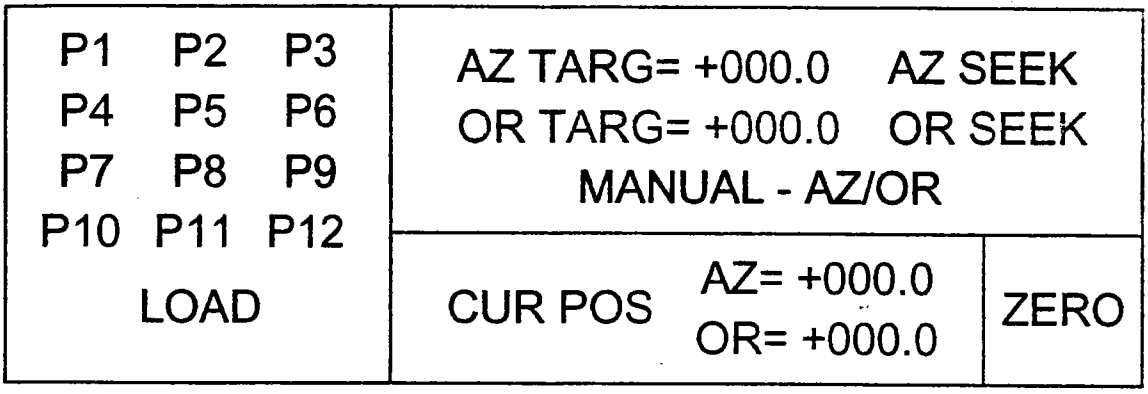

Figure 11. Main Menu Layout

The Twelve Preset Positions are listed below. Table IV is repeated here for the operator's convenience. The positions are in degrees CW ("+") and CCW ("−") from the zero positions. "Az." is "azimuth" and "Or." is "orthogonal."

Pos.	Az.	Or.	Pos.	Az.	Or.	Pos.	Az.	Or.
P1	45	−120	P2	45	0	P3	45	+120
P4	135	+120	P5	135	0	P6	135	−120
P7	225	−120	P8	225	0	P9	225	+120
P10	315	+120	P11	315	0	P12	315	−120

When one of these positions is selected with the Cursor Knob, it may be invoked by pressing the illuminated ENTER key on the Keypad. The ENTER key will remain illuminated during the motion of the azimuth axis (which always moves first) indicating that the ENTER key is still active. The ENTER key may be pressed again to stop the azimuth motion and yet again to restart it. However, during the motion of the ortho-axis (which only moves after the azimuth is at its preset position), the ENTER key will not be illuminated; but it is still active. Pressing it will stop the motion of the ortho-axis and pressing it again will commence the motion of the ortho-axis again. It will now remain lighted.

The LOAD function causes the manipulator axes to move to the azimuth and orthogonal positions defined in the Setup Menu. Select the function with the Cursor Knob. The ENTER key on the Keypad will then be illuminated. Press the ENTER key to invoke the function. The ENTER key will remain illuminated, indicating that it is still active. Pressing it while either manipulator axis is in motion will cause motion to cease. Pressing the ENTER key again will

cause motion to begin again. During the motion, the Cursor Knob will no longer affect the Cursor. This is a safety feature to insure that movement of the manipulator may be stopped quickly if desired. When the manipulator axes reach their respective preset positions, the alarm will beep four times.

The AZ TARG= (azimuth target) parameter is the desired position of the azimuth axis. This parameter is used in conjunction with the AZ SEEK function to move the manipulator to a new azimuth. Select the parameter with the Cursor Knob and key in the new desired value using the Keypad. As the keys are pressed, the corresponding digits will be pushed from right to left into the parameter display. If the azimuth target is set lower than −5 or higher than +365, no motion will occur when the AZ SEEK function is invoked.

The AZ SEEK (azimuth seek) function causes the manipulator azimuth axis to rotate to the position shown in the AZ TARG= parameter. Select the function with the Cursor Knob. The ENTER key on the Keypad will then be illuminated. Press the ENTER key to invoke the function. The ENTER key will remain illuminated, indicating that it is still active. Pressing it before the axis reaches the target azimuth will cause it to cease rotation. Pressing the ENTER key again will cause the axis to again commence rotation. During manipulator motion, the Cursor Knob will no longer affect the Cursor. This is a safety feature to insure that motion of the manipulator may be stopped quickly if desired. When the axis reaches the target azimuth, the alarm will beep twice.

The OR TARG= (orthogonal target) parameter is the desired position of the ortho-axis. This parameter is used in conjunction with the OR SEEK function to move the ortho-axis to a new position. Select the parameter with the Cursor Knob and key in the new desired value using the Keypad. As the keys are pressed, the corresponding digits will be pushed from right to left into the parameter display. If the orthogonal target is set lower than −125 or higher than +125, no motion will occur when the OR SEEK function is invoked.

The OR SEEK (orthogonal seek) function causes the ortho-axis to rotate to the position shown in the OR TARG= parameter. Select the function with the Cursor Knob. The ENTER key on the Keypad will then be illuminated. Press the ENTER key to invoke the function. The ENTER key will remain illuminated, indicating that it is still active. Pressing it before the ortho-axis reaches the target position will cause it to cease rotation. Pressing the ENTER key again will cause the ortho-axis to again commence rotation. During ortho-axis motion, the Cursor Knob will no longer affect the Cursor. This is a safety feature to insure that rotation of the manipulator may be stopped quickly if desired. When the ortho-axis reaches the target orientation, the alarm will beep twice.

The MANUAL-AZ/OR function allows the operator to directly control the movement of the manipulator by means of the Positioner Knob (also known as the Cursor Knob). It is a dual function that transfers control of either the azimuth axis or the ortho-axis orientation to the Positioner Knob When one of these parameters is selected, the ENTER key on the Keypad will be illuminated. Pressing the ENTER key will then place the Positioner Knob in control of the parameter. The ENTER key will remain illuminated, and when pressed again will remove control

of the selected parameter from the Positioner Knob; then the Knob again becomes the Cursor Knob, controlling the position of the Cursor.

When this function is invoked, rotating the Positioner Knob does not directly control the position of the selected axis. Rather, rotating the Knob fills a buffer which empties as the selected axis rotates. It may thus be noticeable that the selected axis continues to rotate for a short time after the operator ceases to rotate the Knob.

1. To manually control the azimuth of the manipulator, select "AZ" with the Cursor Knob and press the ENTER key on the Keypad. The Knob is now the Positioner Knob and controls the position of the azimuth axis of the manipulator. Rotating the Positioner Knob clockwise causes the azimuth axis to rotate clockwise, and rotating the Positioner Knob counter-clockwise causes the azimuth axis to rotate counter-clockwise. To relinquish manual control of the azimuth axis, press the ENTER key again.

2. To manually control the position of the ortho-axis, select "OR" with the Cursor Knob and press the ENTER key on the Keypad. The Knob is now the Positioner Knob and controls the position of the ortho-axis. Rotating the Positioner Knob clockwise causes the ortho-axis to rotate towards larger angles (clockwise), and rotating the Positioner Knob counter-clockwise causes the ortho-axis to rotate towards smaller angles (counter-clockwise). To relinquish manual control of the ortho-axis, press the ENTER key again.

The ZERO function causes the manipulator to perform the following movements in both axes, starting with the ortho-axis and ending with the azimuth-axis. First, the axis will move CCW until it reaches its hard or mechanical limit. Then, it will move CW until it reaches the physical zero position of the encoder. Finally, it will return to logical zero. When both azimuth and orientation motions have been completed, there will be four beeps to indicate that the function has been completed, if the Alarm is on. Select the function with the Cursor Knob. The ENTER key on the Keypad will then be illuminated. Press the ENTER key to invoke the function. The ENTER key will remain illuminated, indicating that it is still active. Pressing it during the motions will cause the motions to stop. Pressing the ENTER key again will restart the motions. During the motions, the Cursor Knob will no longer affect the Cursor. This is a safety feature to insure that motion may be stopped quickly if desired. When both axes reach their preset zero positions, the alarm will beep four times.

Setup Menu. The Setup Menu contains parameters that will either directly affect the user interface of the instrument or will globally apply to each axis of the manipulator.The Setup Menu is entered and exited by simultaneously pressing the two keys on the Keypad labeled "SETUP" (the "1" and "3" keys). This menu is illustrated in Figure 12 which shows the preset limits for both the azimuth (±AZ) and the orthogonal (±OR) axes, the CURSOR RATE, the GPIB address (LISTEN ADDR), and controls for the panel light (PANEL-LIGHT), the alarm (ALARM), load (SET LOAD) and zero (SET ZERO) positions. The modification of each of these parameters is detailed individually below. All modified settings are stored in non-volatile memory so they will be remembered until they are again changed, even through power-cycling of the instrument. To

the "2", "4", and "6" keys on the Keypad. The positional arguments for the azimuth and orthogonal parameters, including those used in the load and zero positions, must be within the range of ±999; this range is further limited by each application as explained below. The Setup Menu cannot be exited if anything is wrong with any of the parameters.

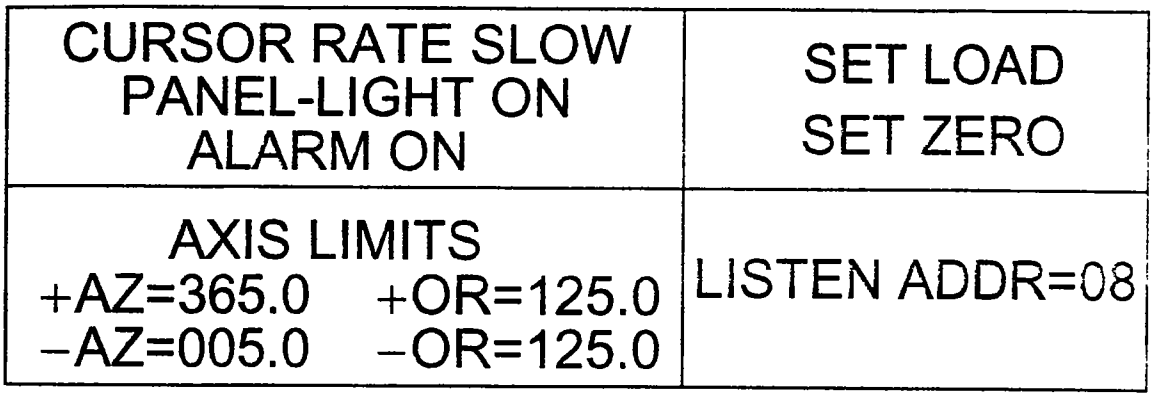

Figure 12. Setup Menu Layout

The +AZ= (azimuth upper limit) parameter defines a programmable clockwise limit of travel (in degrees). This value may not exceed +999 and may not be set lower than the value of the counter-clockwise limit. The default setting is +365, which is also the mechanical limit of clockwise azimuth axis rotation. Even if this parameter is set higher, rotation will stop at +365. Select this parameter with the Cursor Knob and key in the new desired value using the Keypad. As the keys are pressed, the corresponding digits will be pushed from right to left into the parameter display (pressing the ENTER key is not required).

The −AZ= (azimuth lower limit) parameter defines a programmable counter-clockwise limit of travel (in degrees). This value may not be less than −999 and may not be set higher than the value of the clockwise limit. The default setting is −5, which is also the mechanical limit of counter-clockwise azimuth axis rotation. Even if this parameter is set lower, rotation will stop at −5. Select this parameter with the Cursor Knob and key in the new desired value using the Keypad. As the keys are pressed, the corresponding digits will be pushed from right to left into the parameter display.

The +OR= (orthogonal upper limit) parameter defines a programmable upper limit of ortho-axis rotation which is independent of the mechanical limits set at the motor base. This is a "soft" limit which has a maximum value of +999, but the ortho-axis cannot travel above the mechanical limit which is set at +125. It must be set higher than the Orthogonal Lower Limit (−OR=). Even if this parameter is set higher, rotation will stop at +125. Select this parameter with the Cursor Knob and key in the new desired value using the Keypad. As the keys are pressed, the corresponding digits will be pushed from right to left into the parameter display. The default setting is +125.

The −OR= (orthogonal lower limit) parameter defines a programmable lower limit of ortho-axis rotation which is independent of the mechanical limits set at the motor base. This is a "soft" limit which has a minimum value of −999, but the ortho-axis cannot the travel below the

"soft" limit which has a minimum value of –999, but the ortho-axis cannot the travel below the mechanical limit which is set at –125. It must be set lower than the Orthogonal Upper Limit (+OR=). Even if this parameter is set lower, rotation will stop at –125. Select this parameter with the Cursor Knob and key in the new desired value using the Keypad. As the keys are pressed, the corresponding digits will be pushed from right to left into the parameter display. The default setting is –125.

The CURSOR RATE parameter determines the speed with which the cursor will step through the menu items as the Cursor Knob is rotated. There are two settings for the CURSOR RATE, these are SLOW and FAST. To change the setting, select this parameter with the Cursor Knob, and then the setting may be toggled between SLOW and FAST using the "+/-" key on the Keypad. The default setting is SLOW.

The PANEL-LIGHT parameter determines whether or not the Parameter Display will be back lighted. The PANEL-LIGHT may be turned on or off by first selecting it with the Cursor Knob and then pressing the "+/-" key on the Keypad to toggle the setting between ON and OFF. The default setting is ON.

The Audio ALARM parameter determines whether or not the audio alarm will be active. This alarm is used to signal the operator in the event of illegal data entries or upon the manipulator axes reaching a desired value or preset limit. To turn the ALARM ON or OFF, first select it with the Cursor Knob and then press the "+/-" key on the Keypad. When ON the alarm beeps twice for a complete operation and thrice in the event of an illegal entry. The default setting is ON.

The SET LOAD parameter defines the positions which the manipulator axes take when the "LOAD" function is invoked. The default values for LOAD are 0° for both axis positions. To define the LOAD positions, take the following steps. First, position the ortho-axis and/or the azimuth axis where desired for the new LOAD definition using the controls in the Main Menu. Second, go to the Setup Menu, move the cursor to SET LOAD, and press ENTER on the Keypad. If the Alarm is on, there will be a beep to indicate that the new positioning has been saved in the LOAD function.

The SET ZERO parameter may be used by the operator to define the logical "zero" orientation of the manipulator. There are no default values for ZERO; the operator must expect to set both axis positions, although the EMCO installer normally sets them to 0°. To define logical ZERO, use the following procedure. First, position the manipulator orthogonal and azimuth axes in the desired ZERO positions using the controls in the Main Menu. Second, go to the Setup Menu, select SET ZERO, and press ENTER. The manipulator will perform the following movements in both axes, starting with the ortho-axis and ending with the azimuth axis. First, the axis will rotate CCW until it reaches its hard or mechanical limit. Then it will rotate CW until it reaches the physical zero position of the encoder. The controller records the position of the physical zero with respect to the logical zero and returns the axis to logical zero. When both azimuth and orthogonal zeros have been processed, there will be a beep, if the Alarm is on, to indicate that the function is completed. From then on, until they are redefined, the

Menu. Should either axis reach its CW (upper) hard limit, i.e., not find the physical zero of the encoder, it will stop and the alarm will beep three times to indicate that there was an error.

The LISTEN ADDRess parameter is the talker/listener address of the instrument when it is being operated in Remote Mode through the GPIB. To set the address, first select its present value with the Cursor Knob and then use the Keypad to enter the desired value. As the keys are pressed, the corresponding digits will be pushed from right to left into the parameter display. The range of usable addresses is 01 - 31 (address 00 is reserved for the bus controller). After changing the address, power to the Model 5390 must be cycled off and on to make the new address active. The default value is 08.

Model 5390 Remote Mode

The Model 5390 is automatically placed in the Remote Mode when it receives its talker/listener address over the GPIB. The operator may return the instrument to the Local Mode, when it is not locked out, by pressing the LOCAL key ("8") on the Keypad.

Remote Screen. In the Remote Mode, a unique screen, illustrated in Figure 13, is presented to the operator on the Parameter Display.

The Current Positions of both axes of the manipulator are presented in an area entitled CUR POS on the left side of the screen. The units for these values are degrees.

Command Queue. An unlabeled area just to the left of the center of the screen is reserved for a command queue. Displayed here is a list of the last five commands, plus any arguments, received by the Model 5390 over the GPIB. Each command is displayed in its parsed form with all characters in upper case and without additional spaces or illegal characters. A set of examples are shown in this space in Figure 13.

Address Detected Indicator. In the upper half of the screen, just to the right of center is an indicator to show if the instrument has received its talker/listener address. Normally, this area will display the words "ADDRESS NOT DETECTED" to indicate that the instrument has not been addressed as either a talker or a listener on the GPIB. The "NOT" will disappear whenever the instrument is addressed by the bus. Once a command is issued, the message remains "ADDRESS DETECTED" until the command "*RST" is issued, the unit is returned to "Local" and then back to "Remote." or power is cycled off and on.

Local Lock-Out Indicator. In the upper right-hand corner of the screen is an indicator of the status of Local Lock-Out. This indicator will display either "LOCAL LOCK-OUT ON" or "LOCAL LOCK-OUT OFF" according to the status of this function. If the GPIB controller has asserted Local Lock-Out, i.e., LOCAL LOCK-OUT ON, all front panel controls will be rendered inactive; *including the Return To Local key ("8") on the Keypad.*

GPIB Address Indicator. On the right half of the screen, just below center, is a display of the currently selected talker/listener address of the Model 5390 on the GPIB. It is shown as "LISTEN ADDR=nn". The two-digit address is displayed in decimal, e.g., 08 in Figure 13.

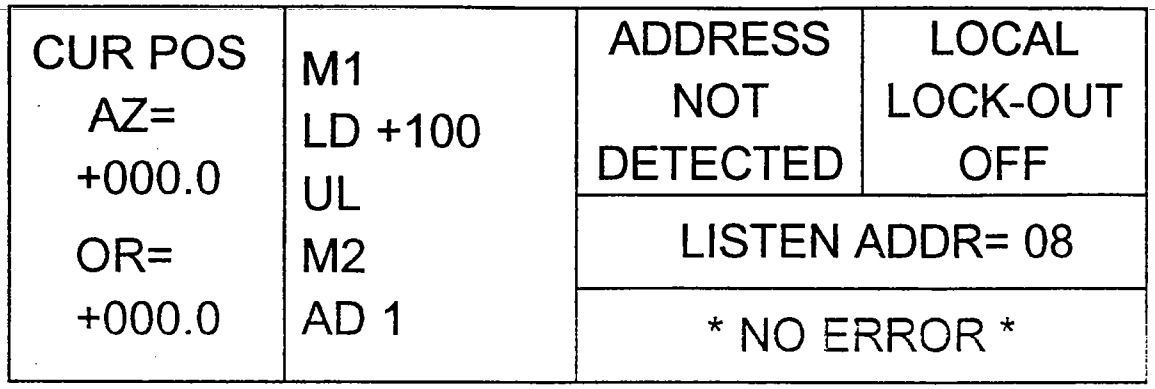

Figure 13. Remote Mode Display Layout

Error Reporting. In the lower right-hand corner of the screen, an area has been reserved for the reporting of errors occurring during GPIB data and command transfers. This area usually contains the message " * NO ERROR * ", but when an error occurs, this message will be replaced by the error message. See Appendix A at the back of this manual for an explanation of these messages.

Return To Local. If the Local Lock-Out is off, the LOCAL key ("8") on the Keypad will be illuminated, indicating that it is active. The operator may return the Model 5390 to the Local Mode by pressing this key. This will cause all motion to cease, the Parameter Display to blank briefly and then return with the Main Menu, and control of the instrument to revert to the front panel.

Programming Remote Operation. The Model 5390 recognizes two sets of commands. These are the Boss Manipulator (Device Unique) Command Set and the IEEE Std 488.2 Mandatory Command Set. For a better understanding of programming GPIB-operated equipment, read [12].

> Note
> All commands described below may be in either lower case, upper case, or a combination of both. It is recommended, although not required, to terminate each command (including its argument, if any) with the delimiter ";". A space is required between a command and any argument that might follow it.

The Boss Manipulator (Device-Unique) Command Set allows the programmer to access all of the features of the Boss Manipulator via the Model 5390. Each of the commands is listed in Table VII, along with a detailed description of its purpose and use. Thoroughly read this section and the section on Programming The Service Request before attempting to use the full range of features of the Model 5390 under GPIB control.

In several of the commands, a decimal argument ±nnn.n is required. The positive sign ("+") and leading zeros are optional. However, the decimal point and fractional part or a zero are required. That is, the argument may take the forms, 35.5, -135.0, +2.7, 054.7, etc.

When using one of the "P..." commands to move the manipulator to preset positions, the limits must be set so as to accommodate the positions required by the commands. If the motion target for an axis is outside the limits, the axis will not move. Also, since the azimuth axis always moves first, if it cannot move because of its target being outside the limits, the ortho-axis will also not move. For example, if "P6" is issued to move the azimuth axis to 135° and the ortho-axis to -120°, but the upper azimuth limit is set to 120°, no motion of either axis will occur.

Notes

During "preset" motion, do not query the position of the azimuth axis while the ortho-axis is moving. This will cause the ortho-axis to travel to its limit.

After the "ST" command is issued, the moving device will not restart motion until a new target command and a new movement command are issued.

Table VII.
Boss Manipulator (Device-Unique) Instruction Set

Mnemonic	Instruction	Description
"AL OFF"	Alarm Off	Turns the audible alarm off.
"AL ON"	Alarm On	Turns the audible alarm on.
"AZ LL?"	Query Azimuth Lower Limit	Issuing this command causes the instrument to respond with the current lower limit of the azimuth axis. The instrument will return a signed decimal value.
"AZ TG?"	Query Azimuth Target	Issuing this command causes the instrument to respond with the current azimuth target. The instrument will return a signed decimal value.
"AZ UL?"	Query Azimuth Upper Limit	Issuing this command causes the instrument to respond with the current upper limit of the azimuth axis. The instrument will return a signed decimal value.
"AZ?"	Query Current Azimuth	Issuing this command causes the instrument to respond with the current position of the azimuth axis. The instrument will return a signed decimal value. (See Table VIII for a programming example.)
"DS?"	Query Device Status	This command is used to determine the origin of a Service Request. Issuing this command causes the instrument to respond with the contents of the Device Status Register. The value returned is in decimal format in the range of 0 to 3. After conversion to binary format, Bit 0 will correspond to the azimuth axis and Bit 1 to the ortho-axis. A bit-value of 1 indicates the device is requesting service. *When this command is issued the register will be cleared upon response.* (For a detailed explanation of the Device Status Register and its function, see "Programming the Service Request" later in this manual.)
"LD AZ ±nnn.n LL" ("+" & leading zeros optional)	Set Azimuth Lower Limit	This command will change the current setting of the Lower (CCW) Limit of the azimuth. A decimal argument in the range of -5 to the value of the Upper Limit, but not greater than +365, is required.
"LD AZ ±nnn.n TG" ("+" & leading zeros optional)	Set Azimuth Target	This command sets the TARGET parameter for the azimuth. A decimal argument within ±999 is required, and must be in the range between the lower and upper active limits.

"LD AZ ±nnn.n UL" ("+" & leading zeros optional)	Set Upper Azimuth Limit	This command sets the upper limit for the azimuth. A decimal argument in the range from the Lower Limit, but not less than -5, to +365 is required. (See Table IX for a programming example.)
"LD OR ±nnn.n LL" ("+" & leading zeros optional)	Set Orthogonal Lower Limit	This command will change the current setting of the Lower (CCW) Limit of the ortho-axis. A decimal argument in the range of ±125 is required. It must be lower than the Upper Limit.
"LD OR ±nnn.n TG" ("+" & leading zeros optional)	Set Orthogonal Target	This command sets the TARGET parameter for the ortho-axis. A decimal argument within ±125 is required, and must be in the range between the lower and upper active limits.
"LD OR ±nnn.n UL" ("+" & leading zeros optional)	Set Upper Orthogonal Limit	This command sets the upper limit for the ortho-axis. A decimal argument in the range of ±125 is required. It must be higher than the Lower Limit.
"OR LL?"	Query Orthogonal Lower Limit	Issuing this command causes the instrument to respond with the current lower limit of the ortho-axis. The instrument will return a signed decimal value.
"OR TG?"	Query Orthogonal Target	Issuing this command causes the instrument to respond with the current ortho-axis target. The instrument will return a signed decimal value.
"OR UL?"	Query Orthogonal Upper Limit	Issuing this command causes the instrument to respond with the current upper limit of the ortho-axis. The instrument will return a signed decimal value.
"OR?"	Query Current Orthogonal Pos.	Issuing this command causes the instrument to respond with the current ortho-axis position.
"P1"	Move to Preset Position #1	Moves the azimuth axis to 45° and the ortho-axis to −120°.
"P2"	Move to Preset Position #2	Moves the azimuth axis to 45° and the ortho-axis to 0°.
"P3"	Move to Preset Position #3	Moves the azimuth axis to 45° and the ortho-axis to +120°.
"P4"	Move to Preset Position #4	Moves the azimuth axis to 135° and the ortho-axis to +120°.
"P5"	Move to Preset Position #5	Moves the azimuth axis to 135° and the ortho-axis to 0°.
"P6"	Move to Preset Position #6	Moves the azimuth axis to 135° and the ortho-axis to −120°.
"P7"	Move to Preset Position #7	Moves the azimuth axis to 225° and the ortho-axis to −120°.
"P8"	Move to Preset Position #8	Moves the azimuth axis to 225° and the ortho-axis to 0°.
"P9"	Move to Preset Position #9	Moves the azimuth axis to 225° and the ortho-axis to +120°.
"P10"	Move to Preset Position #10	Moves the azimuth axis to 315° and the ortho-axis to +120°.
"P11"	Move to Preset Position #11	Moves the azimuth axis to 315° and the ortho-axis to 0°.
"P12"	Move to Preset Position #12	Moves the azimuth axis to 315° and the ortho-axis to −120°.
"PLD"	Move to Preset Load Position	Moves both axes to their preset load positions.

"RTL"	Return to Local	This command will change the state of operation of the instrument from Remote Mode to Local Mode. Execution of this command will cause all motion to cease, the Parameter Display to blank briefly and then return with the Main Menu, and the control of the instrument to transfer to the front panel.
"SET LOAD"	Set Load Position	This command sets the LOAD position in the controller to the current position of the manipulator.
"SET ZERO"	Set Zero Position	This command sets the ZERO position in the controller to the current position of the manipulator.
"SK AZ"	Azimuth Seek	Issuing this command will cause the azimuth axis to commence seeking for its preset TARGET value. The TARGET parameter must be independently set prior to issuing the "SK AZ" command.
"SK OR"	Orthogonal Seek	Issuing this command will cause the ortho-axis to commence seeking for its preset TARGET value. The TARGET parameter must be independently set prior to issuing the "SK OR" command.
"ST"	Stop	This command causes immediate cessation of motion of all active devices.
"ZERO"	Move to Preset Zero Position	Moves the manipulator to the preset ZERO position.

Table VIII.
Programming Example for Query Lower (CCW) Azimuth Limit

```
10    ! no devices are currently active. this is not a requirement
20    ! of the AZ? command.
30    OUTPUT 708;"AZ?;"          ! ready the instrument to respond
40    ENTER 708;APOS             ! read the current azimuth
50    DISP APOS                  ! display the decimal value
```

Table IX.
Programming Example for Upper (CW) Azimuth Limit

```
10    OUTPUT 708;"LD AZ 250.0 UL;"      ! set upper (cw) limit to +250°
```

The IEEE Std 488.2 Mandatory Instruction Set provides standard instructions or commands that are needed in normal GPIB operation of the Model 5390 controller, and makes it compliant with the requirements of IEEE Std 488.2. Each of the instructions is listed in Table X, along with a detailed description of its purpose and use.

Several of the commands in this instruction set either return values in decimal format or need arguments in decimal format. The information being transferred by these decimal numbers makes sense only in binary format since it represents the bit values in an eight-bit binary byte. To interpret the decimal values returned, first convert them to binary format. In this result the least significant bit is Bit 0, the next least significant bit is Bit 1, etc. The information being transferred is contained in the bit values, 1 (set) or 0 (reset or cleared). The use of these bit-values will be explained in Programming the Service Request. Conversely, when forming a decimal argument to use with a function, set up an eight-bit byte, assign each bit a value of 1 or 0, as required to convey the information needed by the command, and convert the binary value to decimal.

Table X.
IEEE Std 488.2 Mandatory Instruction Set

Mnemonic	Instruction	Description
"*CLS"	Clear Status	This command will clear all Event Registers summarized in the Status Byte. (For a detailed explanation of the Status Byte and the Event Registers, see the discussion on "Programming the Service Request" later in this manual.)
"*ESE nnn"	Set the Standard Event Status Enable Register	This command allows the programmer to alter the contents of the Standard Event Status Enable Register. A decimal argument in the range of 0 to 255 is required. This argument, when expressed in binary form, directly represents the bit values of the Standard Event Status Enable Register. (For a detailed description of this register and its function, see the discussion on "Programming the Service Request.")
"*ESE?" (Note the similarity of this command to "*ESR?")	Query the Standard Event Status Enable Register	This command causes the instrument to respond with the contents of the Standard Event Status Enable Register. The response will be a signed decimal number in the range of 0 to +255. This value, when expressed in binary form, directly represents the bit values of the Standard Event Status Enable Register. (For a detailed description of this register and its function, see the discussion on "Programming the Service Request.")
"*ESR?" (Note the similarity of this command to "*ESE?")	Query the Standard Event Status Register	This command causes the instrument to respond with the contents of the Standard Event Status Register. The response will be a signed decimal number in the range of 0 to +255. This value, when expressed in binary form, directly represents the bit values of the Standard Event Status Register. *NOTE: Upon reading this register, its contents will be cleared.* (For a detailed description of this register and its function, see the discussion on "Programming the Service Request.")
"*IDN?"	Identify.	This command offers the programmer the ability to determine the nature of the device located at a given address on the GPIB. Issuing this command causes the instrument to respond with an ASCII character string. The string that is sent, "EMCO,5390,2.9" uniquely identifies the instrument as the EMCO Model 5390 setup to operate the Boss Manipulator.
"*OPC"	Arm the Operation Complete Flag	Issuing this command will cause the instrument to set the Operation Complete bit of the Standard Event Status Register when any moving device has stopped. This command MUST be issued prior to issuing any movement command so that the flag will be set when the device ceases movement. (For a detailed description of this register and its function, see the discussion on "Programming the Service Request.")
"*OPC?"	Query the Operation Complete	Issuing this command will cause the instrument to respond with a single character message. If all moving devices have stopped, the message will be 1, if not it will be 0.
"*RST"	Reset	Issuing this command will initiate an instrument reset. This is similar to turning power to the instrument off and then back on, except that the instrument will remain in the remote mode and The state of the Status Register Data Structure will remain unchanged. However, all moving devices will be immediately stopped and the command queue will be cleared. (For a detailed description of this register and its function, see the discussion on "Programming the Service Request.")

"*SRE nnn"	Set the Service Request Enable Register	This command allows the programmer to alter the contents of the Service Request Enable Register. A decimal argument in the range of 0 to 255 is required. This argument, when expressed in binary form, directly represents the bit values of the Service Request Enable Register. (For a detailed description of this register and its function, see the discussion on "Programming the Service Request.")
"*SRE?"	Query the Service Request Enable Register	This command causes the instrument to respond with the contents of the Service Request Enable Register. The response will be a signed decimal number in the range of 0 to +255. This value, when expressed in binary form, directly represents the bit values of the Service Request Enable Register. (For a detailed description of this register and its function, see the discussion on "Programming the Service Request.")
"*STB?"	Query the Status Byte	This command causes the instrument to respond with the contents of the Status Byte. The response will be a signed decimal value in the range of 0 to +255. This value, when expressed in binary form, directly represents the bit values of the Status Byte. (For a detailed description of this register and its function, see the discussion on "Programming the Service Request.")
"*TST?"	Self Test	This command readies the instrument to respond with a byte indicative of the self-test result. Since the Model 5390 cannot test its internal circuits without destroying the non-volatile parameter values or with absolute certainty of the cause of any failure, the returned message will always be "0".
"*WAI"	Wait to Continue	Issuing this command will cause the instrument to place execution of the next command on hold while there are devices in motion. Once motion has ceased, the next command will be executed normally. Note that while a command is on hold additional commands will not be accepted. Normal operation will continue (the "*WAI" command will be released) after the command on hold has been executed. *The time-out option of the GPIB controller must be disabled before the execution of the "*WAI" command.*

Programming the Service Request (SRQ). The Service Request is a form of interrupt, used by instruments on the GPIB to inform the bus controller of changes in status or the existence of a problem. Once an instrument initiates a Service Request, the bus controller must serially poll all the instruments on the bus to determine the source of the interrupt. Each instrument responds to the serial poll with a Status Byte which indicates whether or not it is the originator of the Service Request. Once the bus controller finds the originator of the interrupt, it may further interrogate the instrument by reading the Status Register Data Structure elements to discern the exact nature of the request for service.

Each instrument incorporates a Status Register Data Structure. Elements of this structure are largely unique to the instrument, however there are several elements which are standard, as defined in IEEE Std 488.2. This data structure provides a means to record "events" and selectively determine if a certain type of "event" should initiate a Service Request. What follows is a discussion of this Status Register Data Structure as it exists in the Model 5390, and how the programmer may use it to properly generate Service Requests on the GPIB.

The Model 5390 may be programmed to initiate a service request upon occurrence of a selected condition. After the selected condition occurs and it initiates a request for service, the Model

5390 will *WAIT INDEFINITELY* for the bus controller to poll it. Upon completion of the poll by the bus controller, the Model 5390 will resume the normal operation state and will be ready to respond to inquiries from the bus controller about its Status Register Data Structure.

There are three types of registers in the Status Register Data Structure. All are eight-bit registers (bytes) with the bits numbered starting from the most significant bit (MSB) to the least significant bit (LSB) as follows: 7 6 5 4 3 2 1 0. The bit numbers also indicate the weight of each bit as a power of two when the binary value is being converted to another format, e.g., decimal. The decimal value equivalent to the eight-bit register filled with all ones is 255.

One of the three registers is the Status Byte, a special register, which is discussed in another paragraph below. The other two registers are, in general, "event" registers and "event enable" registers. These two always exist in pairs, because the "enable" register is a mask for the "event" register, that is, a bit in an "event" register is *logically anded* with its corresponding bit in the companion "event enable" register to make up an event message. If the bit in the "event enable" register is set to 1, the corresponding bit in the "event" register is said to be *enabled*. This term is used in the explanations of specific registers given below.

The Status Byte is a register whose contents form the response to a serial poll initiated by the bus controller. Contained within this register (byte) are two single bit summary messages, and one Master Summary Status (MSS) message. The function of each bit is shown in Table XI.

When the MSS bit (Bit 6) is set to 1 within the Model 5390, e.g., upon completion of an *enabled* event, the instrument will issue a Service Request. Upon receiving a Service Request, the bus controller will serially poll all instruments on the bus. In response to this poll, each instrument will, in turn, send its Status Byte. The bus controller will examine Bit 6 (MSS) of this Status Byte to determine if the associated instrument is requesting service.

Table XI. Status Register (Byte) Data Structure

Bit 0	Not used (reset to 0).
Bit 1	Not used (reset to 0).
Bit 2	Not used (reset to 0).
Bit 3	Not used (reset to 0).
Bit 4	Message Available (MAV). This bit will be set to 1 if there is a message in the instrument output queue. Since the Model 5390 always has a message waiting in the output queue, this bit is always set to 1.
Bit 5	Standard Event Status Summary bit (ESB). This bit will be set to 1 if any of the *enabled* events in the Standard Event Status register occur.
Bit 6	Master Summary Status (MSS). This bit will be set to 1 if any of the *enabled* bits of the Status Byte (Register) are set to 1.
Bit 7	Not used (reset to 0).

The Service Request Enable Register. This register is used in conjunction with the Status Byte (Register). If any bit within this register is set to 1, the corresponding bit of the Status Byte will be enabled and will thus contribute towards the MSS bit. For example, if Bit 5 of the Service Request Enable Register is set to 1, then the corresponding bit (ESB) of the Status Byte will be set to 1, the MSS bit will be set to 1, and a Service Request will be initiated. If the ESB had been

set to 1 but was not enabled because Bit 5 of the Service Request Enable Register was cleared (reset to 0), then the MSS would be cleared (reset to 0), and no Service Request initiated. Note that the bit of the Service Request Enable Register corresponding to the MSS (Bit 6) is not used in the calculation of the MSS.

The contents of this register may be changed using the "*SRE nnn" command, and queried using the "*SRE?" command.

The Standard Event Status Register. This register is a standard structure as defined in IEEE Std 488.2. The bit definition as implemented in the Model 5390 is shown in Table XII.

Table XII. Standard Event Status Register

Bit 0	Set to 1 if an Operation Complete message is initiated. (Op Comp Flag).
Bit 1	Not used (reset to 0).
Bit 2	Not used (reset to 0).
Bit 3	Set to 1 if an internal error occurs.
Bit 4	Set to 1 if an error results from a command execution.
Bit 5	Set to 1 if an illegal command is received.
Bit 6	Not used (reset to 0).
Bit 7	Set to 1 upon the initial power up.

Any enabled bits in this register (see The Standard Event Status Enable Register below) that are set to 1 will cause the Standard Event Status Bit (ESB) of the Status Byte to also be set to 1. In this way, lower level events, such as the detection of an illegal command, can be used to initiate Service Requests. In such an instance, the bus controller would read the Status Byte of the Model 5390 and detect that the MSS and ESB bits were set, indicating that service has been requested because of an event which is defined by the Standard Event Status Register. The bus controller may then query the contents of the Standard Event Status Register, find Bit 5 set and from this determine that an illegal command has been received by the instrument.

The contents of this register may be queried using the "*ESR?" command. *Note that this command will cause the register to be cleared after it is read.* The only other command that will affect the contents of this register is the "*CLS" command, which will clear the register, i.e., reset all bits to 0. The only way a bit within this register can be set to 1 is by detection, within the Model 5390, of an associated event.

The Standard Event Status Enable Register. Each bit of this register may be used to enable the corresponding bit of the Standard Event Status Register. In this way, bits within the Standard Event Status Register may be selectively used to calculate the state of the Standard Event Status Bit (ESB) of the Status Byte, and hence initiate a Service Request. The contents of this register may be altered using the "*ESE nnn" command, and may be queried using the "*ESE?" command.

The Device Status Register. This register contains information regarding the status of the ortho-axis and the azimuth axis. The two least significant bits each correspond to one of the two axes; bit 0 (least significant) corresponds to the azimuth axis, and bit 1 corresponds to the ortho-axis. Each of these bits will have a value of 0 until a device event occurs, i.e., a moving axis

ceases motion, at which time it will be set to 1. This register is used in conjunction with the Device Status Enable Register to determine whether or not an Operation Complete message should be initiated, i.e., setting the Operation Complete bit of the Standard Event Status Register to 1.

The bits in this register are reset to 0 upon one of two conditions: a) the instrument enters the remote mode; or, b) the bus controller issues the "DS?" command and queries the contents of this register. The contents of this register may not be set directly by the programmer, they may only be queried *and reset* using the "DS?" command.

The Device Status Enable Register. The contents of this register determine which of the two axes are to be considered in generating the Operation Complete message. Bit 0, the least significant, corresponds to the azimuth axis and Bit 1 corresponds to the ortho-axis. This register is set up in the firmware so that both axes are always enabled, i.e., both Bit 1 and Bit 2 are set to 1 signifying that both devices shall be considered when determining an Operation Complete condition. Note that an Operation Complete message will not be initiated until both of the axes have had an event, i.e., ceased motion. The contents of this register may not be altered or queried.

Table XIII on page 36 contains a short programming example which is included to clarify the operation and interaction of the registers within the Status Register Data Structure. Additionally, a method of handling a Service Request is shown.

REFERENCES

[1] ANSI C63.4-1992, *American National Standard for Methods of Measurement of Radio-Noise Emissions from Low-Voltage Electrical and Electronic Equipment in the Range of 9 kHz to 40 GHz.*

[2] J. D. M. Osburn, T. E. Harrington and F. Sepulveda, "A Preliminary Evaluation of the Effect of a Dielectric WB TEM Cell Manipulator on Radiated Emissions Test Results," *Electromagnetic Compatibility*, Conference Pub., 396, IEE Ninth International Conference, Manchester, UK, 5 - 7 Sep., 1994, pp. 34-39.

[3] IEEE Std 488.1-1987, *IEEE Standard Digital Interface for Programmable Instrumentation* (ANSI).

[4] IEEE Std 488.2-1992, *IEEE Standard Codes, Formats, Protocols, and Common Commands for Use with IEEE Std 488.1-1987* (ANSI).

[5] EIA RS-414-A-1975, *Simulated Shipping Tests for Consumer Electronic Products and Electronic Components.* (Rescinded; informational only.)

[6] EMCO PN 399169, Rev A, *Model 5300 Series Gigahertz Transverse Electromagnetic (GTEM!™) Cell Operation Manual,* The Electro-Mechanics Company, 1991, pp. 22-37.

[7] D. Hansen, P. Wilson, D. Königstein and H. Garbe, "Emission and Susceptibility Testing in a Tapered TEM Cell," *Proc. 8th Int'l. Zürich Symp. and Tech. Exh. on EMC,* March 1989, pp. 227-232.

[8] P. Wilson, D. Hansen and D. Koenigstein, "Simulating Open Area Test Site Emission Measurements Based on Data Obtained in a Novel Broadband TEM Cell," *IEEE 1989 National Symposium on Electromagnetic Compatibility Record,* 89CH2736-7, Denver, CO, May 23-25, 1989, pp. 171-177

[9] P. Wilson, "On Simulating OATS Near-Field Emission Measurements via GTEM Cell Measurements." *IEEE 1993 International Symposium on Electromagnetic Compatibility Record,* 93CH3310-0, Dallas, TX, August 9-13, 1993, pp. 53-57.

[10] J. D. M. Osburn and E. L. Bronaugh, "Advances in GTEM to OATS Correlation Models," *IEEE 1993 International Symposium on Electromagnetic Compatibility Record,* 93CH3310-0, Dallas, TX, August 9-13, 1993, pp 95-98.

[11] J. Osburn and G. Watkins, "New Test Set-Up Challenges Indoor, Outdoor Options," *EMC Technology,* Vol. 9, No. 6, ICT, 6150 Finchingfield Road, Gainesville, VA 22065, May/June 1990, pp. 37-39.

[12] NI-488.2, MS-DOS Software Reference Manual, Part No. 320282-01, National Instruments, Austin, TX, Tel. 512-794-0100.

[13] J. D. M. Osburn and E. L. Bronaugh, "A Measurement and Calculation Procedure to Remove the 'Gain No Greater than a Dipole' Restriction in the GTEM - OATS Correlation Algorithm," *Proceedings, EMC 94-Barcelona,* 4th International Symposium and Exhibition Technical Normative on Electromagnetic Compatibility, Barcelona, Spain, October 4-6, 1994.

Table XIII.
Programming Example of Operation & Interaction Within the Status Register Data Structure and Handling a Service Request

```
005   REMOTE 708                                  !Place the 5395 in Remote Mode
010   !
015   ! Setup the 5390 to issue a Service Request each time the
020   ! azimuth axis or ortho-axis reaches its target position (ceases motion).
025   !
030   ! 1) Enable Devices to form the Operation Complete Message
035   ! 2) Enable the Operation Complete message to form the
040   !    Standard Event Status Bit summary message (ESB) and
045   ! 3) Enable the ESB to form the Master Summary message (MSS)
050   !    and hence generate a Service Request.
055   !
060   OUTPUT 708;"*ESE 1;"                        !Enable the Op. Comp. (bit 0=1)
070   OUTPUT 708;"*SRE 32;"                       !Enable the ESB (bit 5=1)
075   ! Enable the bus controller to recognize Service Request
080   ! interrupts, and define the interrupt handling subroutine.
085   ENABLE INTR 7                               !Enable SRQ interrupts
090   OUTPUT 708;"*OPC;"                          !Arm the Op. Comp. Flag
095   OUTPUT 708;"SK AZ;"                         !Send Dev. Dep. command
100   ON INTR 7 GOSUB 500                         !Define the interrupt handler
105   OUTPUT 708;"*OPC"                           !Arm the Op. Comp. Flag
110   OUTPUT 708;"SK OR;"                         !Send Dev. Dep. command
...   ...
...   ...
500   ! Upon receiving an interrupt, 1) poll the 5390 (read the Status
505   ! Byte) to determine if it is requesting service; 2) read the 5390
510   ! Status Register Data Structure to determine the nature of the
515   ! request (reading the structure also serves to clear all of the
520   ! registers).
525   !
530   SB=SPOLL(708)                               !Retrieve the Status Byte and
535   IF BIT(SB,6)=1 GOTO 545                     !determine if service is requested.
540   RETURN                                      !If not, return to program.
545   !
550   OUTPUT 708;"DS?;"                           !Query the Device Status Register
555   ENTER 708;DEV_STAT
560   OUTPUT 708;"*ESR?"                          !Query the Standard Event Status
565   ENTER 708;EVT_STAT                          !Register
570   IF BIT(EVT_STAT,0)=1 GOTO 580               !Verify the Op. Comp. bit is set.
575   RETURN                                      !If not, return to program.
580   IF BIT(DEV_STAT,0)=1 GOTO 595               !Verify azimuth axis or ortho-axis
585   IF BIT(DEV_STAT,1)=1 GOTO 595               !has completed operation.
590   RETURN                                      !If not, return to program.
595   !
600   ! Place the user specific measurement routine here ...
605   !
610   RETURN
```

SYSTEM BLOCK DIAGRAMS AND REFERENCE ASSEMBLY DRAWINGS

The following pages contain the Model 5390 and motor base block diagrams and the reference assembly drawings of the platform apparatus. These are provided for information to aid in understanding how the system operates. If repairs are needed, it is best to contact The Electro-Mechanics Company for help, where personnel who are intimately familiar with the system are available.

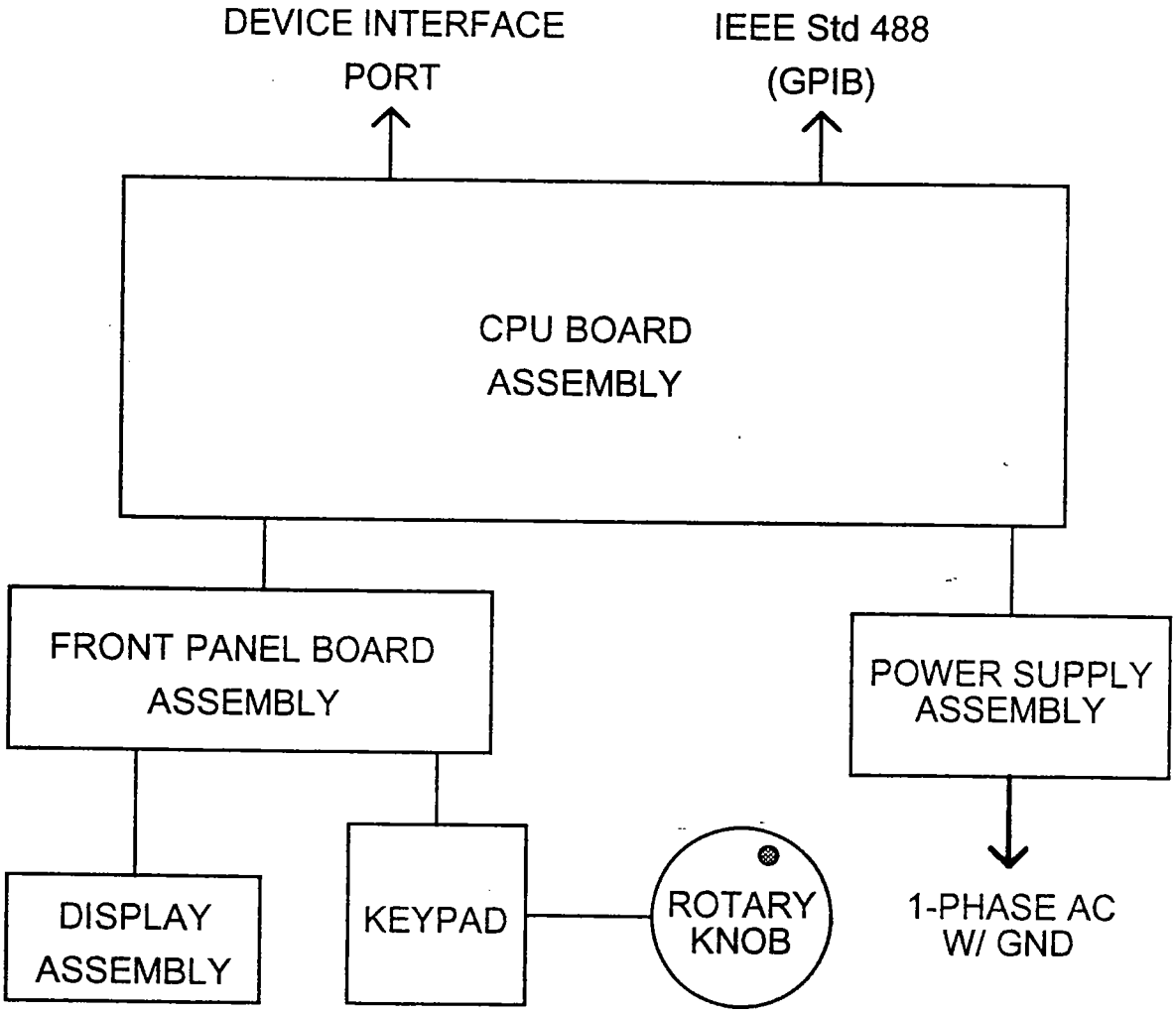

Figure 14. Model 5390 Positioning Controller Block Diagram.

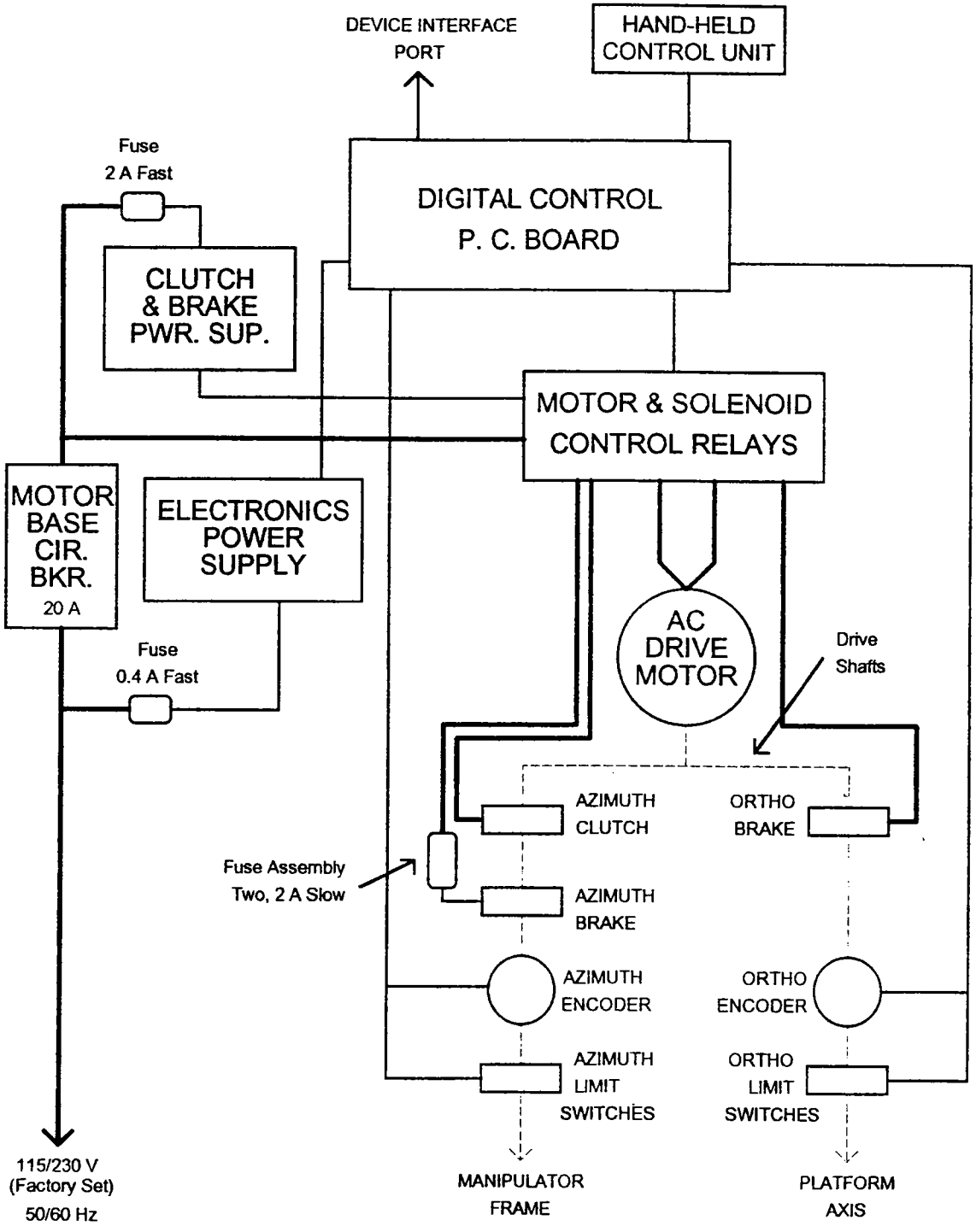

Figure 15. Boss Manipulator Electrical Block Diagram.

APPENDIX A

ERRORS AND ERROR CODES

Connection Errors

If controller power is turned on with the manipulator not connected, incorrectly connected, or without AC power, a two-line error message will appear on the Parameter Display screen instead of the Main Menu. The message is as follows:

"NO RECOGNIZABLE DEVICE PRESENT
CONNECT AND PRESS ENTER FOR RESTART".

This message is displayed if no device (manipulator) is connected or if AC power is not applied to the motor base.

> NOTE
> While the second line of the message suggests leaving the power on while correcting the connection problem, it is better to turn the power off while making any connections. Making connections with the power on, i.e., "hot" connections, can cause transients which might damage the instrument.

Remote Operation Errors

If an error occurs during Remote Operation of the controller, one of the following error messages will appear in the lower right-hand corner of the Parameter Display screen.

1. "BAD or MISSING ARG"; or,
2. "ILLEGAL COMMAND".

These messages will appear in place of " * NO ERROR * " on the Remote Screen. If a command requires a decimal argument, error message 1 will appear if the argument is missing, has too large a number, or contains characters which are not numbers; the argument must lie within the range from 0 to 255 and may be prefixed by a "plus" (+) sign. If a command is sent which is not in the lists in Table VII or Table X, that is, a command which the Model 5390 does not recognize, error message 2 will appear. The error message will continue to be displayed until the third correct command is issued after the one which caused the error.

APPENDIX B

SELECTED PAPERS

The papers listed below on the following selected topics are provided for the convenience of the Boss Manipulator™ user. The papers start after page 45 at the end of this manual.

Perturbing Effects of Manipulator Platform Apparatus

J. D. M. Osburn, T. E. Harrington and F. Sepulveda, "A Preliminary Evaluation of the Effect of a Dielectric WB TEM Cell Manipulator on Radiated Emissions Test Results," *Electromagnetic Compatibility*, Conference Pub., 396, IEE Ninth International Conference, Manchester, UK, 5 - 7 Sep., 1994, pp. 34-39.

Basic Far-Field 3-Measurement, 3-Input Correlation

P. Wilson, D. Hansen and D. Koenigstein, "Simulating Open Area Test Site Emission Measurements Based on Data Obtained in a Novel Broadband TEM Cell," *IEEE 1989 National Symposium on Electromagnetic Compatibility Record,* 89CH2736-7, Denver, CO, May 23-25, 1989, pp. 171-177.

Near-Field 9-Measurement, 9-Input Correlation

P. Wilson, "On Simulating OATS Near-Field Emission Measurements via GTEM Cell Measurements." *IEEE 1993 International Symposium on Electromagnetic Compatibility Record,* 93CH3310-0, Dallas, TX, August 9-13, 1993, pp. 53-57.

Special Measurements for Gain Greater than Dipole and EUT Pattern Estimation

1. J. D. M. Osburn and E. L. Bronaugh, "A Measurement and Calculation Procedure to Remove the 'Gain No Greater than a Dipole' Restriction in the GTEM-OATS Correlation Algorithm," *Proceedings, EMC 94-Barcelona,* 4th International Symposium and Exhibition Technical Normative on Electromagnetic Compatibility, Barcelona, Spain, October 4-6, 1994.

2. J. D. M. Osburn and E. L. Bronaugh, "Advances in GTEM to OATS Correlation Models," *IEEE 1993 International Symposium on Electromagnetic Compatibility Record,* 93CH3310-0, Dallas, TX, August 9-13, 1993, pp 95-98.

[Permission to reprint these papers has been requested.]

APPENDIX C

MANIPULATOR PRESET POSITIONS

The figures in this appendix show the position of the manipulator and EUT for the 12 preset positions listed in Table IV. They are inclusive of the preset positions used in both emissions and immunity measurements. In each figure, the preset position number is given as well as the EUT face and its polarization facing the apex of the GTEM!. Each row of preset positions from Table IV occupies one page in this appendix.

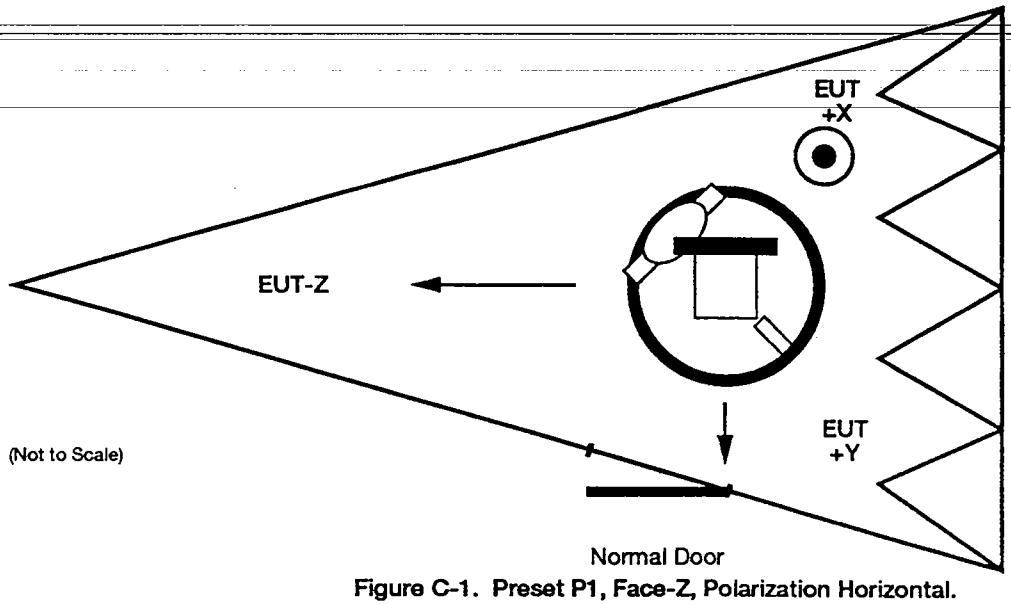

Figure C-1. Preset P1, Face-Z, Polarization Horizontal.

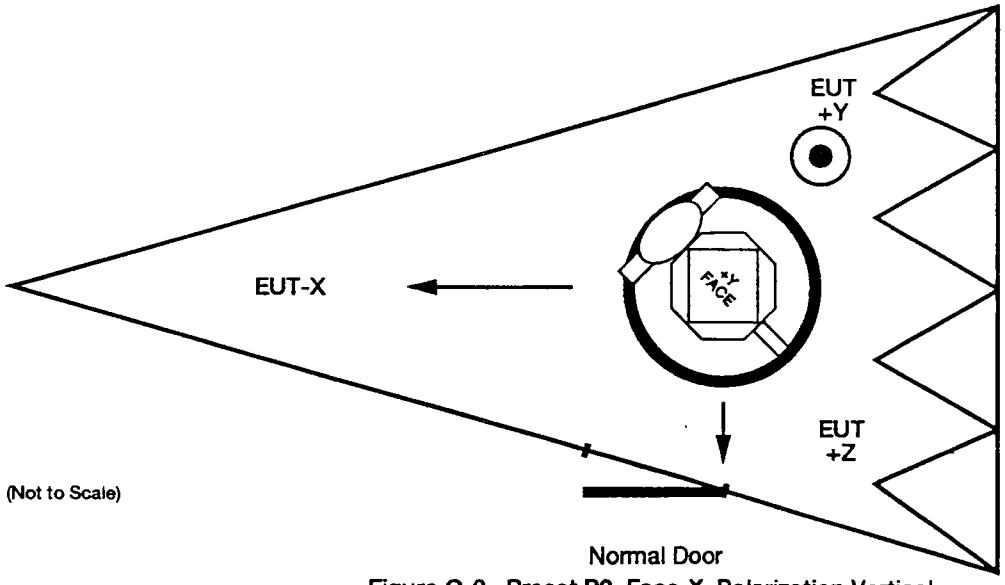

Figure C-2. Preset P2, Face-X, Polarization Vertical.

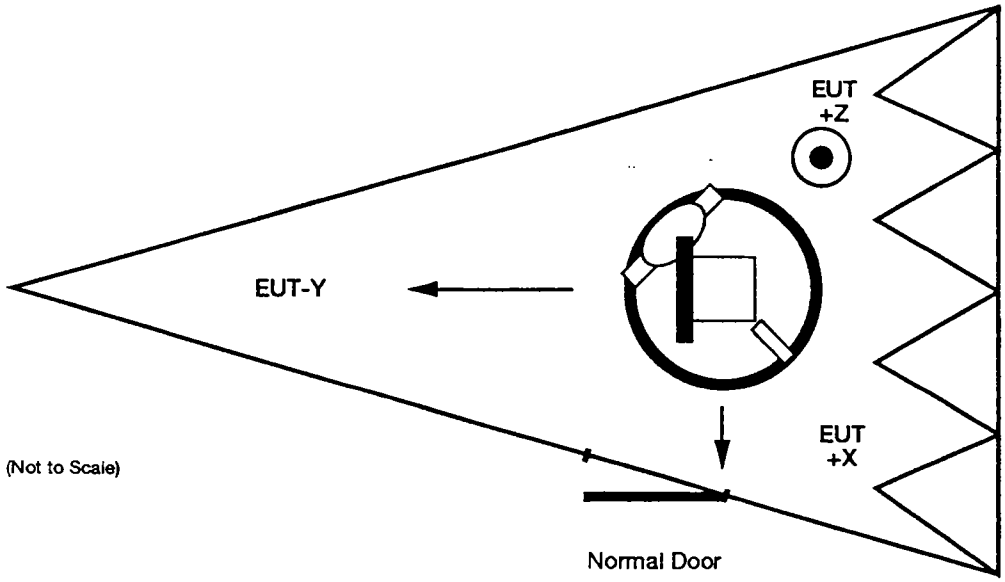

Figure C-3. Preset P3, Face-Y, Polarization Horizontal.

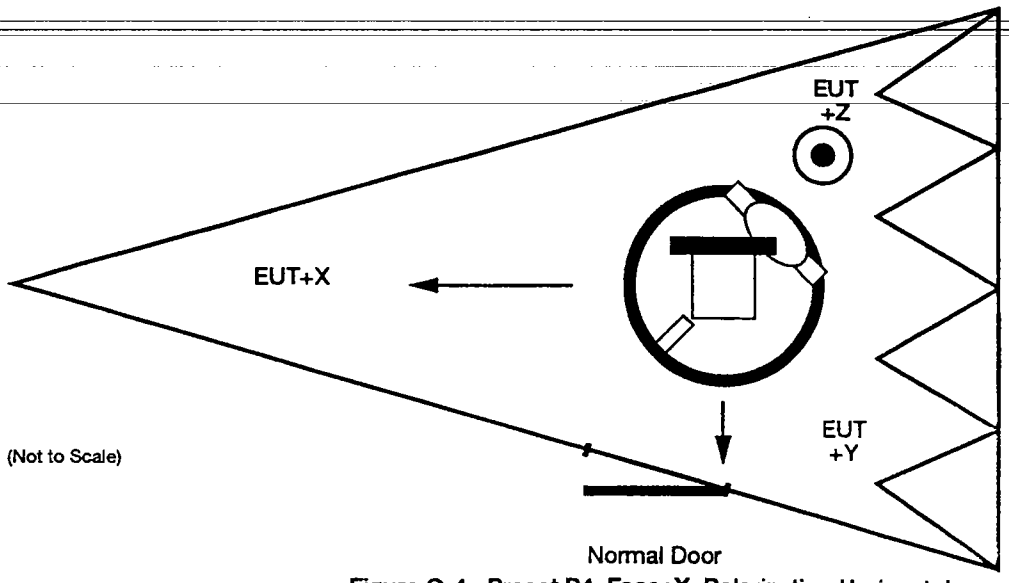

Figure C-4. Preset P4, Face+X, Polarization Horizontal.

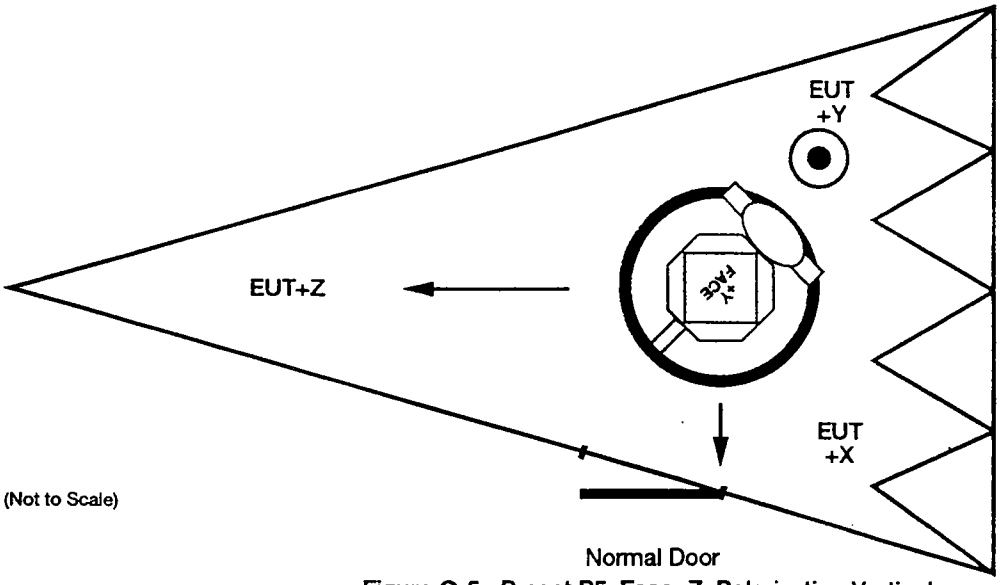

Figure C-5. Preset P5, Face+Z, Polarization Vertical.

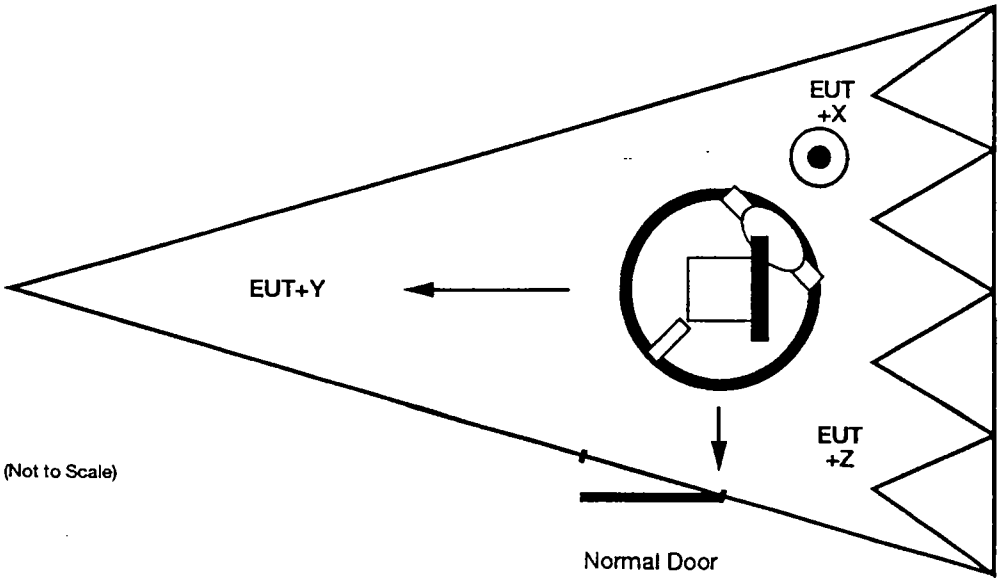

Figure C-6. Preset P6, Face+Y, Polarization Vertical.

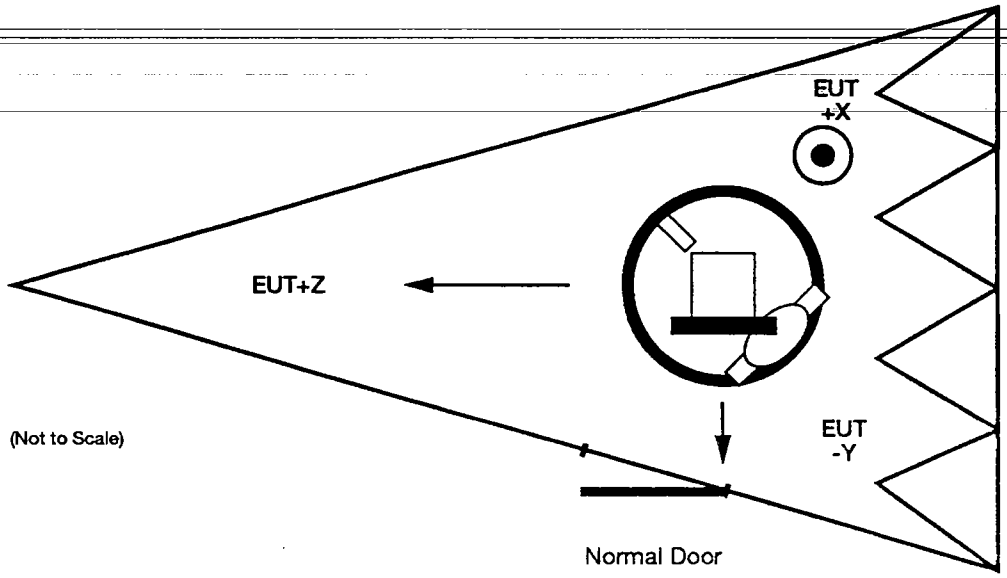

Figure C-7. Preset P7, Face+Z, Polarization Horizontal.

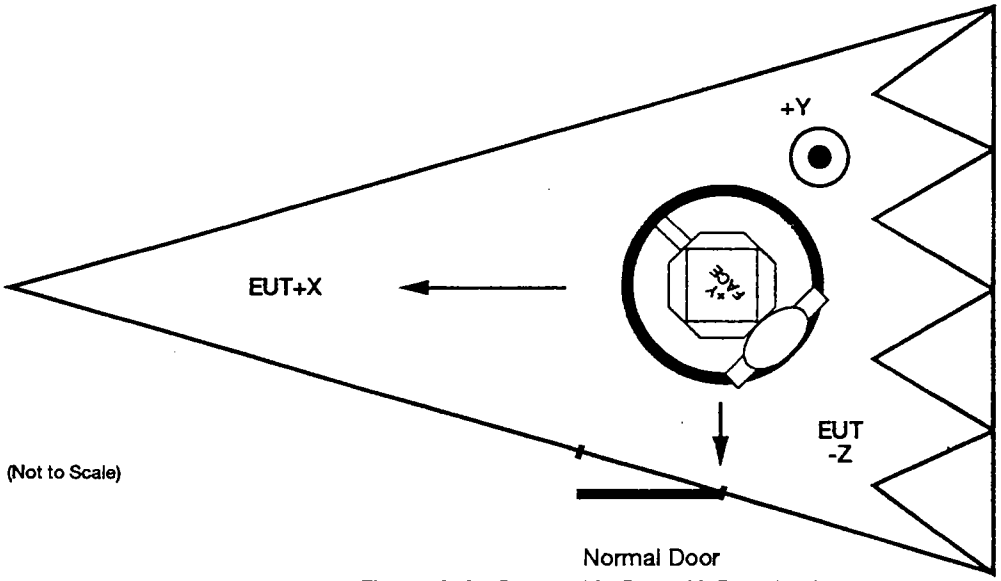

Figure C-8. Preset P8, Face+X, Polarization Vertical.

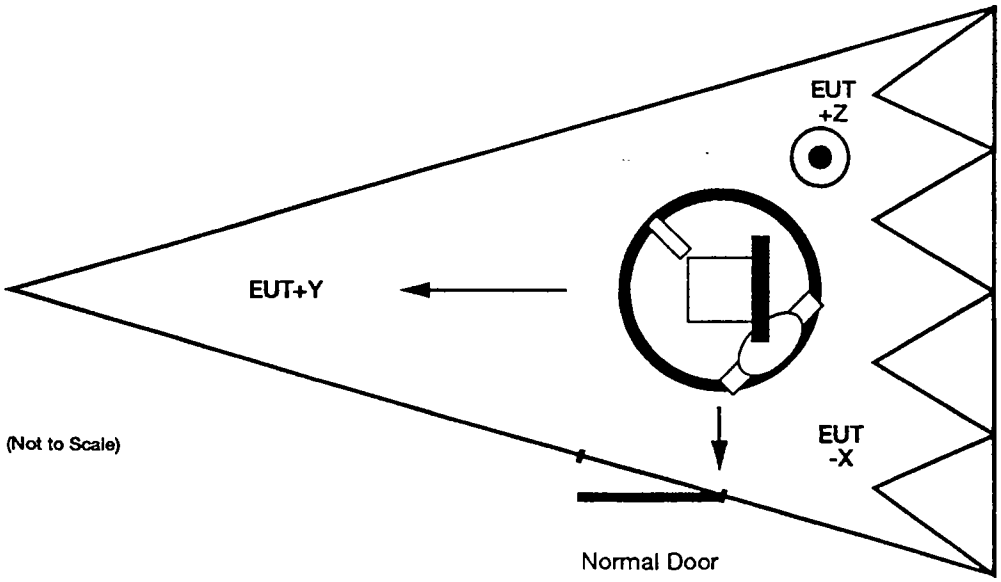

Figure C-9. Preset P9, Face+Y, Polarization Horizontal.

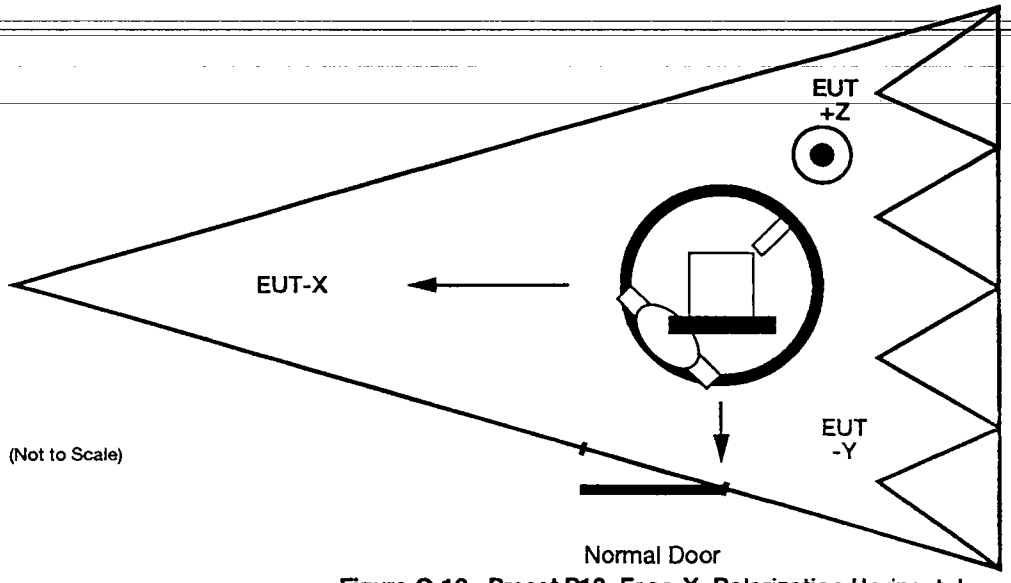

Figure C-10. Preset P10, Face-X, Polarization Horizontal.

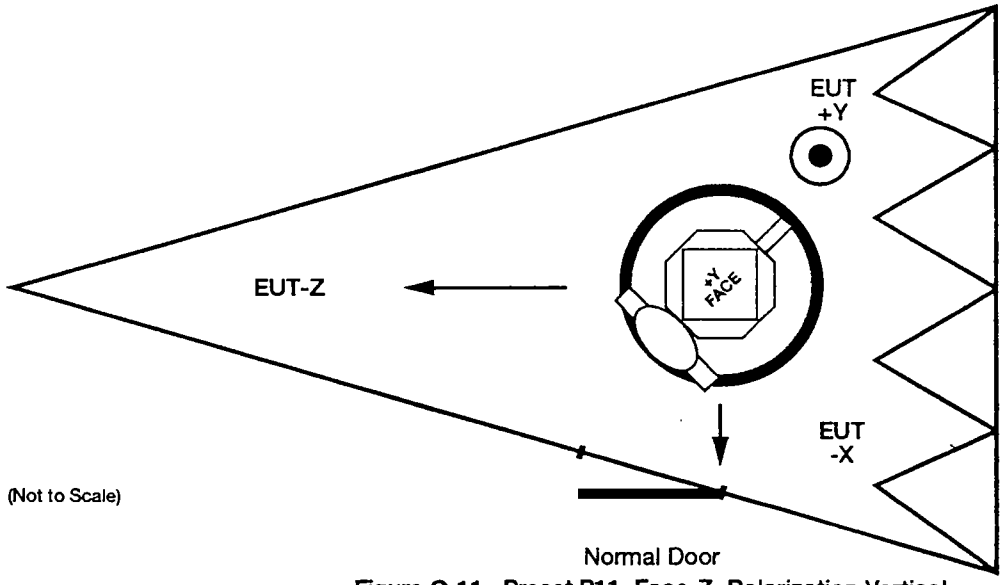

Figure C-11. Preset P11, Face-Z, Polarization Vertical.

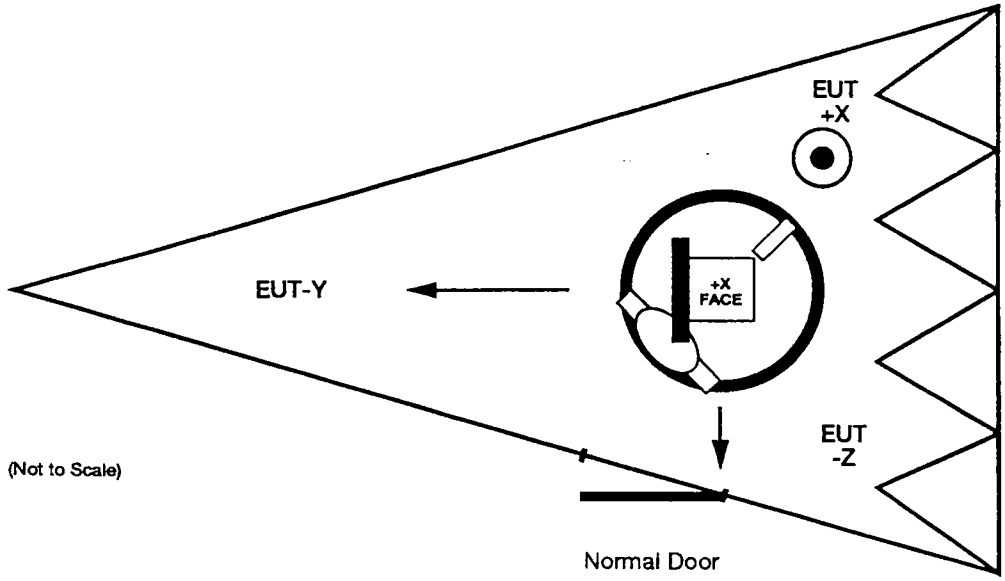

Figure C-12. Preset P12, Face-Y, Polarization Vertical.

A PRELIMINARY EVALUATION OF THE EFFECT OF A DIELECTRIC WB TEM CELL MANIPULATOR ON RADIATED EMISSIONS TEST RESULTS

J D M Osburn, T E Harrington and F Sepulveda

The Electro-Mechanics Company, USA

INTRODUCTION

The recent action by the Federal Communications Commission of the United States, allowing WB TEM radiated cell data to be submitted for type certification measurements, places renewed emphasis on full automation and rapid conduct of these measurements [1]. To allow full automation of radiated emissions testing, an equipment under test (EUT) manipulator has been constructed from dielectric materials, to minimize the interaction of electromagnetic signals originating in the EUT with the manipulator [2]. Since the presence of additional non-EUT materials in the test volume of the WB TEM Cell may interact with the coupling mechanism of the signals to be measured in the cell, it is desirable to evaluate the impact of such interaction of EUT fields with the manipulator. This paper describes preliminary evaluation of the impact of the presence of the dielectric manipulator on radiated emissions test results.

DISCUSSION

Radiated emissions measurements in a WB TEM Cell have historically been accomplished by manual re-orientation of the EUT in the test volume. The physical act of re-orienting the EUT in the test volume to satisfies the need for three orthogonal measurements, but interrupts measurements and precludes full automation of the measurement. To fully automate the radiated emissions measurement, including the re-positioning of the EUT between the three measurements required, an EUT manipulator was constructed from dielectric materials. The relative dielectric constant of the materials employed ranged from about 2.0 to 4.4, with a preference for lower relative dielectric constant materials, where possible. Great effort was made to reduce the presence of any metal component. Metal in the final design is limited to a 7 cm long by 2.5 cm dia drive shaft protruding through the floor of the WB TEM Cell, and two 10 mm dia by 4 cm long bolts. All other components are fabricated from dielectric materials. Use of this manipulator allows full automation of a radiated emissions measurement.

We speculate that the presence of the dielectric material in the test volume of the WB TEM Cell could render inaccurate radiated emissions measurements. Thus it was appropriate to examine the effect the manipulator will have on the accuracy of radiated emissions measurements.

The evaluation was made by performing comparative measurements on a single item using first, the manipulator and second, expanded polystyrene foam. The foam was that was used to position the EUT for the original measurements that showed acceptable correlation of the WB TEM Cell measurements to an open area test site (OATS) [3]. A direct comparison was made between the measurements with and without the manipulator.

PLANNING THE MEASUREMENT

Planning was conducted to provide the best data for the most reasonable comparison. The planning objectives and approach are discussed below.

Object of measurements

The object of the measurements was to provide data that allowing direct comparison of the radiated measurement results with and without the manipulator present, to determine if the manipulating device introduces significant error in the radiated emission measurement.

General Approach

The general approach chosen was to perform comparative measurements with a stable EUT that will allow direct comparison of the data obtained as a measure of the impact of the manipulating device on the overall accuracy of the test results.

Technical Approach

The general technical approach to these measurements is similar to the approach recommended by the ANSI C63 Committee for showing correlation between the WB TEM Cell and an OATS [4]. In general, a statistical approach is used. A set of three measurements was made under each condition, and the average of the three measurements was compared to determine if a significant difference exists under the two conditions.

The "Descriptive Statistics of the Differences" will be used to perform the comparison [5].The differences in the averages of the with and without manipulator E-field readings are used to compute the mean and standard deviation of the differences. These values are the same that are being used to determine acceptability of the particular WB TEM Cell installation for formal measurements for FCC submission.

The radiated emission measurements were performed using automated radiated emissions software [6]. This software allows export of data and correlated E-field values as an ASCII text file. The data was then imported into a spread sheet for calculations.

CONDUCT OF THE MEASUREMENT

Situation

The WB TEM Cell was presented for the initial measurements with the manipulator installed. Therefore, initial measurements were performed using the manipulator.

Test Equipment used and its limitations.

The test equipment used was that immediately available for the conduct of this testing.

Royce Site Source

A Royce Site source was used as the EUT [7]. It is essentially a 10 MHz comb generator with a $(\sin x)/x$ output stable over time. This output is modified by the transmission characteristic of a monopole transmitting antenna. It produces a usable E-field output to around 600 MHz. This device is normally used as an easily operated radiated emissions source to assure continued proper operation of an OATS, on a day-to-day basis.

HP 9590 Spectrum Analyzer

The measurement device was a spectrum analyzer [8]. The one employed had a usable frequency range of 10 kHz to 1.5 GHz, and ±1.5 dB absolute amplitude accuracy. However, it was capable of only modest (5 MHz + 1 % of span, about 0.97 MHz) frequency accuracy. This limitation required special handling of the data during analysis. In a 1 MHz resolution and video bandwidth, it displays about 30 - 35 dB μV input noise.

WB TEM Cell

The WB TEM Cell is of a standard design and was furnished for measurement with the EUT manipulator installed.

Manipulator

The EUT Manipulator, as installed is capable of handling an EUT 0.9 m diameter × 0.7 meters in height. It will handle a total EUT weight of 50 kg.

Testing

Testing was performed as follows:

- Three sets of automated radiated emissions measurements were made using the manipulator to position the EUT for measurements.
- The manipulator was removed.
- Three sets of automated radiated emissions measurements were made using expanded polystyrene foam blocks to position the EUT for measurements.

At the conclusion of all measurements, the data from all six measurement sets was exported from the measurement control software as ASCII files, to enable further analysis.

DATA ANALYSIS

At the conclusion of testing, all data was imported into a spreadsheet as a function of frequency. The extraneous data, recorded as a result of the frequency uncertainty of the measuring instrument, and the noise values, were deleted leaving the E-field data from the six measurements as a function of the measured frequency, as shown in Table I. Also in the Table are the computations performed to reach conclusions about the performance of the manipulator.

The computations performed are:

- Average the three sets of E-Field data from the measurements using the manipulator
- Average the three sets of E-Field data from the measurements using the expanded polystyrene foam blocks
- Subtract the average of the "with manipulator" E-field readings from the average "without manipulator" E- field readings over the entire frequency range.
- Compute the "Descriptive Statistics of the Differences", *i. e.*, the mean and standard deviation of the differences, over the frequency range.

RESULTS

A graphical presentation of the data are shown in Figures 1 and 2. Figure 1 shows a plot of the E-field Values as a function of frequency, with and without the manipulator in the WB TEM Cell. Figure 2 shows the differences in the E-field values with and without the manipulator, as a function of frequency.

As can be seen in Table I, the Descriptive Statistics of the Differences are:

$$\mu = 0.181$$

$$\sigma = 0.586$$

ANALYSIS OF THE RESULTS

Using Descriptive Statistics of the Differences as an indication, the mean and standard deviation of the differences of the E-field values appear to be small. The spectrum analyzer used for measurements is rated at an absolute difference of ± 1.5 dB. This may be interpreted to strongly suggest that the standard deviation of the amplitude measurement could be about 1/3 of those value, or 0.5 dB.

Thus, an ideal amplitude measurement comparison would give a mean difference of 0 dB and a standard deviation of 0.5 dB. Thus, the values computed from the differences of the two E-field measurements are not significantly larger than the ideal values. These differences are a fraction of those found in OATS to WB TEM Cell comparison tests [3,4,5].

CONCLUSIONS

The following conclusions may be drawn from the results of the comparative testing:

- The measured radiated emissions values do not appear to change significantly, over the frequency range measured, whether the manipulator is present or not.
- This set of data showed closer agreement over the lower portion of the frequency range measured. It also seemed to show a possible bias, to measure lower values with the manipulator present, as frequencies increased.

Table I. Comparison Data and Computations

Frequency	Without Manipulator #1	Without Manipulator #2	Without Manipulator #3	Average without Manipulator	With Manipulator #1	With Manipulator #2	With Manipulator #3	Average with Manipulator	Difference in Averages
MHz	dB uV/m	dB uV/m	dB uV/m	dB	dB uV/m	dB uV/m	dB uV/m	dB	dB
45.00	36.36	36.95	36.07	36.46	36.28	36.44	36.29	36.34	0.12
55.00	38.23	38.7	39.05	38.66	38.05	38.53	38.08	38.22	0.44
65.00	39.35	39.85	40.07	39.76	40.00	40.19	40.38	40.19	-0.43
75.00	42.01	42.35	41.92	42.09	41.44	41.96	41.84	41.75	0.35
85.00	44.18	41.92	42.81	42.97	42.98	43.58	43.30	43.29	-0.32
95.00	44.25	44.96	44.46	44.56	43.62	43.84	44.18	43.88	0.68
105.00	45.40	46.07	46.82	46.10	45.76	45.79	46.08	45.88	0.22
115.00	45.40	46.07	46.82	46.10	45.76	45.79	46.08	45.88	0.22
125.00	52.23	52.32	52.38	52.31	52.23	52.91	53.05	52.73	-0.42
135.00	54.19	53.94	54.33	54.15	55.22	54.30	54.60	54.71	-0.55
145.00	54.31	54.22	53.89	54.14	54.66	54.50	54.39	54.52	-0.38
155.00	54.09	53.59	53.41	53.70	54.68	54.10	54.53	54.44	-0.74
165.00	56.93	56.39	56.83	56.72	56.93	56.39	56.83	56.72	0.00
175.00	56.63	56.72	57.31	56.89	56.62	56.41	56.63	56.55	0.33
185.00	55.68	56.44	55.80	55.97	56.16	55.41	55.49	55.69	0.29
195.00	56.61	56.59	56.75	56.65	56.53	56.19	56.57	56.43	0.22
205.00	57.95	57.95	57.95	57.95	57.70	57.61	58.03	57.78	0.17
215.00	58.69	58.9	58.61	58.73	59.05	59.19	59.26	59.17	-0.43
225.00	60.22	60.25	60.17	60.21	60.22	59.36	59.64	59.74	0.47
235.00	60.65	60.59	60.91	60.72	60.85	60.97	61.17	61.00	-0.28
245.00	60.27	60.33	60.15	60.25	60.27	60.43	60.04	60.25	0.00
255.00	59.35	58.81	59.67	59.28	59.76	59.57	59.84	59.72	-0.45
265.00	59.92	59.98	59.93	59.94	60.86	61.08	60.83	60.92	-0.98
275.00	62.14	62.51	62.38	62.34	62.67	62.28	62.47	62.47	-0.13
285.00	62.34	62.63	62.35	62.44	61.11	61.26	61.24	61.20	1.24
295.00	61.46	62.07	62.03	61.85	60.47	60.22	62.00	61.90	-0.05
305.00	61.96	62.29	61.74	62.00	62.54	62.19	62.22	62.32	-0.32
315.00	63.92	64.18	63.68	63.93	63.69	63.70	63.70	63.70	0.23
325.00	62.20	64.34	64.19	63.58	63.88	64.02	63.75	63.88	-0.31
335.00	62.20	64.34	64.19	63.58	63.88	63.66	63.75	63.76	-0.19
345.00	65.03	64.78	64.68	64.83	64.34	64.50	64.12	64.32	0.51
355.00	64.92	64.89	64.55	64.79	63.95	63.73	63.63	63.77	1.02
365.00	64.65	64.09	64.31	64.35	63.82	64.49	64.06	64.12	0.23
375.00	61.78	61.84	62.00	61.87	61.15	60.81	61.62	61.19	0.68
385.00	63.18	62.84	63.21	63.08	61.57	62.07	62.43	62.02	1.05
395.00	63.71	63.79	64.11	63.87	62.65	62.57	62.84	62.69	1.18
415.00	62.56	62.99	63.19	62.91	62.11	61.66	61.93	61.90	1.01
425.00	62.20	61.5	62.15	61.95	60.39	60.58	60.73	60.57	1.38
435.00	59.60	59.94	59.98	59.84	59.18	58.06	59.35	58.86	0.98

Mean of Differences	0.1809
Standard Deviation of Differences	0.5856

Fig. 1 E-Field Data w/wo Manipulator

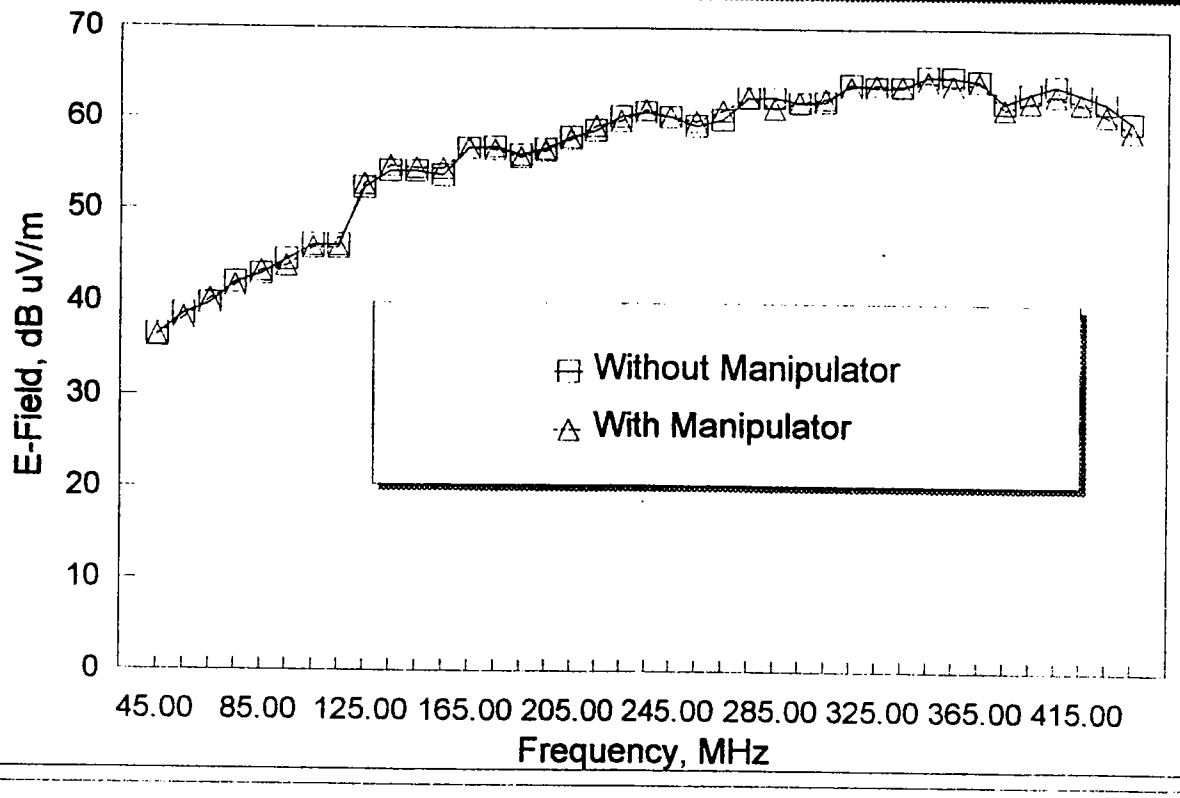

Fig. 2 Differences in Amplitude Data

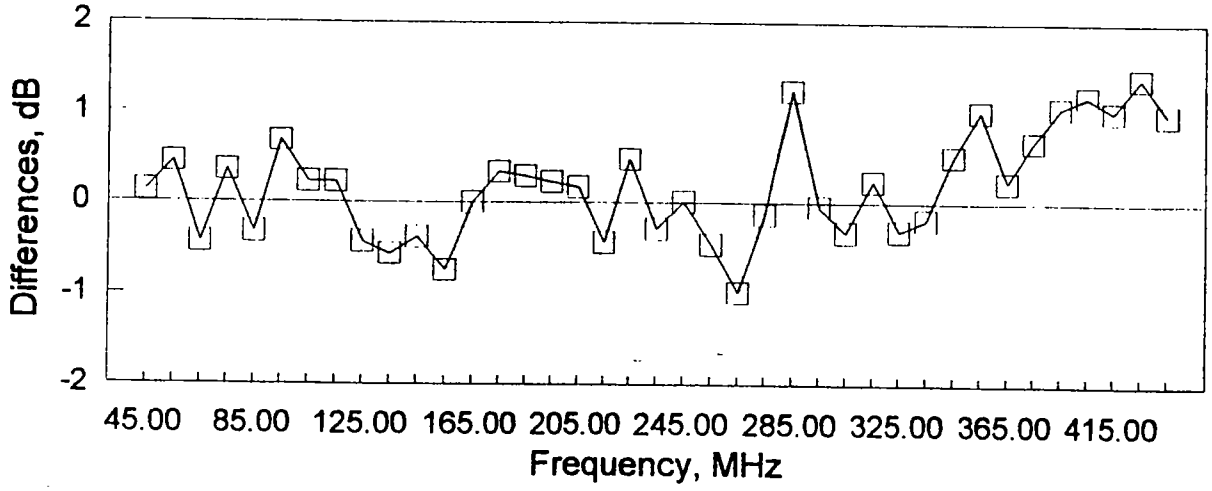

- Additional testing will be needed to completely quantify these differences over frequency.

- The values of the mean and standard deviation for the differences of the manipulator being present and not present are smaller (about 1/5 the values) than those found in a similar comparison of data between a GTEM and an OATS.

- The manipulator can be used without compromising the performance of the GTEM for radiated measurements, at least to frequencies of 500 or 600 MHz.

- It is likely that the WB TEM Cell can be used without any calibration or correction of the measured data to at least 1 GHz.

- If the manipulator does begin to cause inaccuracies in radiated emissions data, it is likely that the data will be due to dielectric losses, and thus can be corrected in the correlation algorithm.

RECOMMENDATIONS

The following recommendations are made to allow a final determination of the impact of a manipulating device in WB TEM Cell radiated emissions measurements.

- Conduct additional testing to assure the small values of the differences in the manipulator measurements hold up over frequency, to at least 1 GHz and preferably to 5 GHz (or even higher).

- Subsequent testing should be planned to employ instrumentation with improved accuracy.

- Subsequent testing should include a variability assessment of the EUT.

SUMMARY

This paper has described the technical issues, the measurements and the results of measurements directed to the determination of the potential error in radiated emissions measurements in a WB TEM Cell due to the presence of a dielectric material manipulator. The general result is that there appears to be no significant statistical difference in the measurements made with the manipulator present and absent.

REFERENCES

[1] FCC Public Notice, "FCC Will Accept GTEM Measurement Data Under Limited Conditions", Federal Communications Commission, 1919 M Street, N. W., Washington, D. C., *Federal Register* 40830, Dec. 2, 1993.

[2] EMCO Announcement, "The BOSS Manipulator", March 1994.

[3] Bronaugh, E. and Osburn, J. D. M, "Radiated Emissions Test Performance of the GHz TEM Cell", Symposium Record, *1991 International Symposium on Electromagnetic Compatibility*, 91CH3044-5, Cherry Hill, New Jersey, August 12-16, 1991, pp. 1 - 8.

[4] ANSI C63/SC1/TG 1-15.1 "Response to FCC Rulemaking Proposal Regarding Acceptability of GTEM Measurements", Project 1-15.1, TEM Device Measurements, ANSI ASC C63 SC-1, 8 August 1993.

[5] EMCO Application Note, "*GTEM! to OATS Correlation Testing to Allow Use of a GTEM! for FCC Type Certification Measurements*", The Electro-Mechanics Company, 2205 Kramer Lane, Austin, Texas, March 24, 1994.

[6] GTEM! Emission Software for HP 8566/68 HP 70000 Series Spectrum Analyzers, Version 3.0, Rev. 1.0, EMC Automation, August 17, 1992.

[7] EMCO Catalog, *Antennas & Accessories for EMC Testing*, The Electro-Mechanics Company, 2205 Kramer Lane, Austin, Texas, 1993, p 57.

[8] Hewlett Packard, *Test and Measurement Catalog*, Published by the Test and Measurement Sector, Santa Clara CA, 1994.

ADVANCES IN GTEM TO OATS CORRELATION MODELS

John D. M. Osburn and Edwin L. Bronaugh
The Electro-Mechanics Company
P. O. Box 1546
Austin, Texas 78767

ABSTRACT

The addition of a GTEM to OATS radiated emissions correlation algorithm to a GTEM allows performance of radiated emissions testing, equivalent to that conducted at an OATS, in the GTEM [1]. The original correlation model and the computational algorithm based on this model accurately addressed the measurement of radiated emissions to commercial standards, over the frequency range of 30 MHz to 1 GHz [2]. This paper examines new additions and expansions to the original model and algorithm. New additions include measurements to telecommunications specifications, measurements from 9 kHz to 30 MHz for electric and magnetic field measurements and measurements to MIL-STD requirements and measurements above 1 GHz.

INTRODUCTION

The Gigahertz Transverse Electromagnetic (GTEM) cell was originally developed to generate intense electromagnetic fields. It was the development of a correlation model that allowed the use of the GTEM as an instrument for the performance of radiated emissions measurements. The correlation model and the attendant computational algorithm allowed the practical aspects of a GTEM to outweigh the inconvenience of the OATS. This paper reviews the original correlation model and the new developments that have expanded the applicability of the GTEM into new areas.

STRUCTURE OF GTEM TO OATS CORRELATION MODELS

An understanding of the basic structure of the fundamental correlation is needed to follow the development of the variations

of the improvements and new approaches described in this paper. This section provides an overview of the general approach to developing OATS based specification limit measurements in a GTEM.

Purpose of Correlation Models

The GTEM to OATS correlation algorithm is used to enable radiated emissions measurements accomplished in a GTEM to be compared directly to the radiated emissions specification limits of any of the international specifications. The radiated emissions values may be computed at different measurement distances, as needed, for determination of acceptable radiated emissions performance.

General Structure of Models

In general, radiated emissions accomplished using a GTEM by measuring the RF voltages that appear at the GTEM RF port, coupled from the EUT, as a function of frequency. These measurements are accomplished with the EUT in three orthogonal positions, centered in the measurement volume of the GTEM. The three positions are assumed in a manner such that the positive X, Y and Z axes of the EUT are sequentially interchanged. The frequency, the three voltages measured at each frequency, the height if the EUT under the septum , the height of the septum over the center of the EUT the measurement distance and the height scan range used for the test antenna maximization search are inputs to the correlation algorithm.

At each frequency, the GTEM correlation algorithm performs the following computations:

Performs a root sum of the squares summation of the three orthogonal voltages,

Computes the total power emitted by the EUT as determined from the summation of the three voltages and the TEM mode equations for the GTEM!,

Computes the current excitation of an equivalent Hertzian dipole when excited with that input power,

Places the hypothetical Hertzian dipole at a specified height over a perfect ground plane,

Computes the horizontally and vertically polarized field strength at appropriate height intervals over the total, operator selected correlation algorithm height, 1 to 4 meters,

Selects the maximum field strength (larger) value of the horizontal or vertically polarized field strengths over the height range selected,

Presents this maximum value for comparison to the chosen EMC specification limit.

CH3310-0/93/0000-0017 $3.00 © 1993 IEEE

The original correlation algorithm is based on the general calculation procedure described above. Application of this model to varying measurement situations has resulted in development of new applications of the original model. Additional development of correlation theory is also described.

The Original Model – The Three Measurement, Three Input Model

The original correlation algorithm model as described above, was initially used for the comparison of GTEM and OATS radiated emissions measurements. This model is described as a three measurement, three input model. The terminology used is meant to be descriptive of the measurement and the correlation process. This model, the three measurement - three input model is the fundamental model for correlation of GTEM data to the OATS measurement. It is the basis of several additional measurement - correlation schemes.

The Twelve Measurement – Three Input Model

This is an addition to the original correlation algorithm. There are EMC specifications that have a differing requirement than the direct comparison of electromagnetic field strength produced by an EUT, as measured on an OATS or in a GTEM , to a field strength specification limit. Other specifications call for the measurement of a maximized specific emanation from an EUT, and then physically replacing the EUT with a resonant "standard" dipole tuned to the same frequency. The input power to this replacement dipole is then adjusted to give the same indication on the measurement instrumentation as the EUT did at that frequency. The specification limit values are in terms of the power input to the "standard" dipole to produce the same instrumentation indication. The original correlation algorithm cannot *directly* produce this output.

Experimentation with measurements to this specification revealed that the fundamental assumption, that of the emanating element in the EUT having gain no greater than a dipole, *is not sound* – particularly as frequencies of the measured emission increase above several hundred MHz. In particular, it was found that the correlation algorithm answers were sensitive to the starting point, or reference face, where the initial measurement was made. This indicates that the radiating element had gain greater than the theoretical Hertzian dipole used in the correlation algorithm to replace the EUT. There are twelve possible starting points for the three-position measurement, six faces with two possible polarizations per face. The three input correlation algorithm provides correct outputs to the correlation process, if the face and polarization with the highest amplitude, and the two associated faces at the Y and Z positions are used as the correlation algorithm input.. Only one of these starting points would give the correct answer as would actually be measured on an OATS.

Remembering that the specification limits are in terms of power input to a tuned dipole, it was apparent that if the correct X, Y and Z inputs were used, then, for the specific correlation algorithms where the EUT is replaced with a dipole, the proper selection of the starting side allows the constraint of gain no greater than a dipole to be met and still provide a correct answer. The twelve-position measurement, three-input correlation approach was devised to allow the development of technically correct answers, while maintaining the correlation algorithm requirement that the emanating element had gain no greater than the dipole.

The twelve-position measurement consists of the measurement of all six faces of a cube enclosing the EUT in both polarizations. Once the twelve measurements are made, the face and polarization having the highest value measured is set as the X, or reference, face and measurement. Since all faces were measured in two polarizations, the information necessary to complete the set of three inputs per the rules for the positive axis interchange are available. Given a specific order of measurements, the Y and Z measurements corresponding to the X measurement selected as having the highest amplitude are input to the correlation algorithm. All three inputs are extracted from the twelve-position measured data and these three related measurements, with the other appropriate data are input to the existing three input correlation algorithm. Since the presumption is that the EUT emitter is a tuned dipole, the correlation algorithm is accurate.

In addition, there is a modification to the correlation algorithm to allow the computation of power to the dipole that is producing the signal.

The Twelve Plus Four Measurement – Three Input Model

The next refinement is to address the assumption that the EUT has gain no greater than a short dipole, a numerical value of 1.5. A variation on the twelve measurement - three input correlation algorithm is to be introduced that allows an estimate of the gain of the emanating element to be made. Starting with the twelve measurements of the EUT, it is then possible to identify the highest emanation from the EUT at any particular frequency. Once this face and polarization is identified, it is then possible to re-orient the EUT such that this face and polarization is the reference face and polarization. Then, measurements are made at the same polarization at an angle of $\pm \pi/4$ to the reference face and at an angle of $\pm \pi/4$ to the cross polarized face. With these three points in each of two perpendicular planes, it is possible to estimate the horizontal and vertical beam widths of the emanation. From this information it is possible to estimate directivity of the emanation. Since the input power and the efficiency of the radiating element will not change, the directivity is an estimator of the gain of the radiating element. This gain estimation is used to replace the value of the gain of a dipole in the correlation algorithm.

The assumption of gain of a dipole is replaced with an assumption that the gain is no more than about 10 dB. If the gain is large with respect to 10 dB, it may not be detected by the

original twelve-position measurements. The additional four measurements are required to allow the estimate of gain to be made. Based on the information obtained by these additional measurements, the gain of the radiating element can be estimated to an approximate precision of ± 2 dB.

The Single Measurement – Free Space Correlation Model

An additional approach is suggested in the recent literature [3]. A wide bandwith TEM cell was used to measure the emanations from an integrated circuit, either in terms of the far field electric field value, or to compute the electric and magnetic free space dipole moments. In this case, only a single axis measurement was accomplished, thus the moments associated with the measurement are limited to one dimension only.

Additionally, relative shielding effectiveness measurements have been reported [4].

Performance of the Three Measurement - Three Input Correlation Algorithm Above 1 GHz

There are complications in using the original correlation algorithm in frequency ranges above 1 GHz. These complications are due to the nature of the antenna that is being used for the accomplishment of the real world measurement on an OATS. If the recommended antenna (a horn antenna) is being used for the real world measurement, comparison measurements as computed by the correlation algorithm will need to have the effect of the ground plane removed from the measurement as the horn antenna is too directional to "see" the reflected component.

On the other hand, if a lower gain antenna (such as a log periodic antenna) is used, the effect of the ground plane should be partially included, at least in the lower portion of the height search range of the correlation algorithm. When the log periodic is used as the receiving antenna, it will "see" the direct path and ground plane reflection path signals at the lower heights of the required one- to four-meter search heights. As the height is increased, the log periodic antenna may not see the reflected path signal and may see the direct path signal and finally may not see either. Since the correlation algorithm output is sensitive to the receiving antenna characteristics, the correlation algorithm for this correlation may have to have a correction for this issue.

New Directions of GTEM to OATS Correlation Models

The development of TEM cell and GTEM correlation algorithm models is still in its infancy. Over the next several years there will likely be many developments advancing the state-of-the-art in correlational algorithm models. Two improvements in coverage and accuracy ale listed below.

The Six Measurement – Six Input Model

A new correlation model requiring either six or nine measurements and six or nine inputs has been presented by the original developer of the three measurement - three input correlation. This advanced model incorporates the near field terms that make possible the measurement of electric and/or magnetic field values from 9 kHz to 30 MHz.

Extension to the Single Measurement Model

Examination of the single axis models led to a differing development. It appears possible that the single axis approach can be used to allow performance of the equivalent of MIL-STD RE102 measurements in a GTEM. In the past, it had seemed difficult to develop a specific mathematical model incorporating the effects of the six surfaces of a shielded enclosure, the metal top test table and the EUT and its multiple images. As a pragmatic alternative, a calibration is possible for the correlation of single axis GTEM measurements to a specific, or even multiple shielded enclosure(s).

A standard radiator can be installed in a GTEM and a single axis voltage measurement performed. The same standard radiator would then be installed in a shielded enclosure in a standard position. A Method RE102 test would be performed. The data from the shielded enclosure, corrected to field strength values will be used to derive a calibration factor for the GTEM voltage measurements. This calibration factor would be applied to the GTEM single axis data to produce a GTEM equivalent MIL-STD-462measurement.

The Future of GTEM to OATS Correlation Models

Based on the directions in correlation algorithm development and the need to provide new and novel uses of the GTEM it seems that the GTEM to OATS correlation models will continue to be developed and as additional EMC measurement applications are defined, the flexibility of the existing models will be used to apply the correlation technology to these new applications. The original three input model, with the addition of additional measurements allowed the GTEM measurement of EUT to new and differently organized specifications. It is anticipated that the new six input correlation algorithm will undergo the same practical expansion to the extension to the new six measurement-six input model.

Summary

In this report on GTEM correlation models and algorithms, an attempt has been made to provide an overview of the current status. The GTEM, as an EMC measurement instrument, is in the earliest stages of development. It will grow to a versatile general measurement instrument over the next several years.

Acknowledgments

The developments described in this paper are the results of a number of talented EMC engineers from Europe and the USA. The authors express their gratitude for the technical input and the friendship of the many individuals who contributed to the developments.

REFERENCES

1. P. Wilson, D. Hansen and D. Koenigstein, "Simulating Open Area Site Emission Measurements Based on Data Obtained in a Novel Broadband TEM Cell," in the *Proceedings of the IEEE 1989 National Symposium on Electromagnetic Compatibility*, 89CH2736-7, Denver, Colorado, May 23 - 25, 1989, pp. 171 - 177.

2. Edwin L. Bronaugh and John D. M. Osburn, "Radiated Emissions test Performance of the GIIz TEM Cell," in the *Proceedings of the 1991 International Symposium on Electromagnetic Compatibility*," 91CH3044-5, Cherry Hill, New Jersey, August 12 - 16, 1991, pp. 1-7.

3. R. R. Goulette, "The Measurement of Radiated Emissions from Integrated Circuits," in the *Proceedings of the 1992 International Symposium on Electromagnetic Compatibility*, 92CH3169-0, Anaheim, California, August 17 0 21, 1992, pp. 340 - 345.

4. Larry K. C. Wong, "Backplane Connector Radiated Emission and Shielding Effectiveness," in the *Proceedings of the 1992 International Symposium on Electromagnetic Compatibility*, 92ch3169-0, Anaheim, California, August 17 0 21, 1992, pp. 346 - 350.

SIMULATING OPEN AREA TEST SITE EMISSION MEASUREMENTS BASED ON DATA OBTAINED IN A NOVEL BROADBAND TEM CELL

P. Wilson, D. Hansen and D. Koenigstein
ABB EMI Control Center
Corporate Research
CH-5405 Baden-Daettwil, Switzerland

ABSTRACT

A new type of EMC test chamber applicable to both radiated emission and susceptibility measurements is discussed. The design is essentially a TEM-cell anechoic-chamber hybrid. A steady input power will generate an almost constant field (better than +/- 4 dB) anywhere in the recommended test volume from dc to frequencies exceeding a gigahertz. Susceptibility testing is done as in a normal TEM cell. Emission testing models test object radiation as due to an equivalent set of multi-poles (in essence electric and magnetic dipoles). The multi-pole components are determined through a sequence of measurements. Once found, the multi-pole model may be used to predict test object radiation both in an ideal free space and above a perfect ground screen. In this manner time consuming emission measurements, such as those required by FCC Rules Part 15 Subpart J or VDE 0871, may be simulated numerically. Both experimental and theoretical data are presented.

1. INTRODUCTION

This paper discusses a new type of EMC test chamber applicable to both susceptibility and emission measurements for frequencies from dc to above a gigahertz. The chamber is in effect a hybrid between a TEM cell and an anechoic chamber. The new chamber seeks to overcome the frequency and size limitations inherent to a standard TEM cell while retaining its basic advantages.

A standard TEM cell consists of a section of rectangular coaxial transmission line tapered at each end to mate with standard (50 ohm) coaxial cable. Thus, a TEM cell connects directly to the generator/receiver. No separate transmitting/receiving antennas are required. The TEM mode simulates a free space plane wave for susceptibility testing. A TEM cell is well isolated from outside ambients and allows one to measure very low radiated signal levels. Conversely, a properly constructed cell will not itself be an interference source. TEM cell design and usage is well documented [1].

The primary limitation to standard TEM cell usage is the size of the test volume which is inversely proportional to the upper operating frequency limit. The upper frequency limit is determined by the apperance of higher-order modes which perturb the desired TEM mode field distribution. The cell tends to act as a high Q cavity and the higher-order mode induced resonances can cause large variations in the field level versus frequency. This occurs when the cell width is on the order of a half wavelength. The test chamber height (the height from the cell floor to the inner conductor) in a normal TEM cell is half the cell width (assuming a square cross section). Thus, the test chamber size in a standard TEM cell is limited to approximately one quarter of the smallest desired operating wavelength. If testing up to 1 GHz (30 cm wavelength) is required then the above arguement would limit the test chamber size to 7.5 cm. This is clearly too small for most practical applications.

An alternative to the standard design is the tapered TEM cell shown in figure 1. It consists of a section of gently flared rectangular coaxial transmission line terminated with a matched load.The end termination is the truely unique feature of the cell. At low frequencies it operates as a circuit element 50 ohm load. At high frequencies the absorber attenuates the incident wave as in an anechoic chamber. The crossover between these two regimes depends on the cell size and the absorber length. The broadband match provided by the termination acts to supress the creation of higher-order modes. The absorbing material significantly reduces the Q of the chamber; thus, what resonance effects that do exist tend to be small. The end result is a field uniformity of better than +/- 4 dB versus frequency (dc to 1 GHz) in the test chamber of an empty cell. These cells have been given the name "GTEM" cells to emphasize their gigahertz capability.

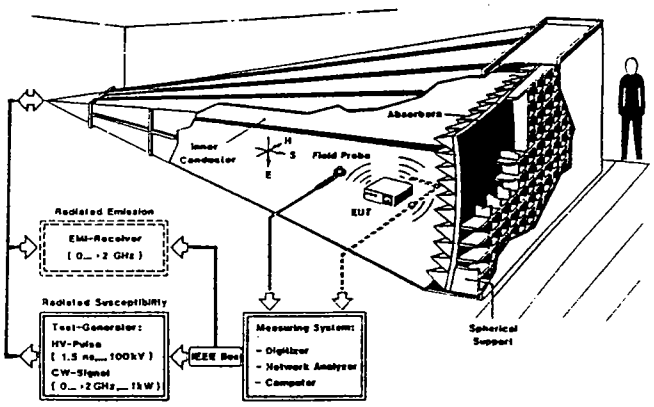

Fig. 1 A tapered TEM cell (GTEM cell)

The design criteria for such tapered cells have been presented previously [2]. Cells have been constructed with test chamber heights of 0.5 m, 1.0 m, and 1.5 m (ABB models GTEM 500, GTEM 1000, GTEM 1500). These are suitable for printed circuit board through box level testing respectively. The inner conductor is vertically offset to create a larger usable test volume. These cells have proven themselves to be valuable engineering tools greatly aiding in the everyday EMI diagnosis of electronics. GTEM type cells have also been recognized in several standards, such as VG 95903 (Part 50). The basic concept may be scaled. Larger cells capable of rack level or automobile testing, are presently under study.

This paper will focus on emission measurements performed in GTEM cells and how the data may be correlated to either free space or ground screen results. For susceptibility measurements, the cell may be used to simulate an incident plane wave. The measurement approach would be similar to that for a standard TEM cell, ground screen or anechoic chamber. Figure 2 shows typical field uniformity data. The vertical electric field and horizontal magnetic field were measured on the floor of a GTEM 1000 cell (final test chamber height 1.0 m) at the point where the inner conductor height was 0.8 m. The two field probes were offset from the cell center by 5 cm. The field uniformity in both cases is +/- 4 dB even beyond 1 GHz (the measurement system was limited to 1.8 GHz; the low frequency noise is due to the measurement equipment not the cell). The width of this cell at the measurement point is 1.6 m. Thus, higher-order mode effects pose a potential problem above approximately 94 MHz. However, no significant resonances appear.

As in a standard TEM cell, the introduction of a test object will perturb the fields and excite the undesired modes. But this is the

CH2736-7/89/0000-0171 $1.00 ©1989 IEEE

case in any test environment. The scattered TEM mode will simulate the scattering of an incident plane wave. The undersired modes should not resonate strongly due to the relatively low Q of the cavity (as compared to a normal TEM cell or shielded room) if the test object size is not too large. Typically, the recommended maximum test object size is one third the test chamber height.

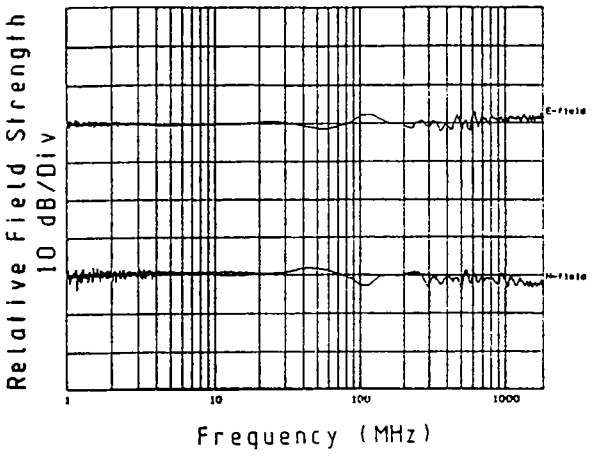

Fig. 2 Field univormity as measured in a GTEM 1000 cell. The low frequency noise is due to the measurement system.

2. EMISSION TESTING IN A GTEM CELL

The typical reference environments for radiated emission testing are free space or a large ground screen. However, TEM cells are transmission lines. Thus, GTEM emission results need to be correlated to these environments if data is to be meaningfully compared. The approach taken here is to model the DUT as a set of multi-poles. At frequencies where the device under test (DUT) is small when compared to a wavelength, the equivalent electric and magnetic dipole moments usually suffice. This method has been successfully used to predict free space radiation based on measurements in standard TEM cells [3-5]. We have extended the analysis to the case of DUT radiation over a ground screen. The basics of the multi-pole approach will be reviewed next. The actual mathematical details are left to the appendix.

Any finite sized current source can be modeled by a multi-pole expansion which will yield the same radiation pattern outside some volume containing the source. The analysis is greatly simplified if only the far-field pattern is considered, as will be done here. If the source is electrically small, then the initial terms of the expansion are sufficient to accurately reproduce the radiation pattern. The leading terms are the electric and magnetic dipole moments. The radiation of both dipole types over a ground screen has been considered. The resulting equations enable one to model any dipole height or orientation over the ground screen and then compute the radiated fields. By combining the DUT equivalent dipole moments we can also predict the fields due to the DUT for any arbitrary configuration. In this manner one can simulate by computer radiated emission qualification tests as prescribed by FCC Part 15 Subpart J or VDE 0871 regulations. These types of emission measurements are very time consuming and thus costly. In addition, background noise at a typical open area test site may make meaningful testing impossible. Thus, GTEM emission testing is a valid alternative, subject to the limitations of the multi-pole model described. The details of the multi-pole model and dipole radiation over a ground screen are left to Appendix A.

The actual DUT equivalent dipole moments, electric and magnetic, are determined through a sequence of GTEM measurements. In essence, the DUT is rotated through the TEM mode so that different dipole moments are strongly coupled. Twelve DUT positions are required to determine the magnitudes of the electric and magnetic dipole moments. The GTEM cell, as opposed to a standard TEM cell, is a one port device. Thus, no relative phase information is available. It is assumed here that the various dipole moments are basically in phase. This assumption should not be overly prohibitive as most DUTs tested for EMC purposes are unintentional radiators and strong phase differentiation is not expected. The details of multi-pole radiation in a GTEM cell and the measurement sequence necessary to determine the dipole moments are left to Appendix B. A much more detailed development of this formulation may be found in [6], as well as in the references already cited.

3. MEASURED DATA: THEORY VERSUS EXPERIMENT

The theory discussed above will now be applied to sample sources in order to verify the usefulness of this approach. We first consider a small self-contained spherical dipole which is a very convenient reference source for site comparisons [7]. It consists of two gold-plated aluminum hemispheres, 10 cm in diameter, which are driven by an internal comb generator based on a 20 MHz clock. It is capable of generating useful 20 MHz harmonics up to 1 GHz. Also, its size is such that it is the electrically small over most of the bandwidth of interest here.

The spherical dipole was first tested in a GTEM cell as an unknown radiator and its equivalent dipole moments were determined according to the sequence outlined in Appendix B. As expected, the GTEM cell tests indicated that it acts primarily as an electrical dipole oriented along its polar axis. However, it does show some lesser magnetic dipole components as well. Quite likely, the metal hemispheres are not thick enough to shield all the direct radiation from the internal circuitry itself. But here this is not a problem since we treat it as an unknown source and it need not be a perfect spherical dipole.

These dipole moments were next used to predict how the spherical source would radiate above a ground screen based on the equations given in Appendix A. The parameters chosen were; height above the ground screen of 0.86 m, spherical source to receiving antenna separation of 10 m, and receiving antenna heights of 1-4 m in 1 m steps. Both the horizontal and vertical electric field were predicted. The frequency range considered was 30-1000 MHz. This configuration is representative of a VDE 0871 radiated emission test for Class B information technology equipment (ITE). It should be noted that the computer program requires negligable time to perform this calculation and plot the predicted emission data.

The spherical radiator was next measured atop the ABB Baden roof top ground screen. The parameters were kept the same as above, except that in the vertical electric field measurement the receiving antenna heights were 2-4 m. The 1 m height measurement could not be performed as the antenna was too large. Acquiring this data took an experienced engineer the better part of two days. Each signal had to be identified against considerable noise by using a very narrow band setting on the receiving equipment. Figure 3 shows the ambient horizontal electric field (noise) 4 m above the ground screen. Local transmitters emit significantly in certain bands as may be seen. Also a number of occasional transmitters and nearby construction noise were also noted. In this case we knew where to look for the desired signals (20 MHz harmonics). For unknown, broadband sources it is often impossible to identify the DUT signal amidst the ambient noise on the ground screen.

The two sets of measurements are compared in figures 4-5. Figure 4 shows the horizontal electric field data, both GTEM predicted (4a) and measured on the roof top ground screen (4b), while figure 5 shows the predicted and measured vertical electric field data. In each case the spherical source was oriented for maximal coupling. Data points exist only at multiples of 20 MHz. The points are connected to show the individual receiving antenna heights more clearly. In the horizontal electric field case (fig. 4) raising the antenna increased coupling at the lower frequencies (less than 400 MHz) while in the vertical electric field the lower receiving antenna position yielded the highest field. This basically

indicates the boundary condition at the ground screen (horizontal electric field equal to zero). At higher frequencies, the wavelength is sufficiently small that we see complicated interference effects between the source and its image.

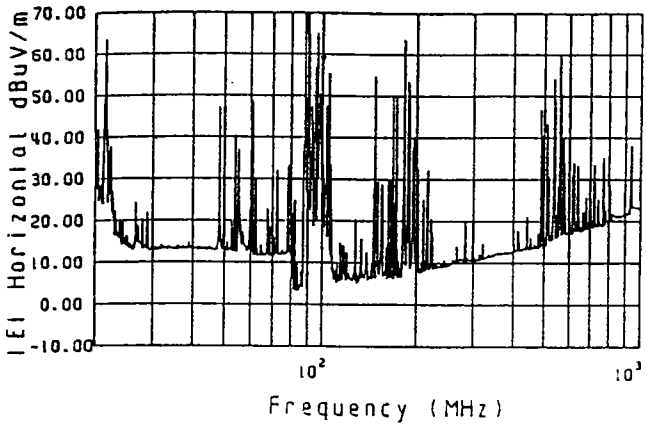

Fig. 3 Ambient noise (horizontal electric field, 4 m height) at the ABB Baden rooftop ground screen.

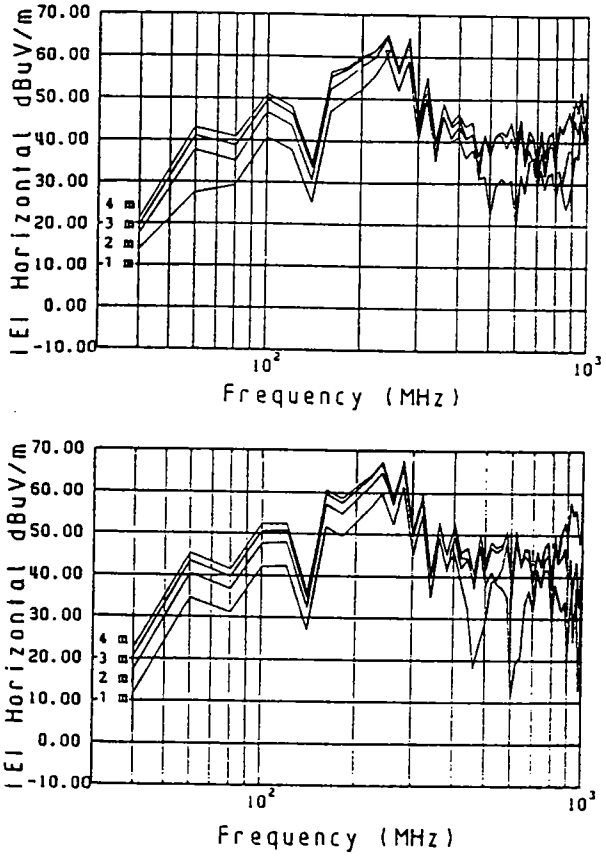

Fig. 4 Horizontal electric field radiated by a spherical source as measured over the ABB Baden rooftop ground screen (upper curve) and as predicted based on GTEM measurements (lower curve). Actual data points are every 20 MHz. The source height is 0.86 m, the source to receiver separation is 10 m, and the receiver height is varied from 1-4 m (1 m steps).

The agreement between the GTEM predicted data and the actual ground screen data is very good. The same model may also be used to predict the free space radiation and the total radiated power.

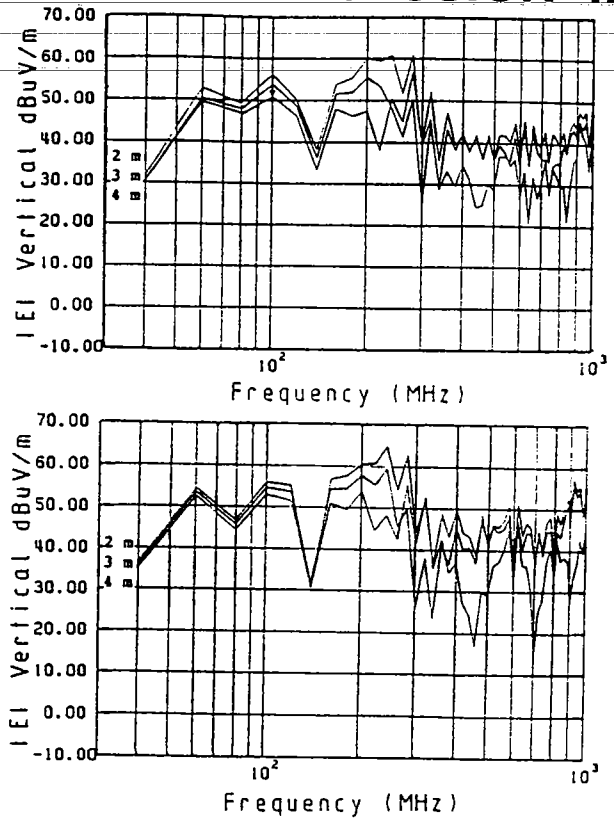

Fig. 5 Vertical electric field radiated by a spherical source as measured over the ABB Baden rooftop ground screen (upper curve) and as predicted based on GTEM measurements (lower curve). Actual data points are every 20 MHz. The source height is 0.86 m, the source to receiver separation is 10 m, and the receiver height is varied from 2-4 m (1 m steps).

The full dipole model requires that the DUT be rotated through a 12 position GTEM test sequence. As outlined in Appendix B, if only the total radiated power is desired, 3 unique measurements positions in the GTEM cell will suffice. This will not allow one to predict the full DUT radiation pattern. But we may use total radiated power to place a reasonable bound on the potential DUT radiation. An unintentional radiator is unlikely to have greater gain than that of a dipole antenna. Thus, the maximum radiated field should not exceed that of a dipole radiating the same total power, when that dipole is oriented for maximal coupling. In the case of the horizontal electric field this will be a horizontal electric dipole and similarly a vertical electric dipole will generate the maximum vertical electric field. In short, the total radiated power as measured in a GTEM cell is used to bound ground screen radiation.

As an example of this approach, a widely available PC was tested. The total radiated power was first determined based on emission measurements in the GTEM 1500 cell (3 orientations). These curves are stored in a computer and correlated to a VDE 0871 Class B configuration using the equations developed in the appendix. The result is shown in figure 6 against the VDE 0871 limits. Recall that the predicted curves, horizontal and vertical, represent worst case envelopes. Thus, based on this data we would expect this PC to pass VDE certification tests. In fact, it carried a label to this effect. The dark area above 200 MHz represents the nominal noise floor (correlated) for the particular receiving equipment used to make the GTEM measurements. This could be lowered by using more sensitive equipment than was available for these tests. Also note that the vertical and horizontal bounds converge above 100 MHz. This indicates that the ground screen no longer strongly affects the maximum field strength and in each case we are probably seeing the direct coupling bound. The whole measurement is automated and requires about one-half hour using a very slow sweep time.

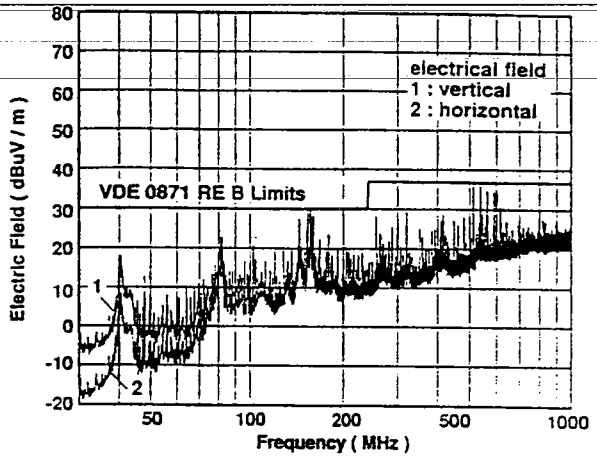

Fig. 6 Simulated VDE 0871 Class B radiated emission test for a PC based on GTEM measurements. Both the horizontal and vertical electric cases are considered. The simulated data represent upper bounds based on maximal coupling assumptions.

4. CONCLUSION

The great advantage of the GTEM multi-pole approach is that, once the multi-poles are determined, a ground screen simulation can be done numerically. Thus, the orientation of the DUT, the height and orientation of the receiving antenna, the separation of the two, and so forth can all be changed by the computer program. This allows one to simulate VDE and FCC emission tests in a fraction of the time it would take to acquire real data. The primary limitations to this method are that accuracy is dependent on the DUT being electrically small and that the DUT must be physically rotated in order to determine its equivalent dipole moments. However, for a wide range of DUTs this method should be an attractive, time and cost saving method for radiated emission testing.

5. REFERENCES

[1] M. L. Crawford, "Generation of standard EM fields using TEM transmission cells," IEEE Trans. Electromagn. Compat., vol. EMC-16, no. 4, pp. 189-195, Nov. 1974.

[2] D. Koenigstein and D. Hansen, "A new family of TEM-cells with enlarged bandwidth and optimized working volume, "Proc. 7th Int. Zurich Symp.and Techn. Exh. on EMC, pp. 127-132, March 1987.

[3] I. Sreenivasiah, D. C. Chang, and M. T. Ma, "A method of determining the emission and susceptibility levels of electrically small objects using a TEM cell," Nat. Bur. Stand., Boulder, CO, Tech. Note 1040, April 1981.

[4] M. T. Ma and G. H. Koepke, "A method to quantify the radiation characteristics of an unknown interference source," Nat. Bur. Stand., Boulder, CO, Tech. Note 1059, Oct. 1982.

[5] G. H. Koepke and M. T. Ma, "A new method for determining the emission characteristics of an unknown interference source," Proc. 5th Int. Zurich Symp. and Techn. Exh., pp. 35-40, March 1983.

[6] P. F. Wilson, D. Hansen and H. Hoitink, "Emission measurements in a GTEM cell: simulating the free space and ground screen radiation of the test device," ABB Research Report (in preparation).

[7] M. L. Crawford and J. L. Workman, "Predicting free-space radiated emissions from electronic equipment using a TEM cell and open-field site measurements," Proc. IEEE Int. Symp. on EMC (Baltimore, MD),pp. 80-85, 1980.

[8] R. E. Collin, Field Theory of Guided Waves, Mcgraw-Hill, New York, 1960.

Appendix A. Multi-Pole Radiation in Free Space and over a Ground Screen

A radiation source (DUT) in free space is depicted in figure A1. A spherical coordinate system (r,θ,φ) is centered at the source. Observation points will be designated by the vector $\bar{r}$ Source points will be designated $\bar{r}'$. We will restrict our attention to the far-field zone where $|\bar{r}-\bar{r}'| \approx r - \hat{r}\cdot\bar{r}'$, $r = |\bar{r}|$, and $\hat{}$ denotes a unit vector. This both simplifies the analysis and represents the primary case of interest.

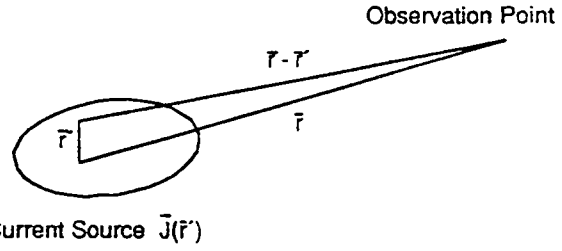

Fig. A1. Radiation source in free space

The electric $\bar{E}(\bar{r})$ and magnetic $\bar{H}(\bar{r})$ fields due to a current density $\bar{J}(\bar{r}')$ distributed over a volume V may be determined from the usual vector potential formulation;

$$\bar{A}(\bar{r}) = \frac{\mu_0}{4\pi}\int_V \bar{J}(\bar{r}')\frac{e^{-jk_0|\bar{r}-\bar{r}'|}}{|\bar{r}-\bar{r}'|}dv',$$
$$j\omega\varepsilon_0\bar{E}(\bar{r}) = \nabla\times\bar{H}(\bar{r}), \text{ and} \qquad (A.1)$$
$$\mu_0\bar{H}(\bar{r}) = \nabla\times\bar{A}(\bar{r}),$$

where ε_0 and μ_0 are the free space permittivity and permeability, k_0 is the free space wave number, and an exp (jωt) time convention is assumed. In the far-zone, the exponent may be approximated as described above and the source to observation point distance in the denominator replaced by r. Thus,

$$\bar{A}(\bar{r}) \approx \frac{\mu_0}{4\pi} f(r)\int_V \bar{J}(\bar{r}')e^{jk_0\hat{r}\cdot\bar{r}'}dv', \text{ where} \qquad (A.2)$$
$$f(r) = \frac{e^{-jk_0 r}}{r}.$$

If the current source is electrically small, then the exponential in the integral may be expanded in a Taylor series about $k_0\hat{r}\cdot\bar{r}'$ Retaining only the leading two terms yields

$$\bar{A}(\bar{r}) \approx \frac{\mu_0}{4\pi} f(r)\int_V \bar{J}(\bar{r}')\left[1 + jk_0\hat{r}\cdot\bar{r}'\right]dv' \qquad (A.3)$$
$$= \frac{\mu_0}{4\pi} f(r)\int_V \left\{\bar{J} + \frac{1}{2}k_0\left[(\bar{r}'\times\bar{J})\times\hat{r} + (\hat{r}\cdot\bar{r}')\bar{J} + (\hat{r}\cdot\bar{J})\bar{r}'\right]\right\}dv'.$$

Defining the electric dipole moment $\bar{P}$, the magnetic dipole moment $\bar{M}$, and the electric quadrupole dyadic $\bar{\bar{Q}}$ in the usual fashion [8], we find that

$$\bar{A}(\bar{r}) \approx \frac{\mu_0}{4\pi} f(r)\left\{\bar{P} - jk_0\bar{M} + \frac{1}{2}jk_0\bar{\bar{Q}}\bar{r}\right\} \qquad (A.4)$$

This basic derivation appears in [3]. The various multi-pole moments are allowed to be complex to account for possible phase differences between the individual components.

We will next consider the far-zone radiation due to $\bar{P}$ and $\bar{M}$. The quadrupole contribution is expected to be small and will be neglected for reasons discussed in Appendix B.

We begin with an analysis of the fields due to the electric dipole. Equation (A.4) indicates that as the frequency approaches zero ($k_0 \to 0$) the electric dipole will represent the dominant contribution. We derive only the radiated electric field since this is the usual field quantity measured; the magnetic field may be found via the wave impedance (far field).

The electric dipole contribution to the potential $\bar{A}(\bar{r})$ is given in (A.4) in terms of spherical coordinates. The resulting electric field may be found from (A.1). However, the result is best expressed in rectangular coordinates since this will facilitate the introduction of a ground screen. Performing the required vector algebra we find that in the far field,

$$\bar{E}_P(\bar{r}) = -j\frac{k_0\eta_0}{4\pi} f(r)\,\bar{F}_P(\bar{r},\bar{P}) \tag{A.5}$$

where now

$\bar{r} = (x,y,z)$, $\bar{P} = (P_x, P_y, P_z)$, $\eta_0 = 120\pi$, $\rho^2 = (x^2 + y^2)$, and

$$\begin{aligned}\bar{F}_P(\bar{r},\bar{P}) = \hat{x}&\left[P_x\left(\frac{x^2}{\rho^2}\frac{z^2}{r^2} + \frac{y^2}{\rho^2}\right) - P_y\frac{xy}{r^2} - P_z\frac{xz}{r^2}\right] \\ +\hat{y}&\left[-P_x\frac{xy}{r^2} + P_y\left(\frac{y^2}{\rho^2}\frac{z^2}{r^2} + \frac{x^2}{\rho^2}\right) - P_z\frac{yz}{r^2}\right] \\ +\hat{z}&\left[-P_x\frac{xy}{r^2} - P_y\frac{yz}{r^2} + P_z\frac{\rho^2}{r^2}\right].\end{aligned} \tag{A.6}$$

It is now a relatively easy matter to introduce a ground screen.

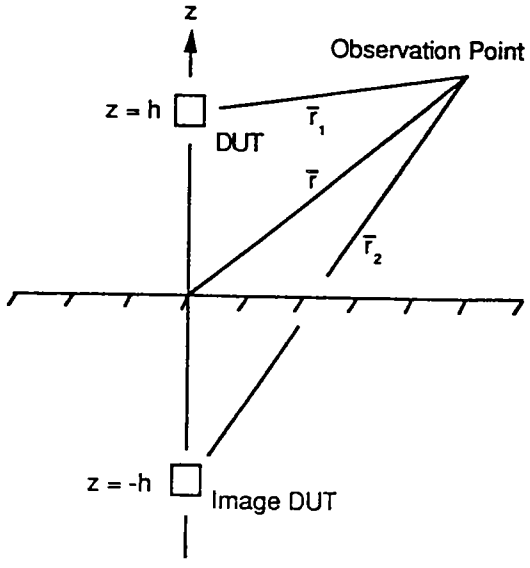

Fig. A2. Radiation source over a ground screen

Referring to figure A.2, let the dipole $\bar{P}$ be at a height h above a perfectly conducting ground screen located in the z=0 plane. This requires that z be replaced by z-h in the expression for $\bar{F}_P$. The field point will again be designated $\bar{r}$. The fields at $\bar{r}$ will be due to both the real source and an image source located a distance h below the ground screen. The vector paths between the observation point and the source and image points are designated $\bar{r}_1$ and $\bar{r}_2$ respectively. The source dipole components are (P_x, P_y, P_z). The image of a positive charge about a perfectly conducting ground screen is a negative charge. Thus, the image of a perpedicular electric dipole is in the same direction while the image of a parallel dipole is reversed. As a result, the image source $\bar{P}_I$ will have dipole components ($-P_x$, $-P_y$, P_z) and the electric field due to the image source is given by $F_P(\bar{r}_2, \bar{P}_I)$. Combining results the total electric field $\bar{E}_P(\bar{r})$ may be written

$$\bar{E}_P(\bar{r}) = -j\frac{k_0\eta_0}{4\pi}\left\{\bar{F}_P(\bar{r}_1,\bar{P})\, f(r_1) + \bar{F}_P(\bar{r},\bar{P}_I)\, f(r_2)\right\} \tag{A.7}$$

where

$$\begin{aligned}&\bar{r}_1 = (x,y,z-h),\ r_1 = |\bar{r}_1|, \\ &\bar{r}_2 = (x,y,z+h),\text{ and } r_2 = |\bar{r}_2|.\end{aligned} \tag{A.8}$$

The magnetic dipole case may be similarly analyzed. One finds that

$$\bar{E}_M(\bar{r}) = \frac{k_0^2\eta_0}{4\pi} f(r)\,\bar{F}_M(\bar{r},\bar{M}) \tag{A.9}$$

where $\bar{M} = (M_x, M_y, M_z)$ and

$$\begin{aligned}\bar{F}_M(\bar{r},\bar{M}) = \hat{x}&\left[M_y\frac{z}{r} - M_z\frac{y}{r}\right] + \hat{y}\left[-M_x\frac{z}{r} + M_z\frac{x}{r}\right] \\ +\hat{z}&\left[M_x\frac{y}{r} - M_y\frac{x}{r}\right].\end{aligned} \tag{A.10}$$

Mimicking the electric dipole analysis, we now introduce a ground screen at a height h below the magnetic dipole. The ground screen is located in the z=0 plane as before. The direct magnetic-dipole far-zone electric field may be found from eqs. (A.9-A.10) simply by replacing z with z-h. The ground screen will also introduce an image source. If we think of the dipole as due to ficticious magnetic charges which retain their polarity when imaged about a perfectly conducting ground screen, then the image dipole $\bar{M}_I$ will have components (M_x, M_y, $-M_z$) respectively. Thus, the electric field due to the image dipole may be found from $\bar{F}_M$ by replacing z with z+h and $\bar{M}$ with $\bar{M}_I$. The total electric field $\bar{E}_M(\bar{r})$ due to a magnetic dipole over a ground screen is thus;

$$\bar{E}_M(\bar{r}) = \frac{k_0^2\eta_0}{4\pi}\left\{\bar{F}_M(\bar{r}_1,\bar{M})\, f(r_1) + \bar{F}_M(\bar{r}_2,\bar{M}_I)\, f(r_2)\right\} \tag{A.11}$$

Combining results we find that the total far-field electric field due to the electric and magnetic dipoles is

$$\bar{E}(\bar{r}) = \bar{E}_P(\bar{r}) + \bar{E}_M(\bar{r}) \tag{A.12}$$

One may also show that the total power P_0 radiated by this source approximation is

$$P_0 = 10k_0^2\left\{|\bar{P}|^2 + k_0^2|\bar{M}|^2\right\} \tag{A.13}$$

Appendix B. Multi-Pole Radiation and Determination in a GTEM Cell

Given a current source, in a GTEM cell shown in figure B1, the fields $\bar{E}^{\pm}$ and $\bar{H}^{\pm}$ excited in the waveguide may be expanded in terms of the normalized waveguide modes $\bar{E}_n^{\pm}$ and $\bar{H}_n^{\pm}$;

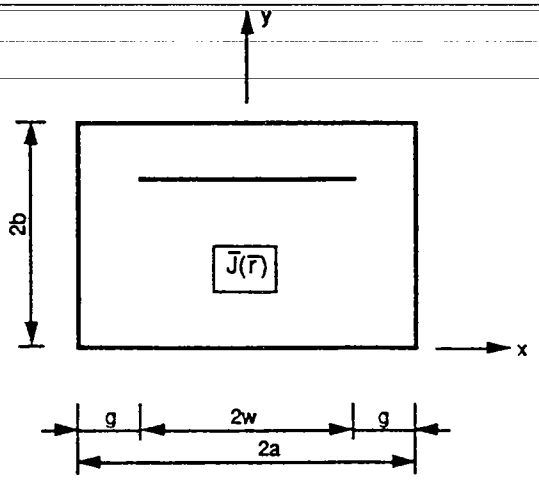

Fig. B1. Radiation source in a GTEM cell

$$\bar{E}^{\pm} = \sum_n \begin{pmatrix} a_n \\ b_n \end{pmatrix} \bar{E}_n^{\pm} \quad \text{and} \qquad \bar{H}^{\pm} = \sum_n \begin{pmatrix} a_n \\ b_n \end{pmatrix} \bar{H}_n^{\pm} \tag{B.1}$$

where $\pm$ indicates the direction of propagation from the source, and a_n, b_n are the forward (+) and backward (-) excitation coefficients respectively. Let z be the direction of propagation and let z=0 be referenced to some suitably chosen origin in the source volume. The normalized waveguide modes may be written

$$\bar{E}_n^{\pm} = (\bar{e}_{nt} \pm \hat{z} e_{nz}) e^{\pm jk_n z}, \quad \text{and} \qquad \bar{H}_n^{\pm} = (\pm \bar{h}_{nt} + \hat{z} h_{nz}) e^{\pm jk_n z}, \tag{B.2}$$

where k_n is the propagation constant of the nth mode. The transverse field components $\bar{e}_{nt}$ and $\bar{h}_{nt}$ are related via the admittance dyadic $\bar{\bar{Y}}_n$,

$$\bar{h}_{nt} = \bar{\bar{Y}}_n \cdot \bar{e}_{nt} \quad \text{and} \quad \bar{\bar{Y}}_n = \frac{1}{Z_n}(\hat{y}\hat{x} - \hat{x}\hat{y}) \; ; \tag{B.3}$$

where Z_n is the wave impedance of the nth mode. The orthonormal condition takes the form

$$\iint_S [\bar{e}_{nt} \times \bar{h}_{nt}] \cdot \hat{z} \, ds = \delta_{mn} \; , \tag{B.4}$$

where the integration is over the cross section S of the waveguide and δ_{mn} is the Kronecker delta function.

The excitation coefficients are related to the current source via

$$\begin{pmatrix} a_n \\ b_n \end{pmatrix} = -\frac{1}{2} \int_V \bar{J}(\bar{r}) \cdot \bar{E}_n^{\mp}(\bar{r}) \, dv, \tag{B.5}$$

where $\bar{J}$ is the current density. The excitation coefficients may be simplified for application here based on two conditions; 1) the source is electrically small and 2) the modes of interest are nearly uniform over the source volume. The former restriction justifies retaining only the leading multi-pole terms. The latter condition allows us to expand $\bar{E}_n^{\pm}$ in terms of a Taylor series about the source volume origin and keep only the first derivative correction,

$$\bar{E}_n^{\pm}(\bar{r}) \approx \bar{E}_n^{\pm}(\bar{o}) + \bar{r} \cdot \nabla \bar{E}_n^{\pm}(\bar{o}) \; . \tag{B.6}$$

Here, $\bar{o}$ denotes an origin chosen in a coordinate system r local to the source volume. It may or may not coincide with the waveguide coordinate system. Subject to this approximation, the excitation coefficients become

$$\begin{pmatrix} a_n \\ b_n \end{pmatrix} = -\frac{1}{2} \left\{ \bar{E}_n^{\mp}(\bar{o}) \cdot \int_V \bar{J}(\bar{r}) \, dv + \int_V \left[\bar{r} \cdot \nabla \bar{E}_n^{\mp}(\bar{o}) \right] \cdot \bar{J}(\bar{r}) \, dv \right\} \; . \tag{B.7}$$

The first integral may be recognized as the electric dipole moment $\bar{P}$. One may show that the second integral is related to the magnetic dipole moment $\bar{M}$ and the electric quadrupole moment $\bar{\bar{Q}}$ [3,8], with the result that

$$\begin{pmatrix} a_n \\ b_n \end{pmatrix} = -\frac{1}{2} \left\{ \bar{E}_n^{\mp}(\bar{o}) \cdot \bar{P} - jk_0 \eta_0 \bar{H}_n^{\mp}(\bar{o}) \cdot \bar{M} + \frac{1}{2} \nabla \bar{E}_n^{\mp}(\bar{o}) : \bar{\bar{Q}} \right\} \tag{B.8}$$

If the electric field is perfectly uniform over the source volume, such that $\nabla E(\bar{o}) = 0$, then the electric quadrupole moment is not needed and will be ignored here for simplicity.

We are primarily interested in the dominant TEM mode (n=0). For the TEM mode both e_{oz} and h_{oz} are zero and the the wave impedance takes the free space value η_0. Expanding the various field terms we find that

$$\bar{E}_0^{\mp}(\bar{o}) = \hat{x} e_{ox}(\bar{o}) + \hat{y} e_{oy}(\bar{o}), \qquad \bar{H}_0^{\mp}(\bar{o}) = \pm \hat{x} e_{oy}(\bar{o}) \mp \hat{y} e_{ox}(\bar{o}) \quad \text{or} \pm \left(\hat{x} e_{oy}(\bar{o}) - \hat{y} e_{ox}(\bar{o}) \right) \; . \tag{B.9}$$

Substituting these results into (B.8) yields

$$\begin{pmatrix} a_o \\ b_o \end{pmatrix} = -\frac{1}{2} \{ [P_x \pm jk_0 M_y] e_{ox}(\bar{o}) + [P_y \mp jk_0 M_x] e_{oy}(\bar{o}) \} \tag{B.10}$$

This result is perhaps more general than needed here. Typically, the DUT will be located centrally in the test chamber (x=0, see fig. B.1). In this case $e_{ox}(\bar{o}) = 0$ and (B.10) reduces to

$$\begin{pmatrix} a_o \\ b_o \end{pmatrix} = -\frac{1}{2} [P_y \mp jk_0 M_x] \, e_{oy}(\bar{o}) \; . \tag{B.11}$$

Because of the particular normalization chosen, the powers carried by the TEM mode in the forward and backward directions are simply $|a_o|^2$ and $|b_o|^2$ respectively. It is, in fact, the power that is actually measured in the proposed scheme to determine the dipole moments.

Each of the three complex components of $\bar{P}$ and $\bar{M}$ represent two unknowns. Thus, we need to determine a total of 6 complex quantities or 12 unknowns, in order to fully specify our two term multi-pole expansion. Clearly, a number of GTEM measurements are required to generate sufficient independent equations.

Similar measurement procedures have been developed for a standard TEM cells [3-5]. The basic approach is to rotate the DUT about an axis, typically the longitudinal axis (direction of TEM mode propagation), through a sequence of $\pi/4$ angular steps. A local coordinate system (x',y',z') is assigned to the DUT and in turn each local axis is aligned with the TEM cell longitudinal axis.

In this manner, each of the dipole moments is at some position strongly coupled to the vertical component of the electric field or the horizontal component of the magnetic field. Clearly, this approach generates numerous equations; solving these for the individual moment components, magnitude and phase can be tedious.

This paper will assume that the dipole moments are in phase. In general, this should not be an unrealistic restriction. Unintentional radiators are not likely to be designed such that they act as highly directive antennas, or such that they have complicated phase differentiation in their radiation patterns. More typically, we expect a box with possible seams and protrusions but with the currents basically in phase.

In a mathematical sense, rotations about any of the axes are equally simple. One need only introduce a rotation angle and perform the necessary bookkeeping. However, physically it is easiest to rotate about the vertical axis, especially when dealing with bulky DUTs. Unfortunately, the electric field in a GTEM cell is primarily vertical as well. Thus, a rotation about the vertical axis only weakly changes the electric field coupling. Consequently, previous TEM cell schemes have used longitudinal axis rotations.Nontheless, rotation about the vertical axis will be considered here.

The TEM mode will be excited according to eq. (B.11). The apex will be chosen as lying in the forward direction; thus, we need to consider the effect of a rotation on a_o. We first introduce a primed coordinate system which is referenced to the DUT. The rotation angle is designated α . In terms of the DUT primed local coordinates, the GTEM coordinate multi-pole moments become

$$M_x = M_{x'}\cos\alpha + M_{z'}\sin\alpha, \quad \text{and} \quad P_y = P_{y'} . \tag{B.12}$$

Thus, as a function of α, $a_o(\alpha)$ is given by

$$a_o(\alpha) = -\frac{1}{2}\left\{P_{y'} - jk_0M_{x'}\cos\alpha - jk_0M_{z'}\sin\alpha\right\}e_{oy}(\bar{o}) \tag{B.13}$$

The power measured by at the cell apex will thus be

$$\left|a_o(\alpha)\right|^2 . \tag{B.14}$$

We take measurements at four positions (multiples of $\pi/4$);

$$\left|\tilde{a}_o(0)\right|^2 = P_{y'}^2 + k_0^2M_{x'}^2 ,$$

$$\left|\tilde{a}_o(\tfrac{\pi}{4})\right|^2 = P_{y'}^2 + \tfrac{1}{2}k_0^2M_{x'}^2 + \tfrac{1}{2}k_0^2M_{z'}^2 + k_0^2M_{x'}M_{z'} ,$$

$$\left|\tilde{a}_o(\tfrac{\pi}{2})\right|^2 = P_{y'}^2 + k_0^2M_{z'}^2 , \text{ and} \tag{B.15}$$

$$\left|\tilde{a}_o(\tfrac{3\pi}{4})\right|^2 = P_{y'}^2 + \tfrac{1}{2}k_0^2M_{x'}^2 + \tfrac{1}{2}k_0^2M_{z'}^2 - k_0^2M_{x'}M_{z'} ,$$

where ~ denotes normalization by $-\frac{1}{2}e_{oy}(\bar{o})$.

If we subtract the last two we additionally have

$$\frac{1}{2}\left\{\left|\tilde{a}_o(\tfrac{\pi}{4})\right|^2 - \left|\tilde{a}_o(\tfrac{3\pi}{4})\right|^2\right\} = k_0^2M_{x'}M_{z'} . \tag{B.16}$$

The notation xx' is introduced to denote the axis alignment; also let

$$M_{1xx'} = P_{y'}^2 + k_0^2M_{x'}^2 , \tag{B.17}$$

$$M_{2xx'} = P_{y'}^2 + k_0^2M_{z'}^2 , \quad \text{and}$$

$$M_{3xx'} = k_0^2M_{x'}M_{z'} .$$

In this case the x' axis is aligned with the x (GTEM cell) axis. For the cases where the y' and z' axes are aligned with the GTEM cell x axis we find that

$$M_{1xy'} = P_{z'}^2 + k_0^2M_{y'}^2 \qquad M_{1xz'} = P_{x'}^2 + k_0^2M_{z'}^2$$

$$M_{2xy'} = P_{z'}^2 + k_0^2M_{x'}^2 \qquad M_{2xz'} = P_{x'}^2 + k_0^2M_{y'}^2 \tag{B.18}$$

$$M_{3xy'} = k_0^2M_{y'}M_{x'} , \text{and} \quad M_{3xz'} = k_0^2M_{z'}M_{y'} .$$

These equations may now be used to solve for $\bar{P}$ and $\bar{M}$, beginning with $\bar{M}$. We find that

$$M_{x'} = \frac{M_{3xx'}M_{3xy'}}{k_0^2M_{3xz'}} \qquad M_{y'} = \frac{M_{3xy'}M_{3xz'}}{k_0^2M_{3xx'}} , \text{ and}$$

$$M_{z'} = \frac{M_{3xz'}M_{3xx'}}{k_0^2M_{3xy'}} . \tag{B.19}$$

Having found the $\bar{M}$ components we may solve for $\bar{P}$;

$$P_{x'} = M_{1xz'} - k_0^2M_{z'}^2 = M_{2xz'} - k_0^2M_{y'}^2 ,$$

$$P_{y'} = M_{1xx'} - k_0^2M_{x'}^2 = M_{2xx'} - k_0^2M_{z'}^2 , \text{ and} \tag{B.20}$$

$$P_{z'} = M_{1xy'} - k_0^2M_{y'}^2 = M_{2xy'} - k_0^2M_{x'}^2 .$$

A difficulty is that some of the $\bar{M}$ components may be zero in which case (B.19) would involve dividing by zero. Thus a program to solve for $\bar{M}$ must first check to see if any of the $\bar{M}_{3\alpha\beta}$ values are zero. If so the equations simplify and the solution is not difficult. We also note that in the notation just developed the total radiated power P_0 (no quadrupole contribution) is given by

$$P_0 = 10k_0^2\left\{M_{1xx'} + M_{1xy'} + M_{1xz'}\right\} \tag{B.21}$$

$$= 10k_0^2\left\{M_{2xx'} + M_{2xy'} + M_{2xz'}\right\} .$$

ON SIMULATING OATS NEAR-FIELD EMISSION MEASUREMENTS VIA GTEM CELL MEASUREMENTS

P. Wilson
EMC Baden Ltd.
c/o ABB Research Center, CH-5405 Baden-Daettwil, Switzerland

The use of a GTEM cell for both near field and far field radiated emission testing is considered. The approach is to model the radiation from the device under test (DUT) as due to an equivalent set of multi-pole moments. A sequence of three, six, or nine GTEM measurements are used to determine the equivalent multi-pole moments for a particular DUT. The multi-pole model allows one to predict both the DUT free space radiation pattern and the DUT radiation over a ground screen. The correlation between GTEM cell and open area test site (OATS) measurements for the far field case (> 30 MHz, 3 m distance) has been examined previously. This paper considers correlation of sources in the near field (< 30 MHz, 1 m distance). Agreement between OATS data and GTEM cell correlated data is very good, better than 2 dB.

Introduction

Any finite sized radiation source may be replaced by an equivalent multi-pole expansion which gives the same field pattern outside some volume bounding the source. If the source is electrically small or if it consists of simple radiating elements, then the initial multi-pole expansion terms should yield an accurate radiation pattern representation. The approach here is to determine the leading multi-pole terms for a given DUT via GTEM cell measurements. These in turn are used to predict the expected free space and ground screen radiation characteristics, including simulated FCC/VDE emission measurements. Both near- and far-field terms are considered.

The basic method has been developed previously for the case of standard two port TEM cells [1-3], as well as for three orthogonal loop antennas [4]. Thus, some of the basic derivation need only be outlined. There are two primary differences between the present work and that derived previously. These are; 1) the GTEM is a single port device as opposed to a standard two port TEM cell and 2) the radiation of the multi-pole expansion will be considered over a ground screen, as well as in an idealized free space.

Previous work has established a correlation between DUT radiation in a GTEM cell and DUT far field radiation over an infinite metallic ground screen based on a three position emission measurement sequence [5-7]. The procedure is to first determine the total radiated power from the DUT under the assumption that the DUT is well modelled by the a set of three orthogonal electric dipoles and three orthogonal magnetic dipoles. Three positions are not sufficient to determine the individual moments of these six dipoles; thus, a detailed DUT radiation pattern cannot be calculated. However, it is noted that maximum far-field levels would occur if only a single dominant dipole (of the six possible) were the source of the total measured radiated power. Therefore, if it is assumed that only a single dipole is radiating (with the same total radiated power) then the actual DUT radiation should be reasonably bounded. This assumption is valid as long as the DUT gain is not considerably above that of a short dipole, which should be the case for unintentional radiators [8]. Note that the maximum gain of a short dipole, $g_{max} = 1.5$, is not too different than that for a resonant half-wave dipole, $g_{max} = 1.64$; thus, even electrically large structures are potentially well represented if they behave like a set of simple dipoles.

In the far field only the electric field is measured and it is not important whether the source is electric or magnetic in nature. However, in the near field, this is not the case. An electric dipole will create high impedance fields and a magnetic dipole will create low impedance fields (with respect to the 377 Ω far field wave impedance). Thus, it is not sufficient to measure only the total radiated power. We need also to know the type of source being measured in order to predict the near fields. Thus, a modification of the far field three position sequence needs to be considered.

This paper will investigate GTEM cell six and nine position emission measurement sequences. The reason for considering more positions is that the individual dipole moments can be determined (min. 6-equations vs. 6-unknowns). Knowing the individual electric and magnetic dipole moments should yield; 1) more accurate DUT far field antenna patterns and 2) estimates as to the DUT near fields. Again, as in the three position model it should be noted that no absolute phase information is available for such a one-port measurement; thus, we again assume that the dipoles are in phase. This is usually not a severe restriction since, typically, one dipole component will be dominant and its phase relative to other components is unimportant for predicting the maximum radiation. The model will be less successful in predicting radiation nulls; however, these are typically not of interest in EMC applications (as opposed to antenna characterisations).

Multi-pole radiation Over a Ground Screen

The multi-pole expansion for an arbitrary electrically small radiator in free space is developed in [1-2] and need not be detailed here. Retaining only the leading electric (P) and magnetic (M) dipole moments the free space fields are given by equation (1) where an

$$
\begin{aligned}
E_x &= K_E\left\{\left[-\frac{y^2+z^2}{r^2}g_1(r)+g_2(r)\right]P_x+\frac{xy}{r^2}g_1(r)P_y+\frac{zx}{r^2}g_1(r)P_z+\frac{z}{r}g_3(r)k_0M_y-\frac{y}{r}g_3(r)k_0M_z\right\}\\
E_y &= K_E\left\{\frac{xy}{r^2}g_1(r)P_x+\left[-\frac{z^2+x^2}{r^2}g_1(r)+g_2(r)\right]P_y+\frac{yz}{r^2}g_1(r)P_z-\frac{z}{r}g_3(r)k_0M_x+\frac{x}{r}g_3(r)k_0M_z\right\}\\
E_z &= K_E\left\{\frac{zx}{r^2}g_1(r)P_x+\frac{yz}{r^2}g_1(r)P_y+\left[-\frac{x^2+y^2}{r^2}g_1(r)+g_2(r)\right]P_z+\frac{y}{r}g_3(r)k_0M_x-\frac{x}{r}g_3(r)k_0M_y\right\}
\end{aligned}
\qquad (1)
$$

$$
\begin{aligned}
H_x &= K_H\left\{\left[-\frac{y^2+z^2}{r^2}g_1(r)+g_2(r)\right]k_0M_x+\frac{xy}{r^2}g_1(r)k_0M_y+\frac{zx}{r^2}g_1(r)k_0M_z+\frac{z}{r}g_3(r)P_y-\frac{y}{r}g_3(r)P_z\right\}\\
H_y &= K_H\left\{\frac{xy}{r^2}g_1(r)k_0M_z+\left[-\frac{z^2+x^2}{r^2}g_1(r)+g_2(r)\right]k_0M_y+\frac{yz}{r^2}g_1(r)k_0M_z-\frac{z}{r}g_3(r)P_x+\frac{x}{r}g_3(r)P_z\right\}\\
H_z &= K_H\left\{\frac{zx}{r^2}g_1(r)k_0M_x+\frac{yz}{r^2}g_1(r)k_0M_y+\left[-\frac{x^2+y^2}{r^2}g_1(r)+g_2(r)\right]k_0M_z+\frac{y}{r}g_3(r)P_x-\frac{x}{r}g_3(r)P_y\right\}
\end{aligned}
$$

CH3310-0/93/0000-0011 $3.00 © 1993 IEEE

exp(jωt) time convention is assumed, r is the source (at the origin) to observation point distance, and

$$f(r) = e^{-jk_0 r} / r$$

$$K_E = -j\frac{k_0\eta_0}{4\pi} \quad \text{and} \quad K_H = \frac{k_0}{4\pi}$$

$$g_1(r) = \left[\frac{3}{(k_0 r)^2} + j\frac{3}{k_0 r} - 1\right] f(r) \qquad (2)$$

$$g_2(r) = \left[\frac{2}{(k_0 r)^2} + j\frac{2}{k_0 r}\right] f(r)$$

$$g_3(r) = \left[\frac{1}{k_0 r} + j\right] f(r)$$

These expressions may also be derived directly using standard dipole fields results [9].

It is now a relatively easy matter to introduce a ground screen. Let the dipole $\bar{P}$ be at a height h above a perfectly conducting ground screen located in the z=0 plane. This requires only that z be replaced by z-h in the field expressions. The observation point will again be designated $\bar{r}$. The fields at $\bar{r}$ will be due to both the real source and an image source located a distance h below the ground screen. The vector paths between the observation point and the real source, and image source are designated $\bar{r}_1$ and $\bar{r}_2$ respectively, where

$$\bar{r}_1 = (x, y, z-h);\ \text{magnitude} = r_1 = \left[x^2 + y^2 + (z-h)^2\right]^{1/2}, \text{ and} \quad (3)$$

$$\bar{r}_2 = (x, y, z+h);\ \text{magnitude} = r_2 = \left[x^2 + y^2 + (z+h)^2\right]^{1/2}$$

The real source dipole components are (P_X, P_Y, P_Z) and (M_X, M_Y, M_Z). The image of a positive electric charge about a perfectly conducting ground screen is a negative electric charge. As a result, the image source electric dipole $\bar{P}_I$ will have components ($-P_X$, $-P_Y$, $+P_Z$). If we think of the magnetic dipole as due to fictitious magnetic charges which retain their polarity when imaged about a perfectly conducting ground screen, then we find that the image dipole $\bar{M}_I$ will have components ($+M_X$, $+M_Y$, $-M_Z$) respectively. Thus, the fields due to the image dipoles may be found by replacing z with z+h, and $\bar{P}$ and $\bar{M}$ with $\bar{P}_I$ and $\bar{M}_I$ respectively. Summing the fields from both the real and image sources gives the fields over a ground screen.

Multi-pole Radiation in a GTEM Cell

The next step is to use a sequence of GTEM cell measurements to determine the various dipole moments. In a mathematical sense, rotations about any of the three axes are equally simple. One need only introduce a rotation angle α and perform the necessary bookkeeping. However, physically it is easiest to rotate about the vertical axis, especially when dealing with bulky DUTs. Unfortunately, the electric field in a GTEM cell is primarily vertical as well. Thus, a rotation about the vertical axis only weakly changes the electric field coupling. Consequently, some previous TEM cell schemes have used rotations about the longitudinal axis. However, only vertical axis rotations will be considered here since they are better suited to the larger DUTs that might be tested in a GTEM cell. If the same source as above is placed in a TEM cell, then the measured voltage will be related to

$$|\tilde{b}_0(\alpha)|^2 = |P_y^2 + k_0^2 M_x^2 \sin^2\alpha + k_0^2 M_x^2 \cos^2\alpha + k_0^2 M_x M_z \sin 2\alpha| \quad (4)$$

where α represents a rotation angle about the vertical axis, and a position factor related to the DUT location in the cell has been normalized out. To generate information about the various moments we evaluate this equation at multiples of ± π/4:

$$|\tilde{b}_0(0)|^2 = |P_y^2 + k_0^2 M_x^2|$$

$$|\tilde{b}_0(\pm\pi/4)|^2 = |P_y^2 + \frac{1}{2}k_0^2 M_x^2 + \frac{1}{2}k_0^2 M_z^2 \pm k_0^2 M_x M_z| \qquad (5)$$

$$|\tilde{b}_0(\pm\pi/2)|^2 = |P_y^2 + k_0^2 M_z^2|$$

This is the basic information available to us via vertical rotations. The ±π/2 equations are redundant. In addition the π/2 equation can be derived from a combination of the others (sum the ±π/4 voltages and subtract the 0 position voltage); thus, vertical rotations generate only three independent equations

$$|\tilde{b}_0(0)|^2 = |P_y^2 + k_0^2 M_z^2|$$

$$|\tilde{b}_0(\pm\pi/4)|^2 = |P_y^2 + \frac{1}{2}k_0^2 M_x^2 + \frac{1}{2}k_0^2 M_z^2 \pm k_0^2 M_x M_z| \qquad (6)$$

Measured Quantities

We need to rotate through three basic axis permutations. These will be designated by the first subscript. In each of the three basic orientations we make a measurement in the basic α = 0 position (1), and two additional measurements (2,3) at α = ±π/4 rotations about the vertical axis. These three measurements 1-3 are designated by the second subscript. Thus, the subscript 23 would refer to the second orientation, -π/4 vertical axis rotation measurement. In the discussion that follows we will make use of the following nine quantities which are determined from the above described GTEM cell measurements.

$$b_{11} = |P_y^2 + k_0^2 M_x^2|$$

$$b_{12} = |P_y^2 + \frac{1}{2}k_0^2 M_x^2 + \frac{1}{2}k_0^2 M_z^2 + k_0^2 M_x M_z|$$

$$b_{13} = |P_y^2 + \frac{1}{2}k_0^2 M_x^2 + \frac{1}{2}k_0^2 M_z^2 - k_0^2 M_x M_z|$$

$$b_{21} = |P_x^2 + k_0^2 M_y^2|$$

$$b_{22} = |P_x^2 + \frac{1}{2}k_0^2 M_y^2 + \frac{1}{2}k_0^2 M_z^2 + k_0^2 M_y M_z|$$

$$b_{23} = |P_x^2 + \frac{1}{2}k_0^2 M_y^2 + \frac{1}{2}k_0^2 M_z^2 - k_0^2 M_y M_z| \qquad (7)$$

$$b_{31} = |P_z^2 + k_0^2 M_y^2|$$

$$b_{32} = |P_z^2 + \frac{1}{2}k_0^2 M_z^2 + \frac{1}{2}k_0^2 M_y^2 + k_0^2 M_z M_y|$$

$$b_{33} = |P_z^2 + \frac{1}{2}k_0^2 M_z^2 + \frac{1}{2}k_0^2 M_y^2 - k_0^2 M_z M_y|$$

The generate the following sum and difference expressions:

$$S_1 = b_{12} + b_{13} = |2P_y^2 + k_0^2 M_x^2 + k_0^2 M_z^2|$$

$$S_2 = b_{22} + b_{23} = |2P_x^2 + k_0^2 M_y^2 + k_0^2 M_z^2|$$

$$S_3 = b_{32} + b_{33} = |2P_z^2 + k_0^2 M_z^2 + k_0^2 M_y^2| \qquad (8)$$

$$D_1 = |b_{12} - b_{13}| = |2k_0^2 M_x M_z|$$

$$D_2 = |b_{22} - b_{23}| = |2k_0^2 M_y M_x|$$

$$D_3 = |b_{32} - b_{33}| = |2k_0^2 M_z M_y|$$

Note that P and k_0M have the same units; thus, it will prove convenient to always work with these quantities.

Multi-Pole Moment Evaluation

Under the assumption that all the dipole moments are in phase we have six unknowns to determine (P_x',P_y',P_z',k_0M_x',k_0M_y',k_0M_z'). This requires 6 independent equations; thus, the minimal number of measurements required in the general case is six. As shall be seen, six measurements will suffice in some cases but not all cases, due to degeneracies in the equations when some of the moment components are zero (or negligible in comparison to the dominant components).

We will consider three routines for determining the dipole moments: 1) a three position model for the case that the source type is known (electric or magnetic), 2) a six position model for the general case assuming no degeneracies, and 3) a nine position model for the general case which allows for degeneracies.

Known Source Model

If we know a priori that the test object is predominately an electric ($P >> k_0M$) or magnetic ($P << k_0M$) source then the three basic position measurements b_{11}, b_{21}, and b_{31} are sufficient. From eq. (7) we see that:

Electric Dipole Source ($P >> k_0M$):

$$P_y'^2 = b_{11}$$
$$P_z'^2 = b_{21} \qquad (9)$$
$$P_x'^2 = b_{31}$$

Magnetic Dipole Source ($P << k_0M$):

$$k_0^2M_z'^2 = b_{11}$$
$$k_0^2M_x'^2 = b_{21} \qquad (10)$$
$$k_0^2M_y'^2 = b_{31}$$

Clearly this case is somewhat artificial, but it makes for a useful check for known sources.

General Source Model - No Degeneracies

In principle the three difference quantities in eq. (8) can be used to solve for the magnetic dipole moments:

$$k_0^2M_x'^2 = \frac{D_1D_2}{2D_3}$$
$$k_0^2M_y'^2 = \frac{D_2D_3}{2D_1} \qquad (11)$$
$$k_0^2M_z'^2 = \frac{D_3D_1}{2D_2}$$

The electric dipole moments then follow either from the basic position data b_{11}, b_{21}, and b_{31},

$$P_y'^2 = b_{11} - k_0^2M_z'^2$$
$$P_z'^2 = b_{21} - k_0^2M_x'^2 \qquad (12)$$
$$P_x'^2 = b_{31} - k_0^2M_y'^2$$

or from the sum data S_1, S_2, and S_3.

$$P_y'^2 = \frac{1}{2}\left\{S_1 - k_0^2M_x'^2 + k_0^2M_z'^2\right\}$$
$$P_z'^2 = \frac{1}{2}\left\{S_2 - k_0^2M_y'^2 + k_0^2M_x'^2\right\} \qquad (13)$$
$$P_x'^2 = \frac{1}{2}\left\{S_3 - k_0^2M_z'^2 + k_0^2M_y'^2\right\}$$

A problem is that one or more of the magnetic dipole moments may be zero, or effectively zero if they are considerably less than the dominant component. Take as an example the case where $M_x' = 0$: in this case D_1 and D_2 reduce to zero and the magnetic dipole moments may not be found via eq. (11). This type of degeneracy makes the six position approach very sensitive to the difference measurements.

General Source Model - Degeneracies Allowed

The basic approach is to first check the three difference values to see if they are all non zero and of the same order of magnitude. If yes then the six position solution may be used. If no, an alternate algorithm is used.

The first step is to compare the difference values D_1, D_2, D_3 to determine whether a degeneracy exists. A degeneracy will be defined as follows: if D_i << Maximum of (D_1,D_2,D_3) then it will be considered to be degenerate. A value of 0.1 to define much less than (<<) yields reasonable results. If a degenerate value exists, for example D_1, then one of three cases must be true:

1) k_0M_x' is small, or

2) k_0M_z' is small, or

3) both k_0M_x' and k_0M_z' are small.

To determine which of the cases applies we form the difference

$$\delta = S_1 - 2b_{11} = k_0^2M_x'^2 - k_0^2M_z'^2 \qquad (14)$$

We then make the following argument:

1) if $\delta = 0$ then k_0M_x' and k_0M_z' are both small, and

$$k_0^2M_x'^2 = D_1/2$$
$$k_0^2M_z'^2 = D_1/2 \qquad (15)$$

2) if $\delta < 0$ then $k_0M_x' << k_0M_z'$, and

$$k_0^2M_z'^2 = |\delta|$$
$$k_0^2M_x'^2 = D_1^2/4/k_0^2M_z' \qquad (16)$$

3) if $\delta > 0$ then $k_0M_x' >> k_0M_z'$, and

$$k_0^2M_x'^2 = |\delta|$$
$$k_0^2M_z'^2 = D_1^2/4/k_0^2M_x'^2 \qquad (17)$$

This algorithm may over estimate one component in the case that k_0M_x' and k_0M_z' are both small but not equal, such that the condition $\delta = 0$ is not exactly met. However, as δ is also small in this case the moments so determined are not significant. The main object of this approach is to find the dominant moment, rather than to accurately determine the insignificant moments. Once the two magnetic moments are found the remaining components are determined as follows:

$$P_y'^2 = \frac{1}{2}\left|S_1 - k_0^2M_x'^2 - k_0^2M_z'^2\right|$$
$$P_z'^2 = \left|b_{21} - k_0^2M_x'^2\right| \qquad (18)$$

$$k_0^2 M_{y'}^2 = \left| S_2 - 2P_{z'}^2 - k_0^2 M_{x'}^2 \right|$$

$$P_{x'}^2 = \frac{1}{2}\left| S_3 - k_0^2 M_{z'}^2 - k_0^2 M_{y'}^2 \right|$$

This example considers the case when D_1 is degenerate. If one of the other differences is degenerate (D_2 or D_3) the same equations (14)-(18) apply after the proper permutation.

Total Radiated Power

Once the various dipole moments have been determined the total radiated power P_0 due to the test object may also be found

$$P_0 = 10k_0^2(P_{x'}^2 + P_{y'}^2 + P_{z'}^2 + k_0^2 M_{x'}^2 + k_0^2 M_{y'}^2 + k_0^2 M_{z'}^2) \qquad (19)$$

Alternately, the total radiated power may be separated electric dipole moment P_{0P} and magnetic dipole moment contributions P_{0M}:

$$P_{0P} = 10k_0^2(P_{x'}^2 + P_{y'}^2 + P_{z'}^2) \qquad (20)$$

$$P_{0M} = 10k_0^2(k_0^2 M_{x'}^2 + k_0^2 M_{y'}^2 + k_0^2 M_{z'}^2)$$

Measurements

To test the above algorithms, a self-contained low-frequency radiator was built. It consists of a comb generator circuit capable of producing the following harmonics:

1) 0.0 - 1.0 MHz; 50 kHz steps

2) 1.0 - 5.0 MHz; 200 kHz steps

3) 0.0 30.0 MHz; 1.6 MHz steps

The circuit is contained in a small metal box and connected either to a 20 cm dipole antenna or a 80 cm^2 square loop antenna. In this way we can create a primarily electric or magnetic source.

Both antenna configurations were measured in the GTEM cell, for all nine orientations and all three frequency ranges for a total of 27 curves for each source. The antennas were placed in a Styrofoam box to facilitate rotations. The DUT height was 41.5 cm below a septum height of 1.3 m, and the DUT was transversely centered.

OATS Measurements

The same two sources were also measured over a ground screen. The electric dipole was measured in the vertical position, 1.13 m over the ground screen, at a distance of 1 m using a monopole antenna. The loop antenna was measured also in the vertical position, 1.11 m over the ground screen, at a distance of 1 m using an active loop antenna. It was not possible to cleanly measure a signal at all frequencies due to interference and the weakness of the source.

Known Source Model

Our test objects are basically known sources; thus, we may use the known source model to determine the moments.

The results of the GTEM correlated measurements and the OATS measurements for the electric source are shown in figure 1, both in absolute terms and the difference between the two (OATS - GTEM). The agreement is very good, < 2 dB for most points. Typically, the GTEM cell data are somewhat higher. This is likely due to the fact that the magnetic dipole moments have been ignored (set to zero); thus, all radiated power is assumed to be due to the electric dipole moments which may have the effect of over estimating their strength.

The equivalent data for the loop (magnetic dipole) are shown in figure 2. Again the agreement is very good with the GTEM data gain being somewhat larger for most points.

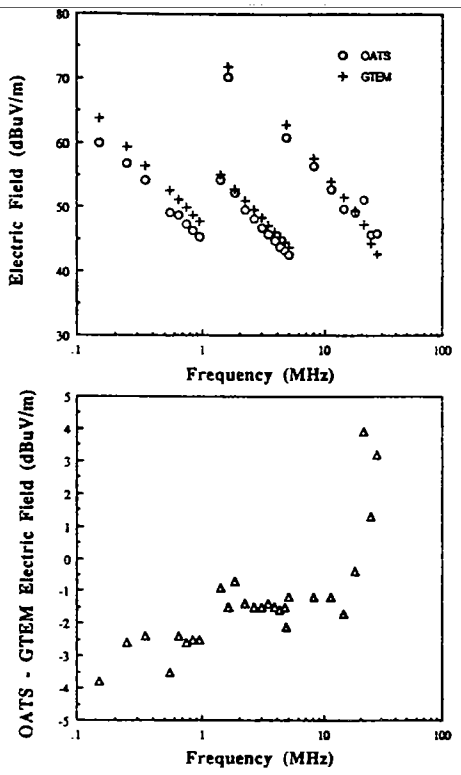

Fig. 1. GTEM cell to OATS data comparison based on the known source correlation sequence: electric dipole source.

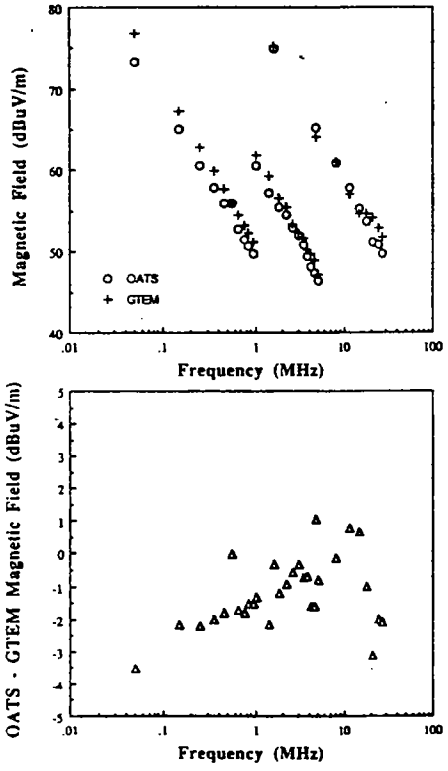

Fig. 2. GTEM cell to OATS data comparison based on the known source correlation sequence: magnetic dipole source.

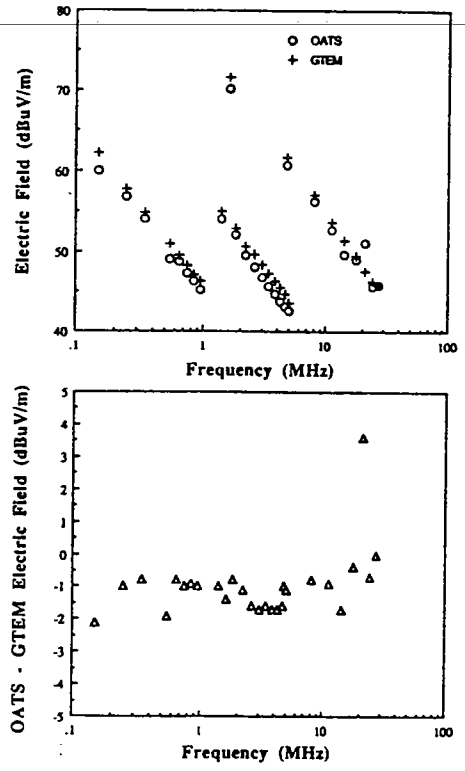

Fig. 3. GTEM cell to OATS data comparison based on the general source correlation sequence: electric dipole source.

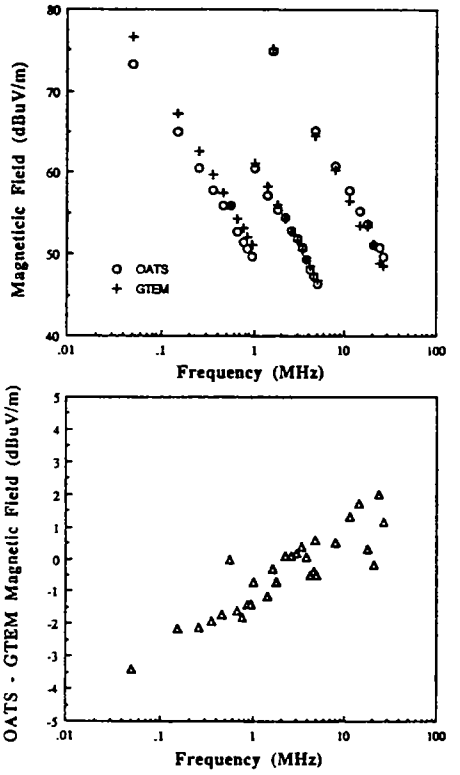

Fig. 4. GTEM cell to OATS data comparison based on the general source correlation sequence: magnetic dipole source.

General Source Model - Degeneracies Allowed

We next apply the general model to the full data. The resulting electric field data are shown in figure 3. In fact the agreement to measurement is better than for the known source model since the dominant component is not over estimated. The agreement is better than 2 dB over the whole range with the exception of a few points. This is basically within the measurement uncertainty of the system. The magnetic field data are shown in figure 4. Again excellent agreement is seen. A slight bias is seen in the data. The active loop antenna used to perform the measurements was later found to be defective. It was crudely recalibrated to give an indication of the error in the antenna gain. We expect that a proper calibration will remove the slight bias in the data and yield even better results.

Conclusion

The use of a GTEM cell for near field emission measurements has been considered. The equations generated here are also applicable to the far field and serve to expand earlier work. An unknown radiator, or DUT, is characterized by an equivalent multi-pole model. Electrically small radiators should be well represented by the leading multi-pole moments; namely, the electric dipole moment, the magnetic dipole moment. It was then demonstrated how a sequence of up to nine GTEM measurements could be used to the individual dipole moments under the assumption that phase differences between the various dipole moments may be neglected. Once the dipole moments are known, both electric and magnetic, the DUT ground screen radiation may be predicted theoretically. In this manner, one may

References

[1] G. H. Koepke and M. T. Ma, "A new method for determining the emission characteristics of an unknown interference source," Proc. 5th Intl. Zurich Symp. and Techn. Exhb. on EMC (Zurich, Switzerland), March 1983, pp. 35-40.

[2] I. Sreenivasiah, D. C. Chang and M. T. Ma, "A method of determining the emission and susceptibility levels of electrically small objects using a TEM cell," Tech. Note 1040, Nat. Bur. Stand., Boulder, CO, April 1981.

[3] M. T. Ma and G. H. Koepke, "A method to quantify the radiation characteristics of an unknown interference source," Tech. Note 1059, Nat. Bur. Stand., Boulder, CO, Oct. 1982.

[4] M. Kanda and D. Hill, "A three-loop method for determining the radiation characteristics of an electrically small source," IEEE Trans. on EMC, vol. 34, no. 1, Feb. 1992, pp. 1-3.

[5] P. Wilson, D. Hansen and H. Hoitink, "Emission measurements in a GTEM cell: simulating the free space and ground screen radiation of a test device," ABB Research Report CRB 89-007, June 1988.

[6] P. Wilson, D. Hansen and D. Koenigstein, "Simulating open area test site emission measurements based on data obtained in a novel broadband TEM cell," Proc. IEEE 1989 Natl. Symp. on EMC (Denver, CO), May 1989, pp. 171-177.

[7] E. Bronaugh and J. Osburn, "Radiated emissions test performance of the GHz TEM cell," Proc. IEEE Intl. Symp. on EMC (Cherry Hills, NJ), Aug. 1991, pp. 1-7.

[8] A. Tsaliovich, "Modeling electronic system radiated field patterns," Proc. 8th Intl. Zurich Symp. and Techn. Exhb. on EMC (Zurich, Switzerland), March 1989, pp. 323-328.

[9] R. Johnson and H. Jasik (Editors), Antenna Engineering Handbook (Second Edition), McGraw-Hill, New York, 1984, Ch. 2.

A Measurement and Calculation Procedure to Remove the "Gain No Greater than a Dipole" Restriction in the GTEM - OATS Correlation Algorithm

John D. M. Osburn
Principal EMC Scientist

Edwin L. Bronaugh
Vice President, Engineering

The Electro-Mechanics Company
P. P. Box 1546
Austin, Texas 78767 U. S. A.

ABSTRACT

This paper describes the evolution of GTEM measurement and correlation computations to remove the most critical assumption in the original correlation algorithm. The assumption was that the equipment under test (EUT) would display the radiation characteristics of a dipole, and the gain of the EUT radiating elements would not exceed that of a dipole antenna. It was found through measurement that there are cases where this assumption did not hold. The first step was to adopt a revised measurement procedure to conform to European Telecommunications Specification measurement practices, the second step was to further modify the measurement and computation to handle the general case where the EUT displays substantial gain characteristics.

SUMMARY

The original GHz transverse electromagnetic (GTEM) cell to open area test site (OATS) correlation algorithm included an assumption that the radiating element from an equipment under test may be modeled as a set of electric and magnetic dipoles [1]. In a practical sense, this assumption treats the radiating element of the EUT, either the entire EUT array or individual radiating elements (slots, apertures, cable segments or complete cable arrays) as if it has the radiation characteristics of a dipole antenna.

This assumption is valid, at least over the lower part of the normal radiated emissions measurement frequency range, where the entire EUT is small with respect to a wavelength. At higher frequencies this assumption may not hold. Consider a 30 cm long slot aperture in an equipment case excited by a 50 % duty cycle, 50 MHz digital clock. The clock signal will produce odd harmonic signals well into the normally measured frequency spectrum. at the fundamental, the wavelength of the excitation is 6 meters long and the slot is 1/20 wavelength long. This slot is, at this frequency, an inefficient radiator. Since the dimensions of the EUT are less than one wavelength, currents flowing around the slot are likely to flow in phase on the entire surface of the EUT. This excitation would produce radiation characteristics similar to a fat

inefficient dipole. At the 11th harmonic, however, conditions have drastically changed. At 550 MHz, the wavelength of the excitation is 0.54 m and the slot is almost optimally excited. The EUT may still have reasonably uniform current flow on its surface, and may still display the approximate radiation characteristics of a dipole. At the 17th harmonic, 850 MHz, this condition will have changed. Here the wavelength is 0.35 m and it is unlikely that the EUT will display dipole characteristics. It is much more likely that the that the EUT radiation characteristics would display directionality. If this is true then the assumption that the radiating element would display gain no greater than a dipole is incorrect.

This problem was first identified when it was noted that the starting position of the EUT in a GTEM measurement influenced the final value of correlated field strength. Testing was being conducted on an EUT where the results would be compared to the ETS [2]. Examination of the EUT at an OATS showed that directional sensitivity was present in the EUT. Further examination of the EUT in a GTEM showed that if the proper starting face for the measurements was chosen, correct answers would be obtained. This was found to be due to the nature of the EMC measurement in the ETS. In the ETS, after maximization of the emission in azimuth on the turntable, and in height with the measurement antenna, the EUT is replaced with a tuned dipole set at the frequency of the emission. The specification limit is in terms of the power, in dBm input to this "replacement" dipole. Since a dipole is assumed in the correlation algorithm, the E-field strength computed by the correlation algorithm showed excellent agreement so long as the proper face and polarization were chosen as a starting position. The only positive assurance of this is to assume the EUT is enclosed by a cube, and to measure each of the six faces of this cube in two polarizations. This assures that the proper face and polarization are chosen for the starting point. Since all faces and polarizations are measured, a total of twelve measurements, the three values (the appropriate X, Y and Z values) are already available from the twelve measurements and may be chosen as inputs to the correlation algorithm. This provided an acceptable procedure for measurement of EUT emissions with undetermined gain values, but having gain in excess of a dipole, to determine compliance with the ETS.

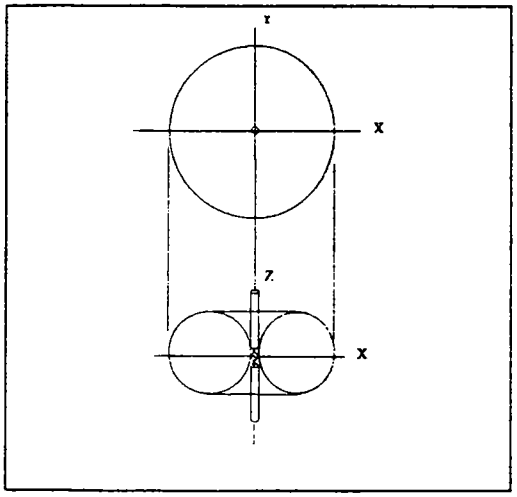

Figure 1. Dipole Radiation Pattern

If one examines the radiation pattern of a dipole, Figure 1, there are two characteristics that can be easily checked from information available from measurements of six faces in two polarizations. As shown in Figure 1, the dipole radiation pattern is omni directional in the X-Y plane. If one chooses the maximum value from the twelve measurements as a reference value, then the co-polarized, adjacent faces in the same orientation should display approximately the same numeric values as the reference.. If they do not, then the assumption of a dipole radiation pattern is in question. In addition if the two adjacent faces of the co-polarized measurement perpendicular to the maximum reference are not substantially below the maximum, then the dipole assumption is also challenged.

Given a set of data of twelve measurements, at any frequency, describing a particular emission, being six faces of an enclosing cube and both polarizations for each face, it is possible to determine if the dipole assumption is appropriate. If this assumption is appropriate, then the maximum value of the emission, chosen as an X reference, and the associated Y and Z values can be used as inputs to the correlation algorithm.

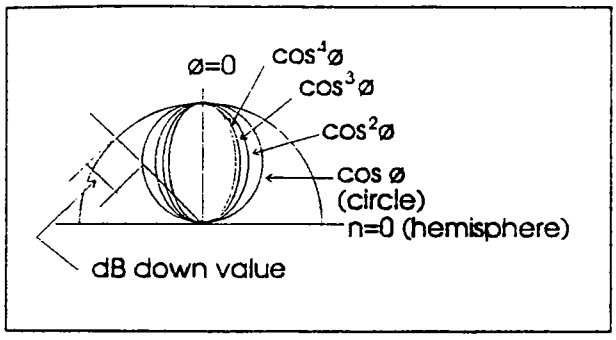

Figure 2. Unidirectional $\cos^n \phi$ Power Patterns for Values of n.

Given that the dipole assumption is not correct, additional steps must be taken to provide an estimate of the gain of the radiating element. A method of estimating this gain is provided in the subsequent paragraph.

Figure 2 shows the power patterns of a unidirectional source whose characteristics are described by $\cos^n \phi$ [3]. As shown in this figure, for $n = 0$, there is a hemispherical power pattern. as n increases, the power patterns become more directional. Of interest here is the behavior of the power patterns off axis. At the left side of Figure 2, a deviation from the hemispherical, or magnitude of omni directional power pattern is noted as "dB down". As shown in this figure, the "dB down" value is between the hemispherical response and the cos ø response. Additional "dB down" responses can be defined for subsequent powers of $\cos^n \phi$. Thus, if values of the drop off of E-field strength were available on any emitter at a specific frequency, an estimate could be made regarding the gain of the radiating element. Numerical estimates of gain are shown in Table I for several values of "dB down".

Table I. Estimated Gain as a Function of "dB down" Values

n	dB down at 45 Degrees	Estimated Beamwidth Degrees	Estimated Gain dB
1	3	120	3
2	6	90	5.1
3	10	75	7.4
4	12	66	9.5

The remaining step is, by measurement, to determine the "dB down" values. At this point the twelve measurements at each frequency are available. Selection of the maximum value at each frequency and testing the twelve points at this frequency for validity of the dipole pattern assumption is a matter of programming. The search through the data set will select the frequencies where the radiation characteristics of the primary assumptions are not valid. The frequency, face and polarization of all signals where the dipole performance assumption are invalid are known. Four additional measurements must be made at $\pm \pi/4$ to the original face and co- and cross-polarized to the original measurement. This allows a reasonable estimate of gain to

be used in the correlation algorithm. This revised gain value is useable as the boresite of the emission is assigned to the original face and polarization of the EUT, at that specific frequency.

The paper will include sample computations and a flow chart highlighting the several data checks and other measurement parameters that are associated with the revised measurement and correlation algorithm.

Incorporation of the revised measurement and computational procedure in the GTEM measurements software will remove the restriction placed by the original assumption of gain no greater than a dipole. This will in turn make GTEM measurements more realistic, and will open the possibility of the GTEM being used for more types of measurements. The incorporation of the revised measurement procedure and computation may prove extremely useful as commercial EMC radiated emission measurement requirements above 1 GHz become more common.

REFERENCES

1 P. Wilson, D. Hansen and D. Koenigstein, "Simulating Open Area Test Site Emission Measurements Based on Data Obtained in a Novel Broadband TEM Cell", *Symposium Record of the 1989 National Symposium On Electromagnetic Compatibility*, 89CH2736-7, Denver, CO, May 23 - 25, 1989, pp. 171 - 177.

2. EUROPEAN TELECOMMUNICATIONS STANDARD, ETS [B] : 1990, Version 3.3.0.

3. J. Kraus, *Antennas*, McGraw Hill, New York, 1950, p.21.